CHARACTERIZATION OF ACID-BASE CATALYSTS

AND

ITS APPLICATION TO CATALYST POISONING

Thesis by

Kiran Bakshi

In Partial Fulfillment of the Requirements
for the Degree of
Doctor of Philosophy

California Institute of Technology
Pasadena, California
1974
(Submitted December 20, 1974)

ACKNOWLEDGEMENTS

It is with great pleasure that I acknowledge the interest and guidance of Professor George Gavalas during the course of this investigation. His constant encouragement and profound advice have played an important role in the development of my scientific personality over the past few years. My studies at Caltech have been immensely enriched by my contact with him.

Special thanks go to George Griffith and the technical staff of the Chemical Engineering shop for their excellent assistance in the fabrication of the experimental apparatus.

I am also thankful to Dr. Dale Powers and Dr. Dana Powers for their assistance in some of the experiments, and Dr. Ramabhadran for his helpful suggestions on my proposition.

I am also grateful to the Chemical Engineering Department for providing me with the financial assistance in the form of Graduate Teaching and Research Assistantships. I would also like to thank Jennifer Burkhart for her help in typing my thesis and publications. Supply of catalyst samples by the various companies is also thankfully acknowledged.

Finally, I would like to express my deep gratitude to my parents for their encouragement, and my wife, Viharika, for her understanding and patience.

ABSTRACT

Several commercial aluminas, silica-aluminas and clays are investigated from a standpoint of catalyst characterization and the influence of partial deactivation on their activities for dehydration of primary alcohols. The states of the various catalysts are characterized by calorimetric titrations with n-butylamine and trichloroacetic acid and the resulting heat of adsorption curves are utilized to obtain acidity and basicity distributions for each catalyst state. A division of these distributions into groups of suitable acidic and basic site pairs leads to the development of a correlation between the acid-base distributions and the catalyst activities. The postulates of the correlation are in agreement with the reaction mechanism previously proposed in the literature.

Several of these catalysts are subjected to poisoning by ammonia and organic bases of different strengths. Subsequent evaluation of the acid-base distributions of the deactivated catalysts show subtle changes in the basicity distributions depending upon the strength of the poison. The correlation developed earlier is used to predict the activities and selectivities of the deactivated catalysts. The good agreement between the predictions and the experimental results substantiate the usefulness of the correlation. Subtle changes in selectivity caused by poisoning have been explained by the corresponding changes in the acid-base distributions, thus proving the importance of such characterization.

Kinetics of methanol and ethanol dehydration over some of these catalysts have been studied to ascertain effects of changes in the catalyst state. The rate expression

$$r = kK_A c_A^{1/2} / (1 + K_A c_A^{1/2} + K_W c_W)$$

describes the experimental data for all the catalysts in their fresh as well as poisoned states. Significant variations in k, K_A and K_W are observed depending upon the catalyst states. Comparison of kinetics on fresh and poisoned catalyst states shows that poisoning increases the K_A and K_W for ether formation in contrast to a decrease in these constants for olefin formation. These variations are attributed to interactions among poison molecules and acid-base site pairs, thereby lending support to the reaction mechanism. Certain implications of nonseparable kinetics are investigated to show significant changes in total conversion and product distribution upon reversal of flow direction through a graded reactor.

TABLE OF CONTENTS

I.
PROLEGOMENA

INTRODUCTION

Deactivation of industrial catalysts plays an important role in their development and utilization. Considerable effort is devoted to extend catalyst life by its proper formulation or by reduction of feed poisons. Process economics however necessitates the use of catalysts under slowly deactivating conditions followed ultimately by either catalyst regeneration or replacement. An investigation of the deactivation process and its influence on the catalyst behavior is hence necessary to design better catalysts and optimize their utilization.

Present investigations deal with two important issues of the deactivation process:

(a) Effect of partial deactivation on reaction kinetics: Many industrial catalysts have to be used under slowly deactivating conditions due either to incomplete removal of feed poisons or to simultaneous coking. From optimization standpoint, a knowledge of the reaction kinetics on a partially deactivated catalyst is hence desirable. For the sake of simplicity, the kinetic models reported in literature have been of separable type, e.g. Butt (1972). However, nonseparable kinetics have certain important implications such as directional effects and change in product distribution as shown by Gavalas (1971). The present work is concerned with an experimental investigation of the nonseparability of kinetics, directional effects and reaction kinetics on a partially poisoned catalyst. The dehydration of primary alcohols on silica-alumina partially poisoned by n-butylamine is selected as a model system to investigate these effects.

(b) Effect of partial deactivation on the state of the catalyst: Proper

understanding of the transformation in catalyst state caused by partial deactivation is certainly necessary to design better catalysts as well as study the deactivation process. However, a definition of the catalyst states in terms of their characteristics is necessary to deal with any changes in them. The present investigation attempts to characterize various aluminas and silica-aluminas, described in Tables A1 - A7, by calorimetric titrations to obtain their acidity and basicity distributions. The relevance of such a characterization in terms of catalyst activity and selectivity may be tested by developing a correlation between the two. Having established a definition of the catalyst state in terms of acid-base distributions of various commercial catalysts, the effect of partial poisoning by a variety of bases on their states and activities is probed. Although the emphasis of this investigation is on the above aspects of partial deactivation, the results are examined relative to a previously proposed reaction mechanism.

The details of these investigations are described in later sections but the principal findings may be briefly described as follows:

Main Results:

Observed kinetic data for methanol and ethanol dehydration on fresh and poisoned states of a silica-alumina catalyst and on other catalysts are given in Tables A10 - A21. The rate expression

$$r = kK_A c_A^{1/2}/(1 + K_A c_A^{1/2} + K_W c_W) \qquad (1)$$

describes the data for all the temperatures and catalysts tested and is in agreement with kinetics reported by other investigators. Figures A1 - A6 describe the fit of the model. From these results it is evident that the

transformation of the catalyst state upon partial poisoning does not have a major influence on the reaction mechanism.

Poisoning, however, does change k, K_A and K_W, thus showing nonseparability of the reaction kinetics. The directional effects described in Tables A8 and A9 along with other data described in the next section show significant changes in both total conversion and product distribution upon flow reversal. The model constants K_A and K_W for the two dehydration products, ether and olefin, are observed to vary differently upon poisoning, thus indicating a different mechanism for each reaction. The difference in this variation of K_A and K_W is explained in terms of two different types of acid-base site pairs, lending support to the mechanism proposed by Figueras et al. (1971) and described schematically in Figures A7 - A8.

The results of calorimetric titrations of various commercial catalysts in their fresh and partially poisoned states are given in Tables A23 - A48. The acid-base distributions obtained from the corresponding heat of adsorption curves show good qualitative correlation with the observed activities of these catalysts. These distributions may thus be used to define the state of the catalyst.

To study the activity and selectivity as a function of the catalyst state, a quantitative correlation connecting the acid-base distributions and the observed activities is desirable. For this purpose, the acid-base distributions of the fresh catalysts are divided into groups of suitable acidic and basic site pairs, and each group is assigned a specific reaction rate by least-squares fitting with the observed rates of dehydration. Such a group analysis results in good correlations for activities for both olefin and ether formation. The estimation of the effective site density for each

group by combination of suitable acid-base site pairs is in accord with the mechanism suggested by Figueras et al. (1971) . The values of the specific rates for olefin and ether indicate that although strongly acidic sites catalyze the formation of both these products, the former is affected more by the strength of the acidic sites. In accordance with the proposed reaction mechanism, ether formation requires basic sites of optimal strength.

Having thus established a correlation between catalyst activities and the state characteristics, further study of the influence of deactivation on the catalyst state may be carried out, and the correlation may be used to predict the activities of partially poisoned catalysts. Effect of poisons of different strengths is studied and the results indicate that the acidity distributions for the deactivated catalysts are predictable from a knowledge of the poisoning level and the corresponding distributions in their fresh state. Poison adsorption selectively destroys the acidic sites displaying the highest heat of adsorption.

The effect of poison adsorption on the basicity distribution, on the other hand, is quite subtle. Weak poisons such as pyridine do not affect the basicity distributions considerably. However, strong poisons such as n-butylamine increase the strength of the strongest basic sites resulting in a change in the basicity distribution. The net effect of poisoning by n-butylamine is a reduction in the number of basic sites having optimal basicity required for ether formation. This explains the behavior of K_A and K_W observed earlier and also explains the increase in selectivity for olefin upon poisoning by a strong base. The activities and selectivities predicted by the correlation are again in good agreement with the experimental results.

CONCLUSIONS

Reaction kinetics on heterogeneous catalysts such as aluminas and silica-aluminas may be, in general, of nonseparable type as shown in the case of alcohol dehydration. Significant directional effects in terms of total conversion and product distribution changes are observed upon flow reversal.

Partial deactivation of these catalysts do not affect the reaction mechanism but significantly change the model constants K_A and K_W for both the reaction products. The variation of K_A and K_W with poisoning is in accordance with the previously proposed reaction mechanism.

The acid-base distributions obtained from calorimetric titrations provide a useful characterization of catalysts in their fresh and poisoned states. The distributions are utilized in developing a group analysis to correlate the observed activities of various catalysts. The postulates used in developing the correlation are in accordance with the reaction mechanism.

The behavior of poisoned catalysts depends on the acid-base distributions in their fresh state and the strength of the poison adsorbed. Weak poisons do not affect the basicity distributions significantly. Strong bases, however, cause a shift in the basicity distribution towards higher strengths. This difference in the behavior of the basicity distribution has a significant effect on the catalyst selectivity. The results show that selective poisoning can be used to produce rather subtle selectivity changes for the catalysts studied.

LITERATURE CITED

Butt, J. B., in "Chemical Reaction Engineering," Advances in Chemistry Series, No. 109, pp. 259-496 (1972)

Gavalas, G. R., Ind. Eng. Chem. Fund., 10, 621 (1971)

Figueras, F., Nohl, A., DeMourges, L., Trambouze, Y., Trans. Faraday Soc., 67, 1155 (1971)

II.

EFFECTS OF NONSEPARABLE KINETICS IN ALCOHOL DEHYDRATION OVER POISONED SILICA-ALUMINA

K. R. Bakshi and G. R. Gavalas*
Division of Chemistry and Chemical Engineering
California Institute of Technology
Pasadena, California 91109

ABSTRACT

The kinetics of methanol and ethanol dehydration over fresh and partially poisoned silica-alumina have been studied in a microflow reactor system. The rate expression $r = kK_A c_A^{1/2}/(1 + K_A c_A^{1/2} + K_W c_W)$ describes the experimental data for all reactions, although the constants for ether formation and olefin formation are entirely different and vary between fresh and poisoned catalysts. Certain effects of nonseparable kinetics, namely directional effects and selectivity changes, were found to be significant in a broad range of conditions. The nonseparability of kinetics and the concomitant variation of the constants K_A, K_W with poisoning can be attributed to interactions among chemisorbed poison molecules and acid-base pairs of sites lending support to a reaction mechanism proposed in the literature.

* To whom correspondence should be directed.

SCOPE

An important consideration in industrial catalyst development is the resistance of the catalyst to deactivation by sintering, coking or poisoning by feed impurities. A great deal of effort is devoted to extend catalyst life by its proper formulation or by reduction of feed poisons. Nevertheless, a catalyst has finite life and must be periodically replaced or regenerated. Between successive regenerations the catalyst is subject to continuous change which affects the kinetics of the main process and poses problems of optimal operation and regeneration policies. Such optimization problems require models describing the kinetics on partially poisoned catalysts, as well as the kinetics of deactivation. For the sake of simplicity and in the lack of more precise information, the kinetic models reported in the literature have been of the separable type. A previous paper of Gavalas (1971) has shown by computer simulation that certain implications of non-separability, such as directional effects, are of considerable importance in catalytic reactor operation. The present investigation is concerned with an experimental investigation of the directional and other kinetic effects of catalyst poisoning in a simple catalytic system, the dehydration of alcohols on aluminas and silica-aluminas. Although the emphasis is on certain kinetic effects of poisoning, the results obtained are briefly examined relative to a previously proposed reaction mechanism.

CONCLUSIONS AND SIGNIFICANCE

The effect of poisoning on the kinetics of alcohol dehydration on several commercial aluminas and silica aluminas has been investigated. The empirical rate expression

$$r = \frac{kK_A c_A^{1/2}}{1 + K_A c_A^{1/2} + K_W c_W}$$

has been found to describe well fresh and poisoned catalysts although the constants k, K_A, K_W vary significantly among the various catalysts and between fresh and poisoned catalysts. The variation of the model constants K_A and K_W due to poisoning can be explained in terms of active sites comprising acidic-basic pairs lending support to a mechanism proposed by Figueras et al. (1971). Three kinetic effects of non-separable kinetics, namely variation of relative activity, variation of selectivity, and directional effects, have been observed. The latter effects, namely the change of conversion and product distribution upon flow reversal in a reactor with a poisoning gradient, can be utilized to optimize catalytic reactor operation.

The rate of a heterogeneously catalyzed reaction depends on the state of the gas, characterized by the concentration c and temperature T, and on the state of the catalyst:

$$\text{rate} = r(c,T;\ \text{catalyst state}) \tag{1}$$

As long as interest is confined to a single and unchanging catalyst, the dependence on the catalyst state is omitted and Eq. (1) takes the familiar form

$$\text{rate} = r(c,T) \tag{2}$$

However, the catalyst state becomes a variable while considering a class of catalysts which differ from each other in their preparation or pretreatment including treatment by moderators and promoters, or due to the action

of deactivation processes including poisoning, fouling, or sintering. In the following we shall mainly be concerned with catalysts differing in their treatment by poisons.

An explicit expression for the dependency on the catalyst state is generally impossible due to the lack of a general quantitative characterization of a heterogeneous catalyst. For this reason, it is useful to consider certain ideal cases allowing simple characterizations and to compare real catalysts against these ideal cases.

An ideal catalyst surface, used in the formulation of the Langmuir isotherm and the Langmuir-Hinshelwood kinetics, is characterized by uniform and noninteracting sites. The expression "noninteracting" means that a chemisorbed species does not modify the properties of neighboring free or occupied sites. A class of such ideal catalysts can be characterized by a single parameter, the density of sites, and the reaction rate can be described by the expression

$$\text{rate} = r(c,T;N) \tag{3}$$

Starting with an ideal catalyst surface, a class of catalysts obeying Eq. (3) could be produced by poisoning at different levels, provided a poison molecule deactivates the adsorbant site completely and does not affect the strength of neighboring sites. If, in addition, reactions involving adsorbed species are monomolecular, i.e. reactions between two chemisorbed species or one chemisorbed species and a vacant site, are excluded, Eq. (3) assumes the separable form

$$\text{rate} = Nr(c,T) \tag{4}$$

The assumptions embodied in the simplified forms (3) and (4) are very restrictive and, in fact, there are numerous investigations indicating

nonuniformity (heterogeneity) or interactions among the active sites. One of the simplest experimental indications of nonideality is the variation of the heat of adsorption with coverage. In kinetic studies, the presence of nonuniformity or interactions has been manifested by the nonlinear variation of conversion with respect to the amount of poison adsorbed (Butt, 1970), or the change of reaction selectivity upon poisoning (Figueras, 1969; Butt, 1970). In general, these studies have involved a single feed composition and the effect of poisoning on the rate in a broad range of concentrations and temperatures has not been investigated.

Chemical engineering studies of catalyst poisoning have been directed towards reactor operation and optimization. Thus, they have focussed on the effects of deactivation on the conversion and selectivity of a single catalyst pellet or of a fixed bed reactor. In all such studies, e.g. Bischoff (1969), Butt (1968), Levenspiel (1972), it has been assumed that the reaction rate is separable, in the sense of Eq. (4), in order to facilitate the kinetic modeling. This work is summarized in the comprehensive review of Butt (1972).

The possibility of nonseparable kinetics, hardly surprising from the chemical standpoint, has certain implications in reactor operation which deserve a more careful consideration. The present study has the purpose to assess experimentally the following effects of nonseparable kinetics attendant upon catalyst poisoning:

(i) a ratio $\rho(c,T)$ may be defined for two catalyst states i and j by

$$\rho(c,T) = \frac{r(c,T;\ \text{catalyst state } i)}{r(c,T;\ \text{catalyst state } j)} \qquad (5)$$

For separable kinetics ρ is constant, so that the variation of ρ in a range of c and T is a measure of the deviations from separable kinetics.

(ii) in the case of multiple reactions, the selectivity varies with catalyst state.

(iii) manifestation of directional effects, i.e. the changes in conversion and product distribution resulting from reversing the direction of flow through a reactor with a poisoning gradient.

The changes in selectivity and the directional effects have obvious practical significance in catalyst production and reactor operation, as has been illustrated in a previous theoretical study (Gavalas, 1971).

The deviations from separable kinetics are specific to the catalyst-reaction system. To the extent, however, that they result from surface nonuniformities and interactions they can be used to characterize a catalyst with respect to a broader class of reactions. The present work employs the dehydration of methanol and ethanol to study a silica-alumina catalyst, fresh and poisoned by n-butylamine. The dehydration of alcohols by alumina catalysts has been studied extensively, as reviewed by Winfield (1960), and Pines and Manassen (1966). Figueras et al. (1971) have investigated the kinetics of dehydration over silica-alumina, including the qualitative effects of a variety of poisons, and have presented a mechanistic interpretation of their results. The present work is devoted to a more complete kinetic study with emphasis on the aforementioned effects of nonseparable kinetics.

EXPERIMENTAL

1. Reagents. Reagent grade methanol and ethanol were used without further purification. Reagent grade n-butylamine was distilled over sodium and percolated over a molecular sieve before use. High purity grade nitrogen and helium were used as diluent and carrier gas, respectively, after drying over a molecular sieve bed.

2. Catalysts. Various commercial catalysts used in the present investigations are listed in Table 1. Most of the poisoning studies were conducted on F49 catalyst. The pelleted catalysts obtained from the suppliers were crushed and fractionated under dry nitrogen to prevent contamination. All the catalysts were stored under dry conditions after a five hour preheating at 250°C under dry nitrogen.

3. Experimental Apparatus and Kinetic Experiments. The general layout of the experimental apparatus is shown in Figure 1A. The kinetic study was carried out in two micro flow reactors immersed in an isothermal fluidized sand bath. The temperatures of both the reactors were maintained within ±0.3°C of the reported values. The reagents were fed by a dual syringe volumetric infusion pump with flow controlled to within 0.5% deviation.

Alcohol was vaporized, mixed with the diluent N_2 and fed to the reactor. A valve matrix preceding the two reactors enabled the use of the reactors in series or in parallel and allowed the reversal of the direction of flow. Identical flow and thermal conditions within the two microreactors, when operated in parallel, enabled simultaneous evaluation of fresh and poisoned catalysts under comparable conditions. The tubes and valves were heated to prevent condensation of the reactant. The analysis of the products was carried out as follows:

(a) Methanol dehydration: Detector--thermal conductivity, He flow rate--30 cm^3/min, Column--10' poropak T at 190°C, Sample volume--1 cm^3.

(b) Ethanol dehydration: Detector--flame ionization, He flow rate--20 cm^3/min, Column--14' of 10% Carbowax 20 M on chromasorb P at 110°C.

4. In Situ Poisoning. Dry N_2 was passed through the catalyst at the reaction temperature until no water or alcohol could be detected chromatographically. The N_2 flow rate was then reduced and a measured volume of n-butylamine solution in benzene was introduced through a mixing tee situated in the vaporizer. The reactor exhaust was monitored chromatographically to detect amine elution, if any. For sufficiently low amine/catalyst weight ratio, no amine eluted, indicating irreversible adsorption. After benzene could no longer be detected in the exhaust, the reactor was ready for resuming the kinetic experiments. The above procedure was repeated when it was desired to increase the level of poisoning.

5. Uniform Poisoning. The poisoning was carried out in a "tumbling batch reactor" consisting of a 1-1/2" O.D. x 3" long stainless steel cylinder tumbling inside a larger, 6" I.D. x 6-3/4" long stainless steel chamber heated by an externally wound heater, as shown in Figure 1B. The entire assembly was controlled at 230°C ± 0.3°C. Two thin detachable discs covering the ends of the internal cylinder were used to increase the heat transfer area. A weighed amount of fresh catalyst was placed in the internal cylinder which could communicate with the gas in the external cylinder only through two fine capillary tubes attached on the side discs. The capillary tubes were designed to attain a controlled and slow poisoning rate. By tumbling

the internal cylinder at a sufficiently high rate, e.g. 50 rpm, the catalyst particles were uniformly exposed to a low poison concentration. The procedure for poisoning consisted in first exposing the catalyst to pure N_2 at 230°C and 6 psig. The N_2 was repeatedly flushed and replaced for a period of 5 hours which was sufficient to stabilize the water adsorbed on the catalyst. A measured solution of n-butylamine in dry benzene was then injected through a septum in the external cylinder. After overnight exposure, no amine could be detected chromatographically. The reactor was then cooled to room temperature and a weighed sample of the catalyst was transferred to the microreactor for kinetic studies.

6. Experimental Conditions. The kinetic experiments were carried out with feed alcohol concentrations in the range 0.001 to 0.024 moles/liter, feed water concentration in the range 0 to 0.0025 moles/liter and temperatures 150°C - 225°C. The total pressure in the reactor was somewhat higher than atmospheric and the pressure drop along the reactor was negligible under all flow conditions. No reaction was observed with an empty reactor at the highest temperatures employed. Low conversions (<6%) were maintained to attain nearly differential conditions, and the measured reaction rates were assigned to the arithmetic average of reactor inlet and outlet concentrations.

Possible mass transfer limitations were tested experimentally and theoretically. Thus, a change of flow rate at constant space velocity and a change of catalyst particle size were found not to affect the rates. Mass transfer coefficients estimated by an appropriate correlation showed film diffusion not to be rate limiting. Similarly, using an effective diffusivity of 10^{-3} cm^2/sec, estimated by the procedure of Satterfield (1970), resulted in a value of the modulus $\Phi \sim 10^{-3}$ assuring the absence of pore diffusional

limitations according to the criterion of Weisz (1954).

The adsorption capacity of F49 for n-butylamine at 200°C was estimated thermogravimetrically at 420 μmoles/g. All poisoning experiments employed poison amounts considerably lower than this capacity. The irreversibility of poison adsorption in the presence of alcohol and water was ascertained chromatographically by the absence of amine in the reactor outlet, and more stringently by the reproducibility of kinetic results over a period of several days of operation.

RESULTS FOR METHANOL DEHYDRATION

1. In Situ Poisoning. Some preliminary kinetic runs were conducted at two methanol concentrations with a fresh and an in situ poisoned catalyst. As shown in Figure 2, the ratio of the rates ρ decreased steeply with initial amine chemisorption but more slowly on further poisoning, indicating that sites with higher activity towards amine chemisorption have also higher activity towards methanol condensation. An alternative explanation could be advanced in terms of interactions rather than nonuniformities of sites. Figure 2 also shows that the ratio ρ depends on methanol concentration, the difference being larger at higher poison levels. Note that the two curves would coincide had the kinetics been separable.

2. Uniform Poisoning. The results reported in Figure 2 do not correspond to any single catalyst state because in situ poisoning results in a gradient of poison concentration along the reactor. To avoid such gradients, the catalyst was poisoned uniformly as described in the previous section, and the kinetic results obtained with this catalyst are as follows:

a. Directional Effects

A series combination of the two reactors, one filled with fresh catalyst, the other with a uniformly poisoned catalyst, establishes a variation of the catalyst state along the flow path. Low space velocities were used to attain high conversions under which the directional effects are significant. As shown in Table 2, as much as 10% difference is observed between the two directions of flow. The difference is more pronounced at low feed concentrations and higher conversions as predicted theoretically by Gavalas (1971). The directional effects are relatively modest in the case of single reactions, especially the ones that are product inhibited, but are expected to be more

pronounced in the case of competitive reactions.

b. Kinetic Experiments and Model Fitting

To investigate the effect of poisoning on the reaction rate, kinetic experiments were carried out on fresh and uniformly poisoned catalyst. Since a strong product inhibition has been reported for alcohol dehydration (Figueras, 1971), the following types of experimental runs were conducted: (i) variation of alcohol concentration at fixed water concentration; (ii) variation of water concentration at fixed alcohol concentration.

The dependence of the rate on alcohol concentration was observed to be less pronounced at higher concentrations, indicating significant surface coverage by alcohol. The data were fitted to the rate expression $r = k'c_A^n/(a + bc_A^n)$ by linear regression varying n from 0 to 2. A minimum residual was obtained for n = 0.5 for the fresh as well as the poisoned catalyst, for all three temperatures and for zero and nonzero feed water concentrations. The results, which for fresh catalyst are similar to those obtained by Figueras et al. (1971), imply a pseudo monomolecular reaction between adsorbed species, while the exponent n = 0.5 may be explained by a dissociative adsorption of methanol.

The data obtained from varying the water concentration at a fixed alcohol concentration were fitted to the form $1/r = A + Bc_W^m/c_A^{1/2}$ varying m from 0 to 2. Least residual was obtained at m = 1 for the fresh and the poisoned catalyst and for all temperatures.

A combination of the above model fitting results suggests the following rate expression

$$r = \frac{kK_A c_A^{1/2}}{1 + K_A c_A^{1/2} + K_W c_W} \qquad (6)$$

for both the fresh and the poisoned catalyst. The constants k, K_A, K_W were determined by nonlinear regression using Marquadt's algorithm and the results are listed in Table 3. A similar model was used by Figueras et al. (1971) for methanol dehydration on silica-alumina. Various other models were derived by Knozinger (1973) from a series of reaction mechanisms differing by one or more elementary steps. At the lower temperature, some of these models were found to fit the present data equally well as Eq. (6), in the sense of yielding very similar residuals. At the higher temperatures, however, Eq. (6) gives substantially lower residuals, for both the fresh and the poisoned catalyst, and hence it was chosen for data fitting in the whole range of conditions.

c. Temperature Effects

The values of the constants k, K_A, K_W, appearing in the kinetic model Eq. (6), are reported in Table 3 for various temperatures. If k is interpreted as the constant of the rate determining step, an estimate of the activation energy can be obtained from a least square fit of the data. Similarly, if K_A and K_W are interpreted as adsorption constants for alcohol and water, then the slopes obtained from their Arrhenius plots can be used to estimate the corresponding heats of adsorption, provided the entropies of adsorption are independent of temperature. The values of activation energies and heats of adsorption so obtained are shown in Table 4. The activation energy for the fresh catalyst is 33 Kcal/mole, in good agreement with the values reported by Winfield (1960).

d. Comparison Between Fresh and Poisoned Catalyst

The kinetic model, Eq. (6), has been found to fit the data with both the fresh and the poisoned catalyst, although (Table 3) the constants

k, K_A, K_W are in each case different. In particular, the constants K_A and K_W, as well as the temperature coefficients for k, K_A, K_W are larger for the poisoned catalyst. The trend for the variation of ρ with c_A as observed during in situ poisoning experiments is in agreement with the effect of larger K_A due to poisoning. An effect of nonseparable kinetics is exhibited in Figures 3 and 4 in terms of the ratio ρ. In each case the solid line represents the ρ predicted from the model, Eq. (6), while the points represent the measurements. The ratio ρ, which is constant in separable kinetics, is seen in Figures 3 and 4 to be subject to significant variations.

RESULTS FOR ETHANOL DEHYDRATION

1. Directional Effects

The directional effects in competitive reactions with nonseparable kinetics are expected to affect the conversion and selectivity upon flow reversal. Two types of experiments were conducted to investigate these effects in ethanol dehydration.

A series combination of two reactors, one filled with fresh F49 catalyst and the other with a uniformly poisoned F49 catalyst, were used to obtain an activity gradient along the flow path. As in methanol dehydration, low space velocities were used to attain high conversions. As shown in Figure 5, as much as 10% change occurs in both ether and ethylene formation rates. The flow reversal has maximum effect at low concentrations and high conversions. The changes in conversions due to flow reversal are in opposite directions for ether and ethylene, hence the selectivity changes by as much as 17% in favor of ethylene upon reversal of flow.

Directional effects were also studied in reactor consisting of a section containing F49 followed by a section containing T126. As shown in Table 5, the rates of ethylene formation and ether formation are changed by as much as 28% and 17% respectively upon flow reversal. Since both changes are in the same direction, the selectivity change is of smaller magnitude.

2. Kinetic Experiments and Model Fitting

Kinetic experiments similar to methanol dehydration were carried out to study the kinetic effects of poisoning. Ethylene and diethyl ether were the only products and the rate of ether formation was observed to be considerably higher than that of olefin formation at 155°C.

a. Kinetics of Ether Formation

The dependence of the rate of ether formation on the concentrations of

alcohol and water was found to be very similar to that of methanol dehydration. Thus the same model, Eq. (6), was used to fit the data and the constants obtained from a linear regression analysis are reported in Table 6 for the two catalyst states, fresh and poisoned. The ratio of the rates of poisoned and fresh catalyst ρ is observed to decrease with increasing alcohol concentration as observed earlier in methanol dehydration. The dependence of ρ on the concentration of water is much less in comparison to the case of methanol.

b. Kinetics of Ethylene Formation

As in the case of methanol dehydration, the kinetic data for ethylene formation can be fitted to the rate expression $r = k'c_A^n/(a + bc_A^n)$ and again the value $n = 0.5$ gives the best fit. This agrees with the conclusion of Figueras et al. (1969) relative to the rate of ethylene production on alumina. The dependence of ethylene formation on water concentration has a similar functional fit as for ether formation. This suggests that the empirical kinetic expression of Eq. (6) may also be used to describe the data on ethylene formation. The fit was indeed found to be satisfactory and Table 6 presents the values of the various constants.

Figures 6 and 7 show the ratio ρ as a function of alcohol and water concentration. In contrast to the case of ether formation, the ratio ρ for ethylene formation increases significantly with water concentration.

c. Effect of Poisoning on Selectivity

As mentioned in section A, an important measure of deviation from separable kinetics is the variation in product distribution or selectivity among different catalyst states. Figures 8 and 9 show the experimentally measured selectivity

$$\sigma = 100 \times \frac{\text{alcohol converted to ethylene}}{\text{total alcohol reacted}} \qquad (7)$$

as a function of alcohol and water concentration for the fresh and the poisoned catalyst. At all concentrations the poisoned catalyst has significantly higher selectivity towards ethylene production.

d. Kinetics on Various Commercial Catalysts

Four different commercial catalysts were investigated relative to the kinetics for ethylene and ether formation. These catalysts varied in method of preparation as well as chemical composition. The rate-concentration data for all catalysts were analyzed in a similar manner as described above. The model of Eq. (6) was found to describe the data well and the constants obtained from a linear regression analysis are reported in Table 7 for the four catalysts. The model constants were found to vary considerably for both ethylene and ether formation among the various catalysts. The effect of alcohol concentration on the selectivity σ for these catalysts is shown in Figure 10. The selectivity is seen to vary as much as twenty fold among the various catalysts tested.

DISCUSSION

The previous results and especially the directional effects and the variations in ρ and σ show that the kinetics of alcohol dehydration are nonseparable with respect to poisoning. This nonseparability is also manifested in the changes of K_A and K_W with poisoning. The changes in K_A and K_W indicate the presence of nonideal effects, namely nonuniformity of the sites or interactions among chemisorbed species. Such interactions must be related to the acidic-basic functions of the catalyst, so that it would be interesting to compare the present results with previous work on the reaction mechanism.

Among previous studies on alcohol dehydration, that of Figueras et al. (1971) can be singled out for its more comprehensive discussion of surface intermediates and reaction mechanism. Their kinetic experiments were performed on silica-aluminas, fresh and poisoned by sodium ions, pyridine and tetracyanoethylene. Although they have not claimed a complete reaction mechanism, they have suggested some of its important features: (i) ether production requires two different types of dissociative alcohol adsorption on an acidic-basic site pair where the acidic site need not be strong. The product water is also dissociatively adsorbed as OH^- on the acidic site and H^+ on the strong basic site. (ii) The production of olefin involves dissociative adsorption on an acidic-basic site pair, where now the acidic site is strong and the basic site could be weak. The product water is dissociatively adsorbed on the same site pair. These mechanistic features as well as their suggestions about the rate determining step of each reaction are compatible with the rate expression Eq. (6). Since the sites involved in ether and olefin production are different, the constants K_A and K_W are expected

to be different as observed in Tables 3, 6 and 7. Figueras et al. did not carry out complete kinetic studies to determine the variation of the constants with temperature and poisoning.

The present kinetic results offer further evidence, through the variation of K_A, K_W, to support the mechanism of Figueras et al. (1971). First of all, it must be emphasized that K_A and K_W, although related to adsorption-desorption equilibria, should not be interpreted as equilibrium constants of Langmuir type isotherms in view of the strong interaction effects of adsorbed methanol and water. The adsorption of water, in fact, is known to directly affect the acidity of the catalyst in general (Fukuda, 1969), and hence its activity with respect to the alcohol dehydration reactions (Butt, 1970).

The comparison of K_W and K_A for fresh and poisoned catalysts presents some interesting evidence regarding the active sites. In the formation of methyl and ethyl ether, the constants K_A and K_W are larger on the poisoned catalyst. This can be explained by the assumption that chemisorption of both alcohol and water involves a strongly basic site. Amine chemisorption on acidic sites would increase the basic strength of the neighboring basic sites resulting in stronger chemisorption as compared to the fresh catalyst. This induction effect may thus result in an increase in overall model constants K_A and K_W.

In ethylene production on the other hand, the two constants K_A and K_W substantially decrease with poisoning, consistent with the view that the reaction requires a strongly acidic site and a weakly basic one. Another piece of evidence for the different type of sites involved in ether and ethylene production is the relative magnitude of the constants K_A, K_W. In the case of ether production the constants K_A and K_W for methanol are quite

close to those for ethanol, considering the difference in the chemisorbed species. In contrast, these constants differ by orders of magnitude compared to the constants for the ethylene formation reaction. These interpretations are also in agreement with Figueras et al. (1968) who observed two different types of chemisorption of ethanol on fresh silica-alumina.

NOMENCLATURE

A, B	Linearized model constants
a, b, k'	Linearized model constants
c	Concentration vector
c_A	Alcohol concentration in gas phase, moles/liter
c_W	Water concentration in gas phase, moles/liter
c_P	Poison concentration in adsorbed phase, moles/g. catalyst
E_A	Activation energy for rate determining step, Kcal/mole
k, K_A, K_W	Nonlinear model constants as in Eq. (6)
N	Site density
Q_A	Heat of adsorption for alcohol, Kcal/mole
Q_W	Heat of adsorption for water, Kcal/mole
R	Universal gas constant
r	Rate of product formation, mole of product/hr-g catalyst

GREEK LETTERS

ρ	Rate ratio defined by Eq. (5)
σ	Selectivity defined by Eq. (7)
Φ	Thiele modulus

LITERATURE CITED

Bischoff, K. B., Ind. Eng. Chem. Fundamentals, 8, 665 (1969)

Butt, J. B., Rohan, D. M., Chem. Eng. Sci., 23, 489 (1968)

Butt, J. B., Dabrowski, J. E., Bliss, H., J. Catalysis, 18, 297 (1970)

Butt, J. B., in "Chemical Reaction Engineering", Advances in Chemistry Series, No. 109, pp. 259-496 (1972)

Figueras, F., Renard, P., DeMourges, L., J. Chem. Phys., 65, 1393 (1968)

Figueras, F., DeMourges, L., Trambouze, Y., J. Catalysis, 14, 107 (1969)

Figueras, F., Nohl, A., DeMourges, L., Trambouze, Y., Trans. Faraday Soc., 67, 1155 (1971)

Fukuda, Y., Matsuzaki, I., J. Res. Inst. Catalysis, Hokkaido Univ., 17, No. 3, 192 (1969)

Gavalas, G. R., Ind. Eng. Chem. Fundamentals, 10, 621 (1971)

Knozinger, H., Kochloefl, K., Meye, W., J. Catalysis, 28, 69 (1973)

Levenspiel, O., J. Catalysis, 25, 265 (1972)

Pines, H., Manassen, J., Advan. Catalysis, 16, 49 (1966)

Satterfield, C. N., "Mass Transfer in Heterogeneous Catalysis", p. 41, M.I.T. Press, Massachusetts, (1970)

Weisz, P. B., Prater, C. D., Advan. Catalysis, 6, 167 (1954)

Winfield, M. E., "Catalysis" (Emmett, P. H., ed.), vol. 7, pp. 93-182, Reinhold, New York, (1960)

Table 1. Commercial Catalysts for Alcohol Dehydration Study

Catalyst Code	Supplier	Chemical Composition
KSFO	Chemetron Corporation	Montmorillonite Clay Acid Activated
F49	Filtrol Corporation	74% SiO_2 17.5% Al_2O_3 4.5% MgO
AHC	American Cyanamid Company	76% SiO_2 24% Al_2O_3
T-126	Chemetron Corporation	Activated γ-Alumina
F-1	Aluminum Company of America	γ-Alumina Support

Table 2: Directional Effects in Dehydration of Methanol

	c_A (x 10^3)	Percentage Conversion		Ratio
		Forward[1]	Reverse	(Reverse/Forward)
A.	0.684	56.36	53.00	0.9404
	1.472	43.53	41.10	0.9442
	2.21	37.47	34.54	0.9218
	3.95	30.68	27.70	0.9029
B.	1.04	57.42	52.44	0.9129
	1.987	49.87	47.28	0.9481
	3.99	37.50	34.45	0.9187
	7.48	27.35	24.77	0.9057

Conditions: A. Catalyst weight = 3.64 g T = 190°C

Total feed rate = 0.237 moles/hr.

B. Catalyst weight = 3.64 g T = 190°C

Total feed rate = 0.142 moles/hr.

[1] Forward direction implies fresh catalyst bed followed by poisoned catalyst bed along the flow path.

Table 3. Model Constants for Dehydration of Methanol

Product: Dimethyl Ether

A. Fresh Catalyst

Temperature (°C)	k (x 10^3)	K_A	K_W
160	3.8346	4.8017	772.58
170	9.3058	3.2796	662.61
182	25.1730	2.0401	576.93

B. Poisoned Catalyst

Temperature (°C)	k	K_A	K_W
160	2.052	7.1010	2145.17
170	5.176	4.7315	1856.76
182	14.755	2.9735	1540.47

Table 4. Temperature Dependence of Model Constants for Dehydration of Methanol

Catalyst	E_A [1]	Q_A [2]	Q_W [3]
Fresh	33.50	30.51	5.212
Poisoned	35.15	31.01	5.944

[1] $E_A = -R \frac{d \ln k}{d\ 1/T}$

[2] $Q_A = R \frac{d \ln K_A}{d\ 1/T}$

[3] $Q_W = R \frac{d \ln K_W}{d\ 1/T}$

Table 5. Directional Effect in a Graded Reactor

Experimental conditions:

1.	Catalysts:	0.61g F49; 4g T126
2.	Temperature:	200°C
3.	Feed Concentration c_A:	1.45×10^{-2} moles/liter
4.	Forward Flow Direction:	T126 followed by F49
5.	Reverse Flow Direction:	F49 followed by T126

Rate of Ethylene Formation:

a. Forward: 7.03×10^{-4} moles/hr g catalyst bed

b. Reverse: 9×10^{-4} moles/hr g catalyst bed

Percentage increase upon flow reversal: 28.02%

Rate of Ether Formation:

a. Forward: 1.15×10^{-2} moles/hr g catalyst bed

b. Reverse: 1.35×10^{-2} moles/hr g catalyst bed

Percentage increase upon flow reversal: 17.39%

Table 6. Model Constants for Dehydration of Ethanol at 155°C

Product: Diethyl Ether

Catalyst	k (x 10^3)	K_A	K_W
Fresh	3.4746	6.17	546.4
Poisoned	0.8696	9.062	650.12

Product: Ethylene

Catalyst	k (x 10^3)	K_A	K_W
Fresh	0.08547	282.6	77540
Poisoned	0.04219	69.9	17750

Table 7. Model Constants for Various Commercial Catalysts

Catalyst	Ethylene			Diethyl Ether		
	k ($\times 10^3$)	K_A	K_W	k ($\times 10^3$)	K_A	K_W
KSFO	15.95	81.5	4035	256	2.3	224
F49	4.62	97.0	3000	156	2.0	134
AHC	0.68	49.0	6492	5.55	14.2	2240
F1	0.007	134.5	45800	0.236	78.0	23400

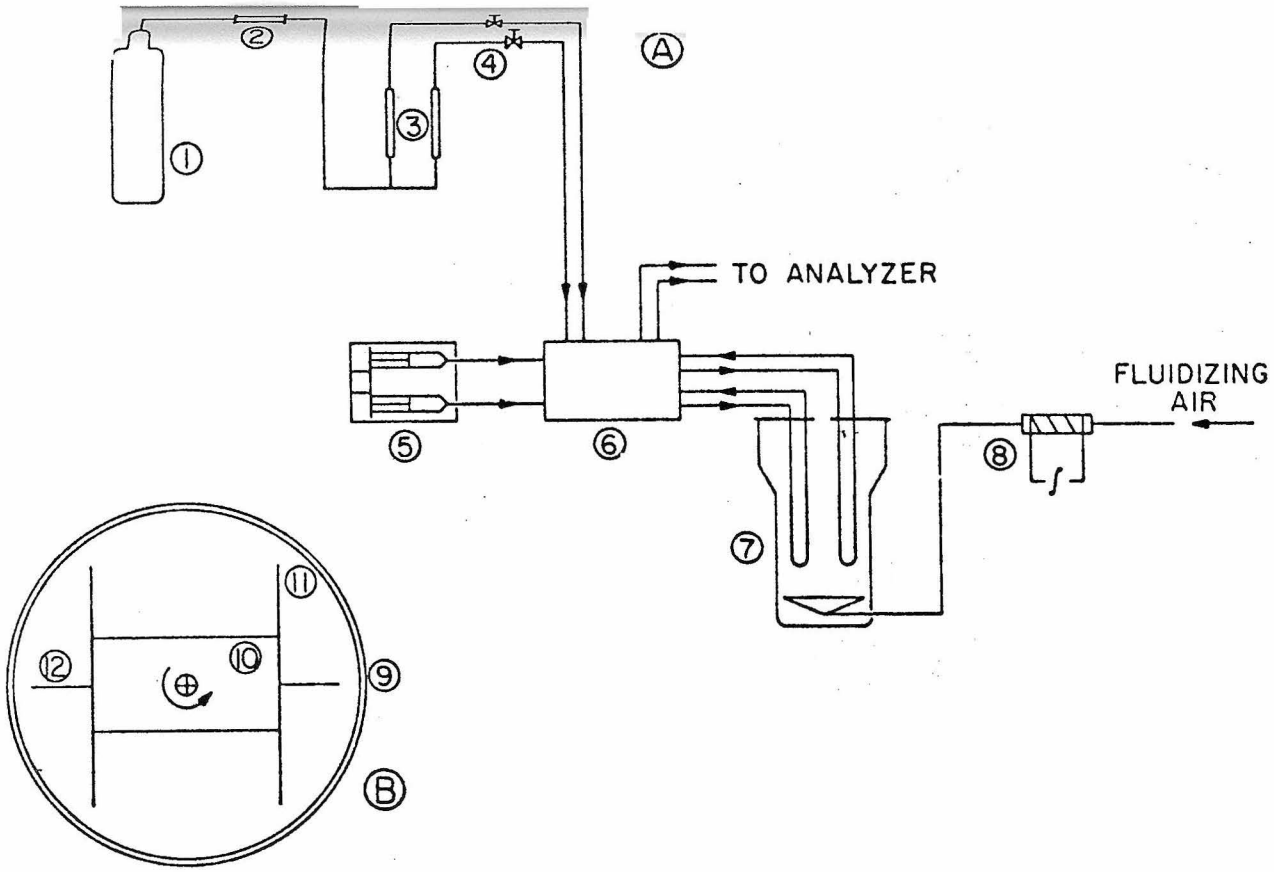

Figure 1. Schematic diagram of experimental apparatus

(1) Nitrogen Cylinder
(2) Gas dryer
(3) Rotameters
(4) Micrometer needle valves
(5) Volumetric infusion pump
(6) Vaporizer
(7) Fluidized sand bath with microreactors
(8) Air preheater
(9) Heated chamber
(10) Tumbling reactor
(11) Heat transfer discs
(12) Capillary

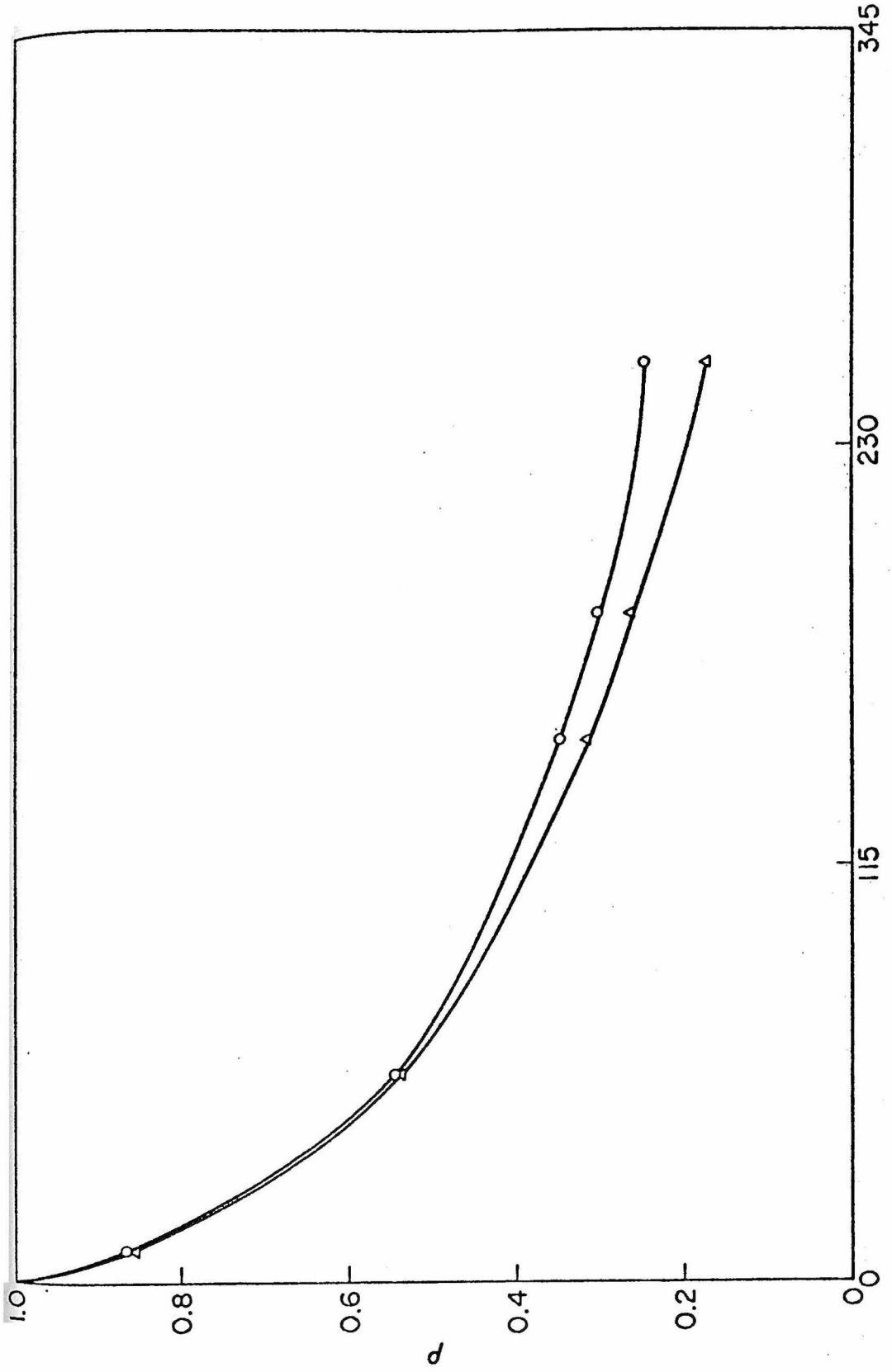

Figure 2. Effect of in situ poisoning on methanol dehydration

Run conditions: weight of catalyst 4.3 g.; temperature 170°C;
(o) c_A = 0.006; (Δ) c_A = 0.022

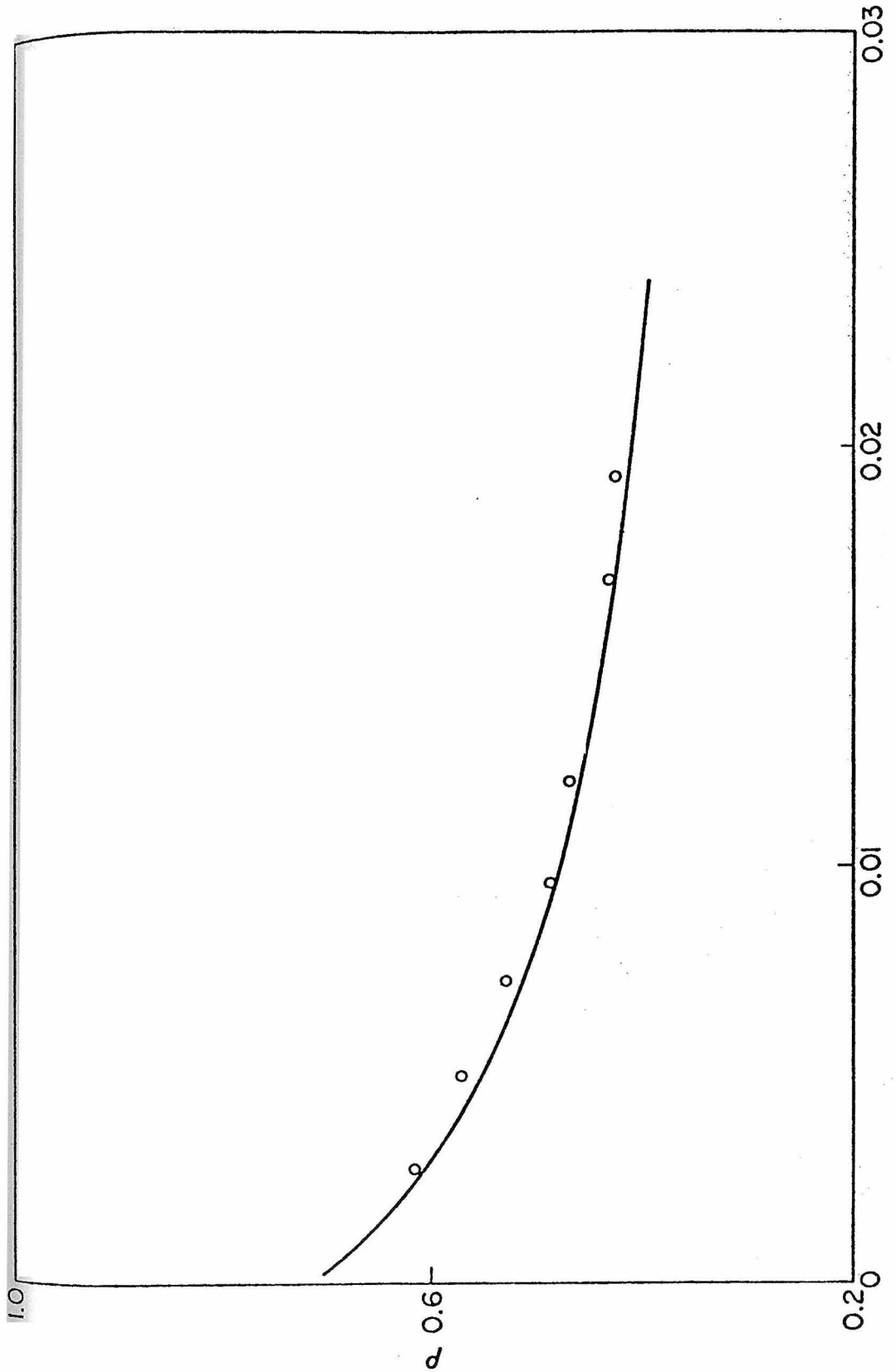

Figure 3. Effect of water on ρ for methanol dehydration

Run conditions: c_A = 0.0102; T = 170°C

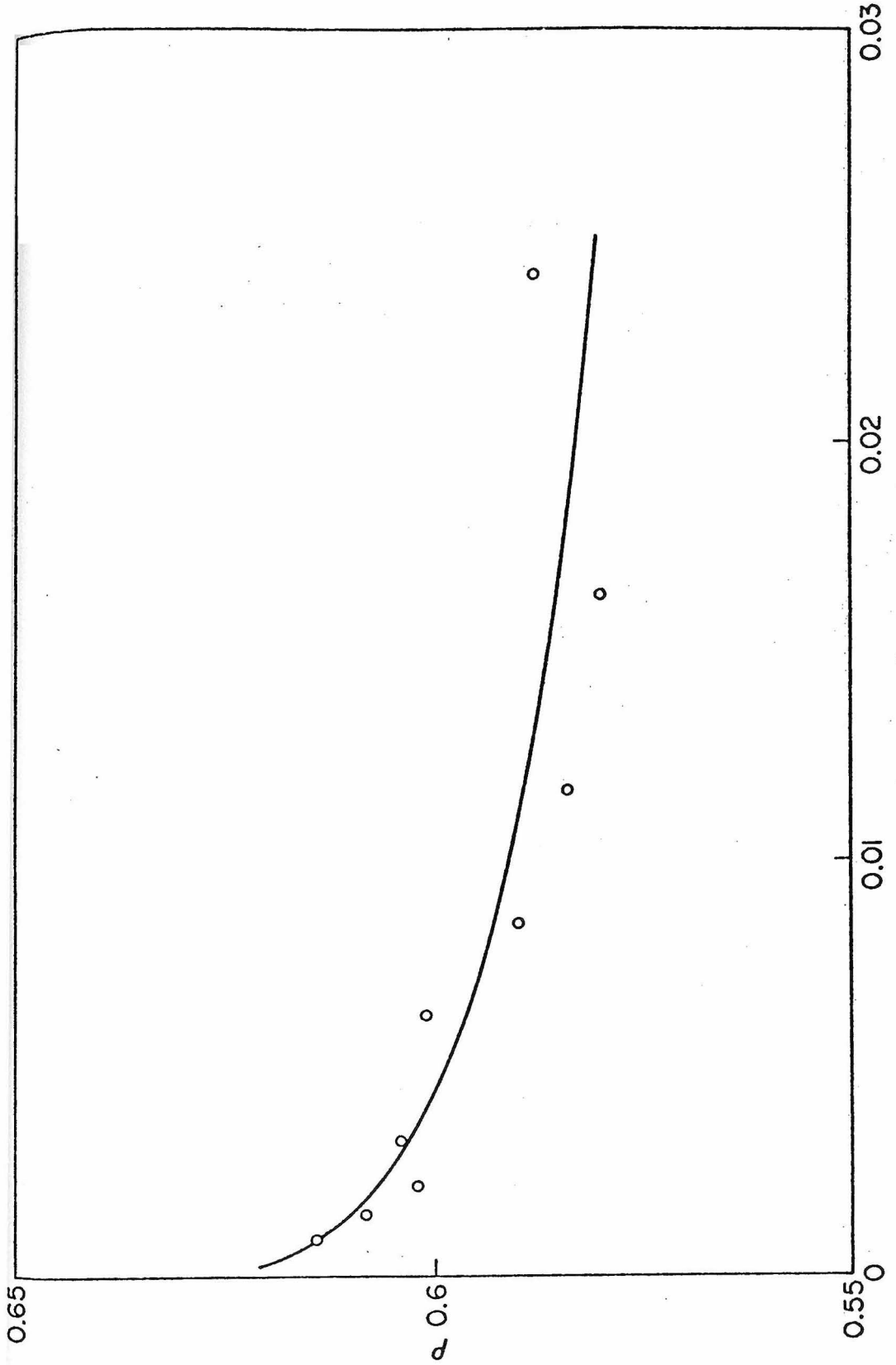

Figure 4. Effect of alcohol on ρ for methanol dehydration

Run conditions: c_W (feed) = 0.00025; T = 160°C

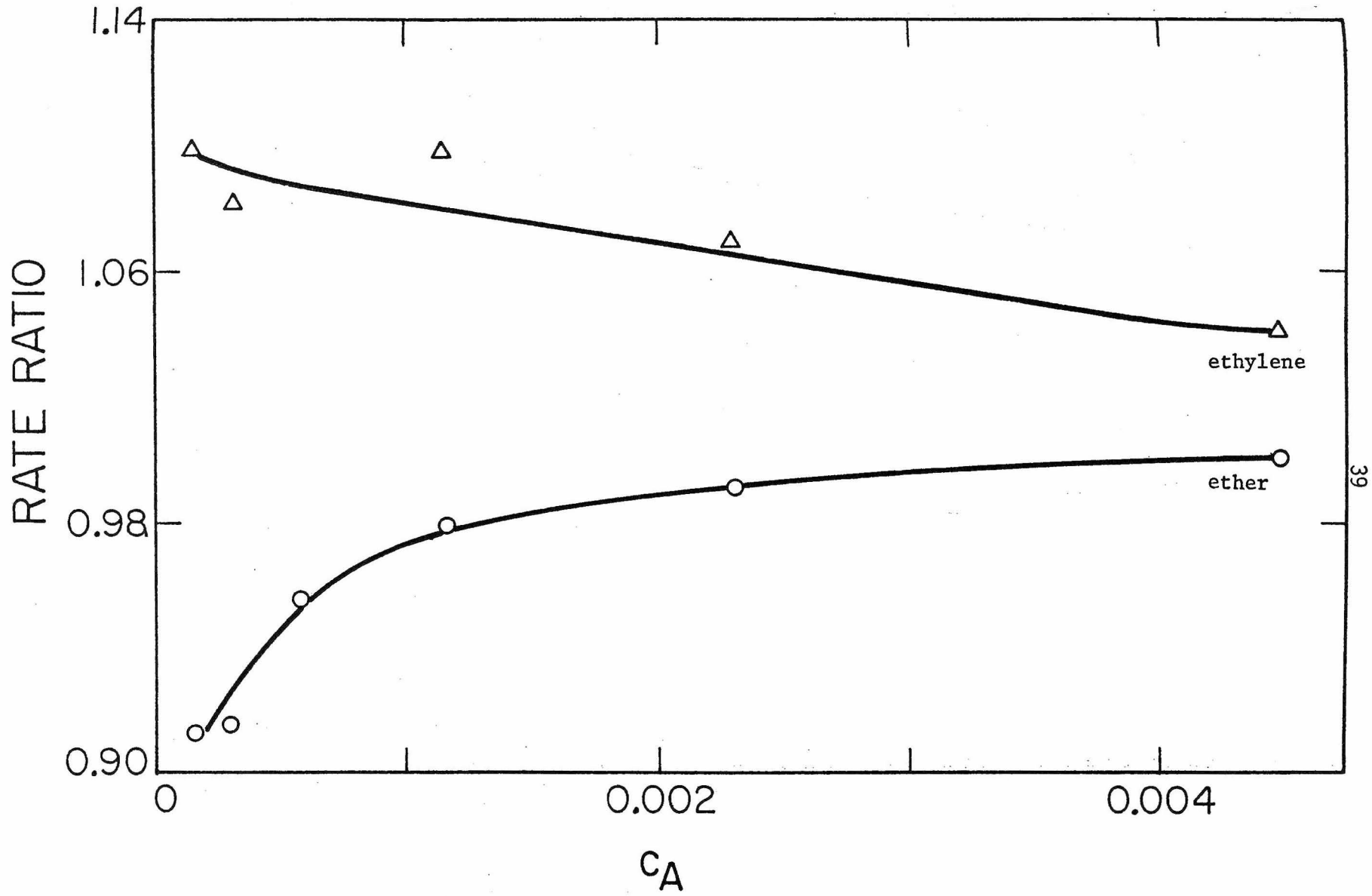

Figure 5. Directional effects in dehydration of ethanol

Run conditions: T = 170°C; c_W (feed) = 0

Rate ratio = (reverse rate)/(forward rate)

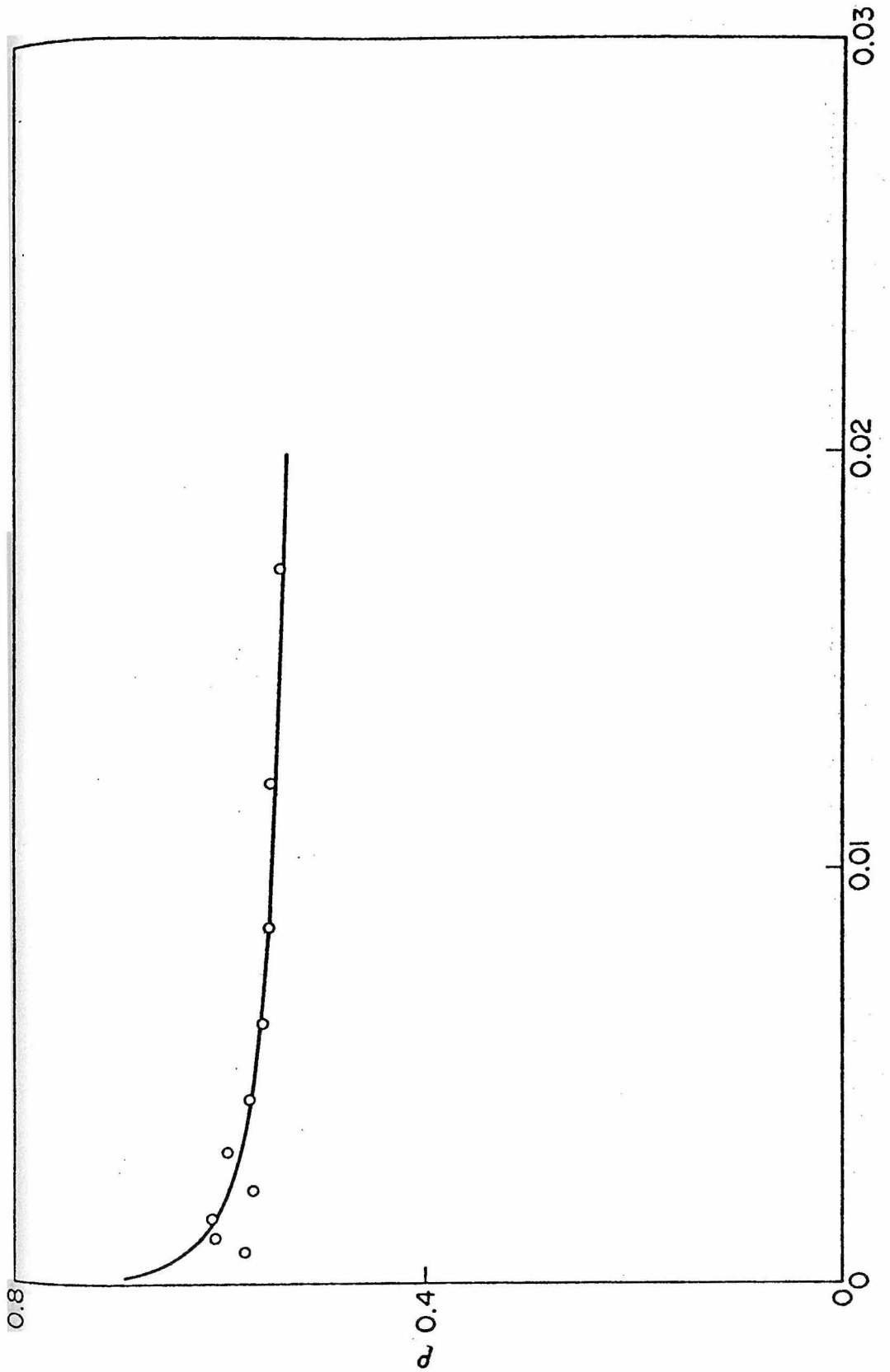

Figure 6. Effect of alcohol on ρ for ethylene formation

Run conditions: C_W (feed) = 0; T = 155°C

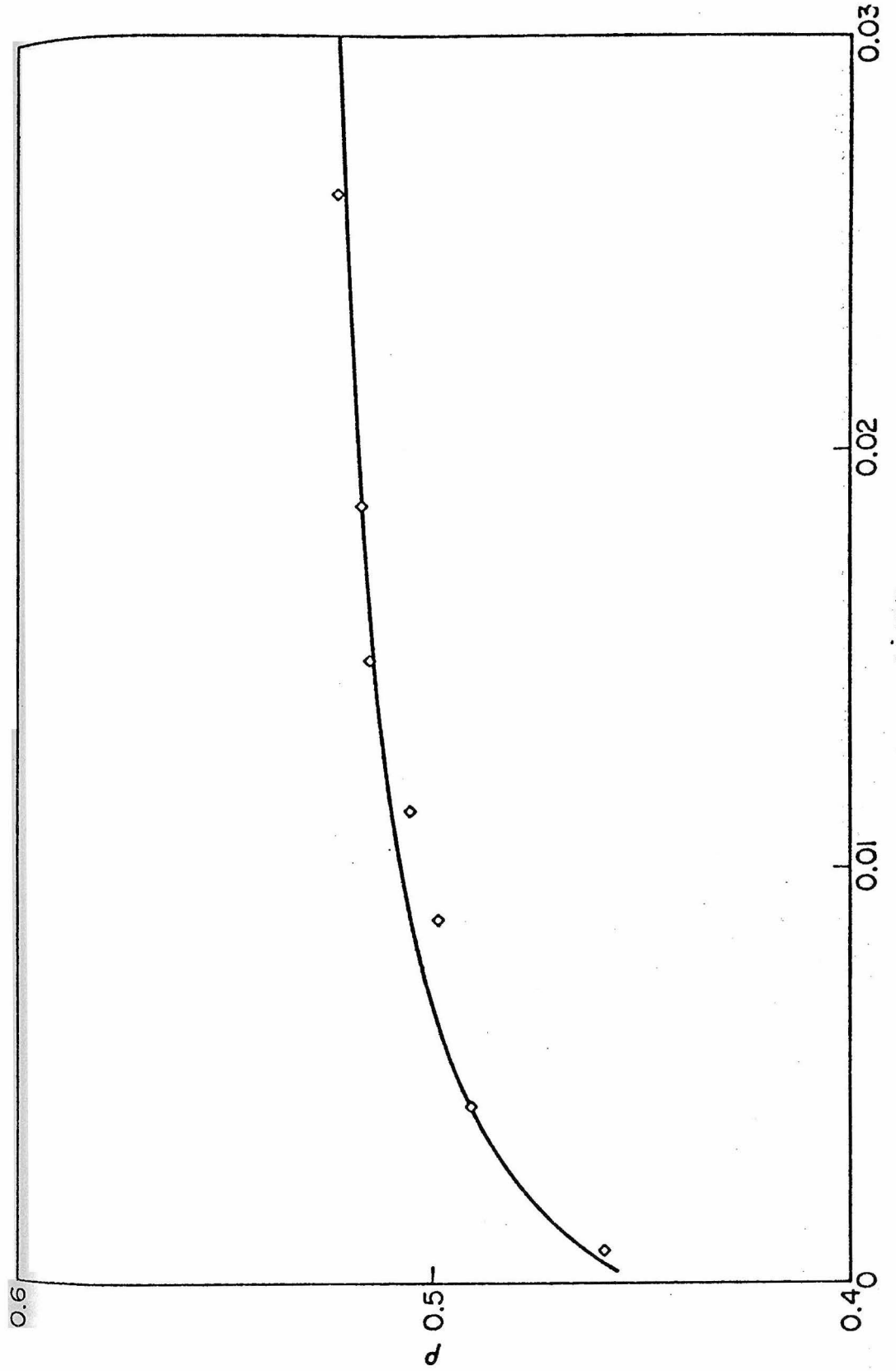

Figure 7. Effect of water on ρ for ethylene formation

Run conditions: c_A = 0.0128; T = 155°C

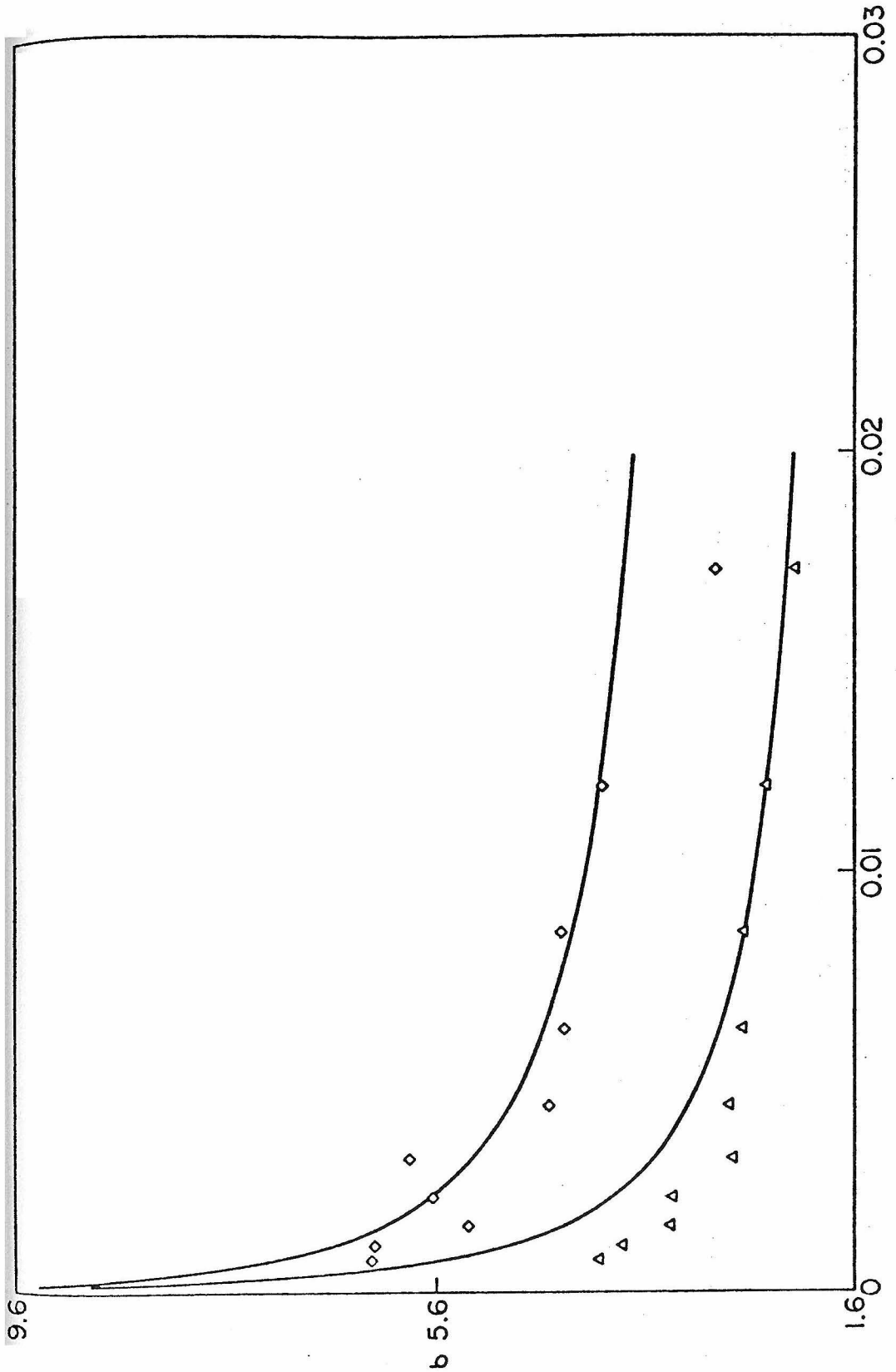

Figure 8. Effect of alcohol on selectivity σ

Run conditions: c_W (feed) = 0; T = 155°C;
(△) fresh catalyst; (◇) poisoned catalyst

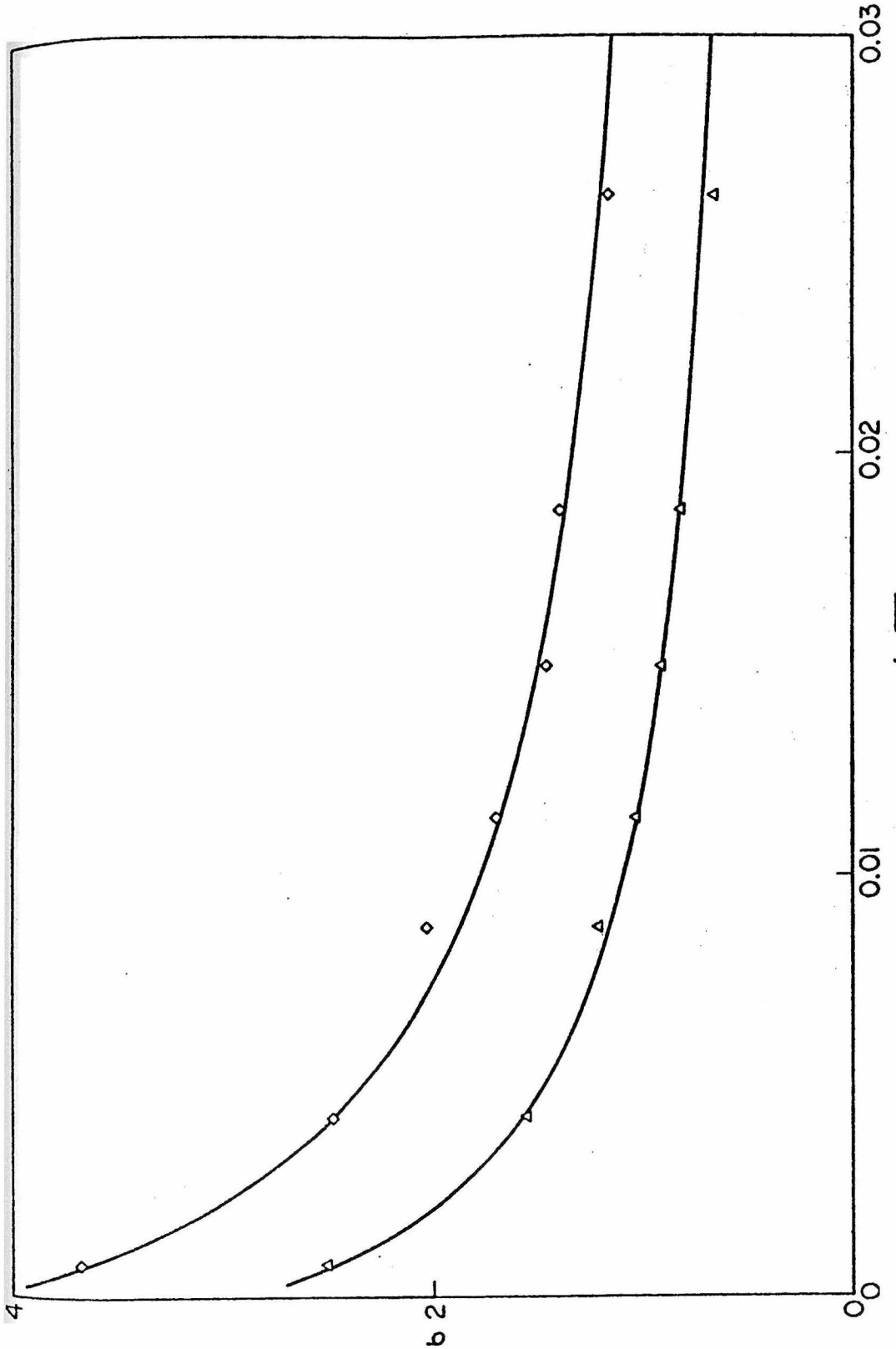

Figure 9. Effect of water on selectivity σ.

Run conditions: c_A = 0.0128; T = 155°C;
(△) fresh catalyst; (◇) poisoned catalyst

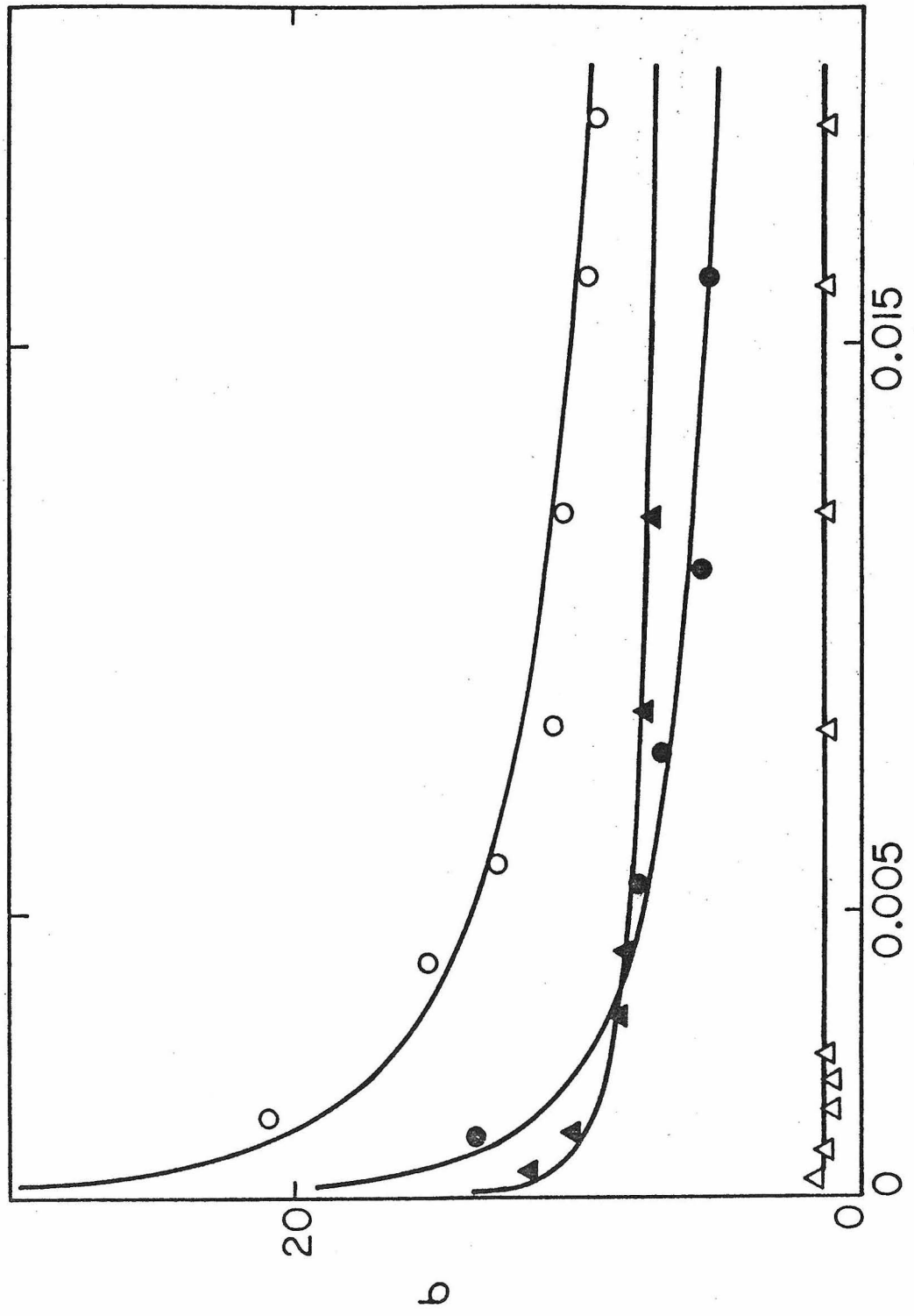

Figure 10. Effect of alcohol concentration on σ for various catalysts
Run conditions: C_W(feed) = 0; T = 225°C
(o) KSFO; (●) F49
(▲) AHC ; (Δ) F1

III.

Characterization of Acid-Base Catalysts by Calorimetric Titration

I. Correlation with Alcohol Dehydration Activity

K. R. Bakshi and G. R. Gavalas*

Division of Chemistry and Chemical Engineering
California Institute of Technology
Pasadena, California 91125

ABSTRACT

Several commercial aluminas, silica-aluminas and clays are characterized by calorimetric titration with n-butylamine and trichloroacetic acid. The heat of adsorption distributions obtained by titration are found to be sufficient measures of surface acidity and basicity in correlating catalyst activity towards alcohol dehydration. A correlation is obtained by dividing the distributions into groups of suitable acidic and basic site pairs, and assigning to each group a specific reaction rate by least-squares fitting with the observed rates of dehydration. The correlation describes well both olefin and ether formation and provides support for a reaction mechanism proposed in the literature.

*To whom correspondence should be directed.

INTRODUCTION

Catalyst development and utilization requires information about the dependence of the catalyst activity and selectivity on the state of the catalyst as well as the modification of the catalyst state due to pretreatment and deactivation processes. Such an interrelation between pretreatment or deactivation, catalyst state, and reaction kinetics presupposes, above all, a suitable and reproducible method of catalyst characterization. Site density or surface area has served as one important parameter characterizing various catalysts but is clearly insufficient for catalysts possessing sites of various strengths. A proper characterization includes specification of a strength parameter along with corresponding capacity parameter thus resulting in a site strength distribution characteristic of the catalyst state.

Acidic catalysts such as alumina, silica-alumina and zeolites display a particularly wide variation in site strength and have been studied by a number of different methods. A review of the methods for the determination of the surface acidity distribution has been given by Tanabe (1970).

Originally reported by Walling (1950) and Benesi (1957), a colorimetric titration of acidic catalysts with an n-butylamine solution using a variety of Hammett indicators has been extensively employed by many workers. Hirschler (1963) improved upon these titrations by using H_R indicators and showed that Hammett indicators fail to resolve acidities of catalysts with different activities. Both these titrations characterize the catalyst surface in terms of an acidity distribution divided into distinct groups of acidic strengths equivalent to the acidity constants of the various indicators employed. The titre value within each group serves as a capacity

parameter to represent the site density possessing the corresponding group strength.

Adsorption of a gaseous base such as ammonia followed by evacuation of the catalyst at various temperatures (Webb, 1957) or a differential thermal analysis (Bremer et al., 1968) has also been employed to characterize acidic catalysts. The evacuation temperature and the amount of base retention serve as the strength and capacity parameter respectively. Amenomiya et al. (1967) have developed a temperature programmed desorption technique to obtain site strength in terms of desorption temperature. Topchieva (1964) and Tanabe et al. (1966) developed calorimetric titrations to obtain the total acidity of various catalysts by measuring the heat of adsorption of a base. The heat of adsorption and the titre values serve as the strength and capacity parameters respectively.

Although all these methods have been employed to characterize acidic catalysts, some of them show distinct limitations when used in certain specific cases. The thermal adsorption-desorption techniques are restricted to thermally stable gaseous bases and hence are useful in characterizing the catalysts possessing relatively weak sites only. Since the colorimetric titrations depend upon visual changes of indicator colors, they cannot be easily employed in characterizing colored acidic catalysts. Moreover, the color changes for some of the Hammett indicators are not easily perceptible, thereby introducing uncertainty in results (Drushel et al., 1966).

In conjunction to their acidic sites, the catalysts under discussion possess basic sites (Peri, 1965) which play an important role in certain reactions such as alcohol dehydration (Pines et al., 1968; Bakshi and Gavalas, 1974). The characterization of the basicity using colorimetric titrations has not been possible (Tanabe, 1964) due to unavailability of

suitable indicators. Calorimetric titration on the other hand has been used successfully for estimating the total number of basic sites of a silica-alumina catalyst (Tanabe, 1966).

The most useful aspect of a catalyst characterization method is its ability to distinguish between catalysts of different activities and to correlate the activity with the capacity parameter of the catalyst. Development of such correlations have been extensively attempted for acidic catalysts using one of the methods described earlier. Polymerization of olefins (Tarama, 1962), xylene isomerization and cracking of Cumene (Covini et al., 1967), catalytic cracking (Mone et al., 1973) have all been investigated on silica-alumina and zeolites to show good correlation between the catalyst activity and the total acidity measured by amine titrations. Such correlations between catalyst activity and acidity have been reviewed by Tanabe (1970). Most of the correlations employ either total acidity or acidity above certain indicator levels to represent the total number of active sites. The contribution of the various sites is assumed to be the same, independent of site strength.

Since a non-uniform catalyst owes its activity to sites having distinctly different strengths, the contribution from various sites is not expected to be identical. Yoneda (1967) has attempted to correlate activity of non-uniform catalysts for olefin oligomerization by employing amine titrations to characterize acidity distributions. Investigating a sufficient number of comparable catalysts, he has obtained the relative activity of sites having different acidic strength. It must be noted that most of the aforementioned correlations were developed for single reactions and have not attempted to correlate catalyst selectivity in the case of competitive reactions.

The present work is concerned with the characterization of acid-base catalysts in terms of their acidity and basicity distributions and attempts to correlate their acid-base characteristics with their activity for the dehydration of methanol and ethanol. The dehydration of alcohols by alumina and silica alumina has been studied extensively (Winfield, 1960; Pines and Manassen, 1966; Figueras, 1971). The reactions have been shown to require basic as well as acidic sites (Figueras, 1971) therefore the present work has emphasized the distribution of both functions. Among various methods of catalyst characterization, calorimetric titration providing the heat of adsorption as a function of coverage has been found to be the most convenient as a measure of the acidity and basicity distributions. Since the dehydration of ethanol provides ethylene and ether, the correlation developed here includes the catalyst selectivity as well as its activity.

EXPERIMENTAL

1. Reagents: Reagent grade methanol, ethanol and n-butylamine were used without further purification. Reagent grade benzene was dried by percolation over a molecular sieve bed before use. Anhydrous ammonia, supplied by Mathesan Gas Products, was used without further purification.

2. Catalysts: Commercial catalysts used for this investigation are shown in Table 1. The pelleted catalysts were finely crushed and fractionated under dry nitrogen to prevent contamination. All catalyst samples were pre-treated at 300°C under dry nitrogen for five hours and stored under dry conditions before use.

Two of the commercial catalysts, KSFO and AHC, were impregnated with MgO using aqueous solution of magnesium acetate followed by calcining at 500°C for four hours.

3. Activity Measurements: Evaluation of catalyst activity for alcohol dehydration was carried out in a differential microreactor suspended in a well-mixed air bath. The reactor temperature was maintained within ± 0.2°C of the reported values by a proportional temperature controller. Alcohol, fed by a multi-speed infusion pump, was vaporized and mixed with dry nitrogen to attain the desired feed concentration. The reaction products were analyzed by a flame ionization detector after separation on a 10% Carbowax 20m column. The details of the experimental set-up are described elsewhere (Bakshi and Gavalas, 1974).

4. Ammonia Adsorption Capacity: Thermogravimetric analysis was employed to quantitatively obtain the ammonia adsorption capacity of various catalysts. A 950 DuPont TGA system was used to determine the decrease in weight of a catalyst sample upon thermal desorption at various temperatures. The TGA

assembly was flushed at room temperature with flowing helium for two hours and about 30 ∿ 50 mg. of powdered catalyst sample was placed in the sample pan of the TGA. The catalyst sample was heated to 500°C under flowing dry helium, was maintained at that temperature for one hour, and was subsequently cooled to room temperature under dry helium. The sample was then saturated with ammonia by passing anhydrous ammonia for two hours until no further increase in weight could be recorded. After discontinuing the ammonia flow, the TGA chamber was flushed with helium and the temperature of the sample was raised and maintained at 150°C under dry helium till no further weight decrease due to ammonia desorption could be detected. This procedure was repeated at 50°C temperature increments up to 500°C and the sample weight was continuously recorded. This procedure enabled an estimation of the ammonia adsorption capacity of various catalysts at different temperatures.

5. Rate Recovery Experiments: The partial recovery of activity attendant upon thermal desorption of a weak poison such as ammonia was used as another characterization of various catalysts. The catalyst sample was pretreated to 500°C, as indicated earlier, and was subsequently cooled to 100°C. Ammonia diluted with dry nitrogen was passed over the catalyst for four hours to completely saturate the sample at that temperature. The flow of ammonia was then discontinued and the catalyst was heated to a higher temperature under dry nitrogen flow. The thermal desorption was carried out for two hours after which the activity of the catalyst for alcohol dehydration reaction was measured in the flow microreactor. This procedure was repeated at different desorption temperatures for all catalysts.

6. Calorimetric Titrations: In principle, calorimetric titrations involve

measurements of heat of adsorption of a liquid reactant as a function of the amount adsorbed. In the present study the calorimetric assembly consisted of a Dewar flask equipped with a Beckman thermometer, a magnetic stirrer and a microburette, and was insulated with a thick cork. About 3 ∿ 5 g. of powdered, pretreated catalyst was placed in 100 ml. dry benzene in the Dewar flask and stirred. The contents of the calorimeter were allowed to equilibrate with the surroundings for about one hour before the titrations. The temperature rise due to stirring was read at definite time intervals. The titrations were carried out by stepwise addition of aliquots (0.3 ∿ 0.5 ml.) of a standardized reactant from a microburette. The bath temperature was read every 30 seconds for about 10 ∿ 15 minutes after each addition. The total rise in temperature was corrected for the slight contribution from stirring to give the rise due to the heat of adsorption. The latter temperature rise was observed to level off after about two to three minutes after each addition.

The above procedure was repeated with subsequent increments of reactant additions till no temperature rise due to heat of adsorption could be observed. The standardized reactant solutions used were 0.909 M n-butylamine in dry benzene for acidity measurements and 0.44 M trichloroacetic acid in dry benzene for basicity measurements. The heat capacity of the calorimeter and its contents was evaluated by measuring the temperature rise in 10 minutes due to passage of a d.c. electric current through a nichrome wire heater immersed in the calorimeter. The energy input in this time interval was estimated from voltage drop measurements across the nichrome heater and a 1.69 ohm standard resistor in series with the heater.

A theoretical estimation of the time required for liquid phase diffusion in porous catalysts was carried out by a procedure described by

Satterfield (1970) using an effective tortuosity factor of 6 and porosity of 0.4 for the powdered catalysts. The estimated value of the diffusion coefficient was 2×10^{-6} cm^2/s with a corresponding characteristic diffusion time of one to two minutes for 100 micron particles. It follows that the observation time of 10-15 minutes for each incremental titre addition is sufficient for completion of chemisorption provided the kinetics of chemisorption is not rate limiting.

RESULTS

1. Activity Measurements: The activity of various commercial catalysts for dehydration of methanol and ethanol was measured under identical conditions of feed concentration and temperature. The only products observed were dimethyl ether during methanol dehydration and diethyl ether and ethylene during ethanol dehydration. The rates of formation of various products listed in Table 2 show wide variations of activity and selectivity among the nine catalysts tested.

2. Ammonia Adsorption Capacity: Since the dehydration activity of the catalysts tested is known to be impaired by chemisorption of ammonia and organic bases, a correlation was attempted between the ammonia adsorption capacity and the activity of the catalysts. The results of the thermogravimetric analysis of F49, AHC and F1 catalysts are shown in Table 3 in terms of ammonia retained at various temperatures. The adsorption capacity of a catalyst sample at a given desorption temperature is evaluated from the difference in weight of the sample at that temperature and the weight of the dry catalyst at 500°C. The results in Table 3 indicate that ammonia adsorption capacity at temperatures above 250°C is in the order F49 > AHC > F1. As shown in Table 2, the activity for both ether and olefin formation follows the same order. The result is not surprising since the ammonia retained at higher desorption temperatures is attached to the stronger sites which are expected to make the major contribution to the dehydration reactions. Although reactivity and ammonia adsorption capacity maintain the same order among the catalysts, a quantitative correlation between the two properties does not appear feasible in view of the fact that reactivity varies much more rapidly than ammonia adsorption capacity. For example, F49 shows a thousand-fold activity for olefin formation as compared to F1,

while the corresponding ammonia adsorption capacity ratio is only two even for the strongest sites measured at 450°C. A further desorption at temperatures above 500°C may perhaps be required to provide a significant distinction between the two catalysts. Furthermore, although the catalytic activities for both ether and olefin formation follow the same qualitative order as that of acidity evaluated in terms of ammonia adsorption capacity, the relative variations in the selectivity shown in Table 2 indicate that the catalyst characterization follows different correlative patterns for the two dehydration reactions.

3. Rate Recovery Experiments: The relative recovery of catalyst activity attendant upon desorption of ammonia at various desorption temperatures is reported in Table 4 for F49, AHC and F1 catalysts. The activity recovery at all desorption temperatures follows the order F1 > AHC > F49 for both ether and olefin formation, thus indicating that weaker sites are responsible for the activity of F1 whereas much stronger sites are responsible for the activity of F49. These results show the same trend with the relative activities of these catalysts as shown in Table 2 as well as with the ammonia adsorption capacity as shown in Table 3. The relative recovery pattern for olefin formation in comparison with ether formation for all catalysts tested indicate that the effect of ammonia adsorption is larger on ethylene than on ether formation at all desorption temperatures. From the difference in relative recovery rates between two successive desorption temperatures, it is apparent that the stronger acidic sites contribute more to the activity than the weaker sites. Any attempt at a characterization of these catalysts would thus involve the intrinsic heterogeneity of the catalyst surface in terms of its acidity distribution.

4. Calorimetric Titrations: Calorimetric titration of solid catalysts against standard reagents involves evaluation of heat of adsorption from a knowledge of heat capacity of the calorimetric system and the temperature rise upon addition of a differential amount of the reagent to the calorimeter. The heat release thus calculated represents an average heat of chemisorption for the amount of reagent added. The titration results are thus obtained as average differential heats of chemisorption for successive equal additions of the reagent. The results for various catalysts titrated are as follows:

a. Acidity Distribution: The calorimetric titrations for acidity measurements are reported in terms of heat of adsorption of n-butylamine solution at room temperature. A representative set of differential heat of adsorption curves is shown in Figure 1 for some of the catalysts. Invoking an assumption that chemisorption of n-butylamine on a stronger acidic site results in a higher heat of adsorption, the acidic strength of these catalysts can be arranged in the order KSFO > F49 > AHC > F1. Since the same order is exhibited in their relative activities (Table 2), the acidity measurements obtained through calorimetric titrations appear to provide a good method for catalyst characterization.

In order to obtain a quantitative correlation between the acidity distribution and the relative activities of the various catalysts, the differential heat curves are divided into groups each of which spans a range of heats of adsorption as indicated in Figure 1. The limits of each group are selected by an inspection of the relative activities of various catalysts. Table 5 shows the acidity distributions in terms of groups A_1 - A_5 of Figure 1. Assuming that all acidic sites contribute to the catalytic

activity and that the relative contributions depend upon the strength of the acidic sites, there appears to be a general qualitative agreement between the relative activities (Table 2) and the acidity distributions shown in Table 5.

The acidity distributions follow the same order as the ammonia adsorption capacity of F49, AHC and F1 catalysts. The results obtained in the rate recovery experiments are also in good qualitative agreement with the acidity distributions of Table 5 in that the weaker sites of F1 show higher rate recovery upon thermal desorption of ammonia as compared to the AHC and F49 catalysts.

Before proceeding further we may note certain properties of the acidity distributions that are important in the group analysis given below. For all the catalysts titrated, the differential heat curves are concave in nature, indicating a decrease in differential heat of adsorption upon subsequent additions of n-butylamine. This effect may result from either inherent heterogeneity of the catalyst surface or from the effect of previously adsorbed n-butylamine which may render the neighboring acidic sites weaker by induction. Since the surface induction effect would be expected to be different for other bases, a partial titration of the catalyst to a known extent by a stronger base such as KOH, followed by calorimetric titration with n-butylamine, is generally expected to result in a complementary acidity distribution only if the inductive effect is insignificant during these titrations. The results from Table 5 indicate that upon partial titration of KSFO with 0.12 mmol/g. of KOH, an equivalent number of strong acidic sites of A_2 are destroyed as measured by n-butylamine titrations. The complementary nature of these titrations suggest that the

variations in differential heat curve with coverage results from the inherent surface heterogeneity and not from the surface induction effect of previously adsorbed n-butylamine. This important issue certainly requires further investigation.

b. Basicity Distributions: The basicity measurements of various catalysts obtained by calorimetric titrations are reported in terms of differential heats of adsorption of trichloroacetic acid. A representative set of differential heat curves is shown in Figure 2 for some of the catalysts. The variation in the differential heat of adsorption with successive additions of the reactant indicates the heterogeneity of the catalyst surface. As in the case of the acidity distributions, the differential heat curves for basicity have been divided into groups of basicities as indicated in Figure 2, and the basicity distributions thus obtained are shown in Table 6. The presence of MgO in impregnated catalysts and in F49 is evidently related to the strong basicities of these catalysts. In agreement with observations reported recently by Figueras et al. (1971), the γ-alumina T126 and F1 possess stronger basicity than silica-alumina.

The results of acidity and basicity titrations on AHC using different amounts of stepwise additions are shown in Figure 3. The differential heat curves for acidity and basicity depicted in this figure indicate the reproducibility of the titrations.

5. Catalyst Characterization and Group Analysis: The qualitative agreement among the results obtained in ammonia adsorption experiments, rate recovery experiments, relative activities for dehydration reactions and the acid-base distributions obtained by calorimetry suggest that these characteristics could be utilized to develop a quantitative correlation for the activities

and selectivities of the catalysts tested. The surface heterogeneity suggests that the acid-base sites of each catalyst may be subdivided into groups of different strengths so that the catalytic activity observed for a given chemical reaction is a sum of contributions from all such active groups.

All the active sites within a group are assumed to contribute equally to the overall catalyst activity independently of the catalyst considered. Thus the contribution by a group i to the activity of the j^{th} catalyst is given by $(f_i\ s_{ij})$ where fi, the specific rate, depends on the strength of the group i, reactant concentration and temperature but not on the catalyst state. Under these assumptions, the overall reaction rate r_j on j^{th} catalyst of unit weight can be expressed as:

$$r_j = \sum_{i=1}^{N} f_i s_{ij} \qquad (1)$$

where N is the number of effective groups. The site density s_{ij} for each catalyst can be estimated from the strength distribution obtained by experimental methods such as calorimetric titrations. The reaction rate data for M different catalysts under identical concentration and temperature conditions, along with a detailed knowledge of their strength distributions, enable an estimate of the specific rates f_i by the method of least squares provided M, the number of catalysts tested, is larger than N, the number of groups used to correlate the catalytic activities.

6. Group Analysis for Ethylene Formation: The reaction mechanism discussed earlier (Figueras, 1971) for ethylene formation requires a dissociative chemisorption of alcohol on an acid-base site pair, where strong acidity is more effective. Since the presence of a basic site is necessary for adsorption and subsequent reaction, only those acidic sites which have

adequate basicity in their neighborhood are effective. A determination of the effective site density s_{ij} to be used for group analysis thus requires consideration of acid-base pairs of varying acidic and basic strengths. The acidity and basicity groups used for this investigation are shown in Tables 5 and 6 for various catalysts. Different models involving association of an acidic site with various basic groups alone or in combination are attempted to determine the effective s_{ij}. A set of specific rates f_i is determined by a least square fit for each model and the fit for different models are compared in terms of their residuals as shown in Table 7. The results in Table 7 imply that a model requiring an interaction between an acidic site with weak basic sites in the groups ($B_4 + B_5$) gives the best least square fit. Table 8 presents the specific rates and the comparison between observed rates and rates predicted by the group analysis. The agreement between predicted and observed rates is also shown in Figure 4. The significant variation in the specific rates substantiates the assumption that the contribution to the total activity by acidic sites weaker than the A_5 group is negligible and hence these sites need not be considered in the group analysis. The necessity of a weak basic site for dissociative chemisorption of alcohol and subsequent reaction reported earlier (Figueras et al., 1971) is reflected through a better correlative fit of the model using the basicity ($B_4 + B_5$). Table 9 shows the actual contributions by each group towards ethylene formation. Comparing the relative contribution of the group with the highest acidic strength for a given catalyst to the total observed rate on that catalyst, it is apparent that almost all catalysts tested owe above 90% of their olefin formation activity to their strongest acidic group, with the exception of KSF and ALC catalysts. Even

in these two catalysts, the contribution by their strongest acidic group is above 75% of the total activity for olefin formation.

7. Group Analysis for Ether Formation: In contrast to the mechanism for olefin formation, the formation of ether has been suggested to involve the interaction between a dissociatively adsorbed alcohol intermediate with a surface alkoxide and involves two acid-base site pairs with strong basicity required for alkoxide formation (Figueras, 1971). An attempt at applying group analysis to ether formation would thus require a careful consideration of the acid-base distributions while evaluating s_{ij}.

Denoting by X and Y the active sites involved in the dissociative adsorption of alcohol to a carbonium ion and an alkoxide respectively, we must investigate the acidity and basicity required in each of the two types of sites. The simplification is made that the sites X must be separated to groups X_i due to their wide variation of activities while the Y sites may be considered in a single group. Various models and their fit with the data are listed in Table 10. The models of set A assume that X_i requires acidity alone while Y requires basicity alone, in some optimal range. A comparison of the models in set A shows that $Y = B_1 + B_2$ gives the minimum residual error, thus establishing an optimal span of basicity for alkoxide formation and subsequent reaction to ether.

Since association of strong acidic sites with weak basic sites yields better correlation for ethylene formation which also requires a dissociative adsorption of alcohol, the models in set B of Table 10 explore the effectiveness of the same type of pairs in evaluating X_i. The definition of Y is again based on similar interpretation as for the models of set A. Comparison of the residuals in this set suggests that the best fit model is the

one involving alcohol adsorption on acidic sites associated with weak basic sites in the groups $(B_4 + B_5)$, i.e., $X_i = (A_i, B_4 + B_5)$, with another alcohol adsorbed as an alkoxide on basic groups $Y = (B_1 + B_2)$.

Alkoxide formation has been suggested to involve strong basic sites associated with acidic sites of suitable strength (Figueras, 1971). The models in set C hence define Y as only those $(B_1 + B_2)$ sites which are associated with an optimal acidity. The definition of X_i is that of set B. Comparison of the residuals indicates that the optimal acidity required for alkoxide formation comes from $(A_4 + A_5)$. It is thus suggested that ether formation requires interaction between two types of adsorbed alcohol molecules. One type of alcohol adsorption requires acidic sites associated with weak basic sites i.e., $X_i = (A_i, B_4 + B_5)$ and the other chemisorbed alcohol molecules requires an optimal basicity associated with weak acidity i.e., $Y = (B_1 + B_2, A_4 + A_5)$. The residual for this model is the least among all models in sets A, B or C.

A comparison of the observed rates with the rates predicted by the group analysis using the best-fit model is shown in Table 11 for diethyl ether and Table 12 for dimethyl ether formation. The specific rates reported in Tables 11 and 12 show the effect of acidic strength on f_i. The agreement between the predicted selectivity and the experimentally measured selectivity in ethanol dehydration is shown in Figure 5.

The details of group analysis showing the actual contributions by each group towards diethyl ether formation are given in Table 13. Comparing the relative contribution of the group with the highest acidic strength in each catalyst, it is apparent that with the exception of ALC, all catalysts tested owe above 85% of their ether formation activity to their strongest acidic

group. ALC owes its different behavior to a higher number of acidic sites in the A_3 group as compared to the A_2 group as shown in Table 5.

DISCUSSION

Successful application of group analysis in predicting activity and selectivity of various acid-base catalysts indicates that the relative contributions from various active groups on a catalyst depend exclusively on the number density of sites within each group. The composition or pretreatment history of the catalyst is manifested only through their effect on the site densities in each group. The quantitative correlation of catalyst activities requires a reproducible method of determination of densities and strengths in each effective group of sites.

Although ammonia adsorption capacity and rate recovery experiments exhibit the correct trend of catalytic activities, a quantitative correlation fails partially due to the weaker basicity of ammonia giving the improper resolution but more so because the basicity distributions required for the dehydration activity are not determined by these methods. Calorimetric titrations provide a better method of catalyst characterization yielding both acidity and basicity distributions which can be used for quantitative correlation of relative catalytic activities as indicated by group analysis.

Although the acid-base distributions of various catalysts are characteristics of the surface, they are dependent upon the experimental method (such as calorimetric titrations) employed in their evaluation and they can be used as a unique set of catalyst characteristics only when a standard experimental procedure is adopted. The division of these distributions into groups of different strengths is obviously not unique but is nevertheless suggested by a qualitative agreement with the relative activities of various catalysts. The value of this division is exhibited in the successful prediction of the rates of both ethylene and ether formation using the same groups for all

catalysts. The same groups with similar specific rates yield good predictions of catalytic activities for methanol dehydration.

The models employed to determine s_{ij} in group analysis appear to be in qualitative agreement with the reaction mechanism proposed for the two dehydration reactions (Figueras, 1971). Ethylene formation requires a dissociative adsorption of ethanol on a strong acidic site associated with a weaker basic site. The strong dependence of the group activity constants on acidity indicate that indeed stronger acidic sites contribute to olefin formation much more effectively than weaker sites. A model based on acidity distribution associated with weak basic sites in the group $(B_4 + B_5)$ results in a better correlative fit than a model based on acidity distribution alone, thus indicating the necessity of weak basic sites for the dissociative chemisorption and subsequent dehydration.

The estimation of the effective site density s_{ij} from the product of site densities in A_i and $(B_4 + B_5)$ inherently assumes a random distribution of acidic and basic sites on the catalyst surface independent of the catalyst composition. Imposition of any particular preference in their relative geometric distributions on the catalyst surface (such as weak acidic sites neighbored by strong basic sites) would lead to different effective site densities s_{ij}. The assumption of randomicity of site distributions leads to successful modeling of catalytic activities etc. but is by no means proven by such results.

The reaction mechanism for bimolecular dehydration of alcohols leading to ether formation requires an interaction between a dissociatively adsorbed alcohol molecule with a surface alkoxide obtained from chemisorption of another alcohol molecule on an acid-base site pair. Earlier mechanistic

evidence (Figueras, 1971) indicates that a strong basic site is effective in alkoxide formation whereas a strong acidic site is effective in the dissociative adsorption of alcohol and further dehydration. The results of the group analysis using various models to evaluate the effective site density s_{ij} indicate that the best correlative fit is obtained when s_{ij} is evaluated by the product of two separate combinations of acid-base pairs. As in ethylene formation, acidic sites A_i associated with weak basic sites (B_4 + B_5) form one combination, while the other is formed by strong basic sites in the group (B_1 + B_2) associated with weaker acidic sites in the group (A_4 + A_5). The latter combination may be interpreted to represent surface alkoxide formation which requires a strong basic site associated with a weaker acidic site. The exclusion of this combination in evaluating s_{ij} for ethylene formation is in agreement with the reported observation (Knozinger, 1968) that the surface alkoxide does not appear in the IR spectra of t-butyl alcohol (which forms only olefin upon dehydration) on silica-alumina, and hence is not expected to be an intermediate in olefin formation.

The dependence of s_{ij} for ether formation on basic sites in the groups (B_1 + B_2) associated with acidic sites in (A_4 + A_5) groups appears to explain the alkoxide formation required for the bimolecular dehydration reaction. A better correlative fit using this particular combination of basicity and acidity suggests that although a catalyst surface may exhibit basic sites stronger than (B_1 + B_2), the latter are optimal for alkoxide formation as well as subsequent reaction with the intermediate formed on A_i and (B_4 + B_5) site pair combination. Each acid-base site pair combination included in evaluation of s_{ij} represents different chemisorption steps for the two alcohol molecules and the product of these combinations required for the best

correlative fit inherently assumes a random distribution of these combinations on the catalyst surface as before.

The results of the group analysis show that for most of the catalysts tested, the main contribution to the total activity for both dehydration products comes from a single group involving the strongest acidic sites. The catalyst surface thus assumes a pseudo-homogeneous behavior for these reactions and explains the reason for obtaining the same kinetic model for the catalysts KSFO, F49, AHC and F1 reported earlier (Bakshi and Gavalas, 1974).

CONCLUSIONS

Acid-base distributions obtained by calorimetric titrations provide a useful characterization of acid-base catalysts. These distributions may be divided into groups of sites of different strengths and a group analysis may be applied to correlate the total catalytic activity and selectivity for alcohol dehydration reactions.

The specific rates for both ethylene and ether increase with the acidic strength of the group. The effective site density employed for group analysis assumes random distribution of sites on the catalyst surface and allows for certain acid-base site pair associations consistent with a previously proposed reaction mechanism.

NOMENCLATURE

A_i Acidity in i^{th} group defined by Table 5

B_i Basicity in i^{th} group defined by Table 6

f_i Specific rate for i^{th} group

r Rate of product formation, mole of product/hr-g catalyst

r_{ob} Experimentally observed rate of product formation

r_{pr} Predicted rate of product formation

r_j Rate of product formation for j^{th} catalyst

s_{ij} Effective site density in i^{th} group for j^{th} catalyst

W Amount of titer adsorbed, mmol/g. catalyst

$-\Delta H$ Heat of adsorption, kcal/mole

GREEK LETTERS

σ Selectivity defined by Table 2

σ_{ob} Experimentally observed selectivity

σ_{pr} Predicted selectivity

LITERATURE CITED

Amenomiya, Y., Cvetanovic, R. J., Advan. Catalysis, 17, 103 (1967)

Bakshi, K. R., Gavalas, G. R., AIChE Journal (Submitted for Publication, 1974)

Benesi, H. A., J. Am. Chem. Soc., 78, 5490 (1956)

Bremer, H., Steinberg, K. H., Intern. Congr. Catalysis, 4th Moscow, Preprints of Papers, No. 76 (1968)

Covini, R., Fattore, V., Giordano, N., J. Catalysis, 9, 315 (1967)

Drushel, H. V., Sommers, A. L., Anal. Chem., 38, 1723 (1966)

Figueras, F., Nohl, A., DeMourges, L., Trambouze, Y., Trans. Faraday Soc., 67, 1155 (1971)

Hirschler, A. E., J. Catalysis, 2, 428 (1963)

Knozinger, H., Buhl, H., Ress, E., J. Catalysis, 12, 121, (1968)

Mone, R., Moscou, L., J. Catalysis, 30, 417 (1973)

Peri, J. B., J. Phys. Chem., 69, 211 (1965)

Pines, H., Manassen, J., Advan. Catalysis, 16, 49 (1966)

Satterfield, C. N., "Mass Transfer in Heterogeneous Catalysis," p. 33, M.I.T. Press, Massachusetts (1970)

Tanabe, K., Yamaguchi, T., J. Res. Inst. Catalysis, Hokkaido Univ., 11, 179 (1964)

Tanabe, K., "Solid Acids and Bases," Academic Press, New York (1970)

Tarama, K., Teranishi, S., Hattori, K., Ishibashi, T., Shokubai (Tokyo), 4, No. 1, 69 (1962)

Topchieva, K. V., Moskovskaya, I. F., Dobrokhotova, N. A., Kinetics and Catalysis (USSR), (Eng. Transl.), 5, 910 (1964)

Walling, C., J. Am. Chem. Soc., 72, 1164 (1950)

Webb, A. N., Ind. Eng. Chem., 49, 261 (1957)

Winfield, M. E., "Catalysis" (Emmett, P. H., ed.), vol. 7, pp. 93-182, Reinhold, New York (1960)

Yoneda, Y., J. Catalysis, 9, 51 (1967)

Table 1

Commercial Catalysts for Alcohol Dehydration

Catalyst Code	Supplier	Chemical Composition
KSF	Chemetron Corporation	Acid treated montmorillonite clay
KSFO	Chemetron Corporation	Acid treated montmorillonite clay
F49	Filtrol Corporation	74% SiO_2 17.5% Al_2O_3 4.5% MgO
AHC	American Cyanamid Company	75% SiO_2 25% Al_2O_3
ALC	American Cyanamic Company	87% SiO_2 13% Al_2O_3
T-126	Chemetron Corporation	Activated γ-Alumina
F1	Aluminum Company of America	γ-Alumina

Table 2

Dehydration Activity of Various Catalysts

Catalyst	Rate of Product Formation[1] Dimethyl Ether ($r \times 10^3$)	Ethylene ($r \times 10^4$)	Diethyl Ether ($r \times 10^3$)	Percentage Selectivity[2] σ
KSFO	30.98	105.3	29.9	14.97
KSFO + M[3]	25.1	62.4	24.0	11.50
KSF	3.05	33.8	2.98	36.20
F49	12.47	26.9	14.20	8.65
ALC	3.25	5.66	2.39	10.60
AHC	2.00	1.10	1.30	4.06
AHC + M[3]	2.69	1.00	1.54	3.15
T126	4.58	0.105	2.27	0.23
F1	0.197	0.027	0.129	1.04

1 Experimental Conditions:

Reaction temperature: $200^{o}C$
Feed methanol concentration: 6.77×10^{-3} moles/liter
Feed ethanol concentration: 6.64×10^{-3} moles/liter

2 Selectivity σ is defined by

$$\sigma = \frac{\text{Amount of ethanol converted to ethylene}}{\text{Total ethanol conversion}} \times 100$$

3 Catalysts + M denote impregnated catalysts

Table 3

Ammonia Adsorption Capacity of Various Catalysts

Desorption Temperature °C	Mmol. of Ammonia Retained/g. catalyst		
	F49	AHC	F1
400	0.2522	0.1582	0.1188
350	0.5156	0.3640	0.1422
300	0.7408	0.5974	0.2633
250	0.9343	0.8655	0.4197
200	1.1471	1.1742	0.6102
150	1.4700	1.5452	0.8572

Table 4

Activity Recovery for Various Catalysts

Desorption Temperature °C	Percentage Activity Recovery[1]					
	F49		AHC		F1	
	Ethylene	Ether	Ethylene	Ether	Ethylene	Ether
200	2.08	4.35	28.97	49.00	71.30	89.92
250	2.64	4.50	32.35	66.57	**	**
300	5.62	11.60	40.00	74.79	87.04	97.67
350	14.50	23.40	46.20	77.38	97.80	99.00
400	26.80	33.80	59.70	87.25	**	**
465	47.50	70.00	97.80	98.87	**	**

** Data not available

1 Experimental conditions:

Alcohol feed concentration: 6.64×10^{-3} moles/liter
Reaction temperature: 200°C

Table 5

Acidity Distributions of Various Catalysts

Catalyst	Acidity[1] mmol/g catalyst				
	A_1	A_2	A_3	A_4	A_5
KSFO	0.0	0.24	0.05	0.04	0.06
KSFO + M	0.0	0.21	0.06	0.05	0.11
KSF	0.033	0.037	0.015	0.012	0.015
F49	0.0	0.136	0.104	0.06	0.09
ALC	0.0	0.02	0.22	0.08	0.13
AHC	0.0	0.0	0.24	0.08	0.15
AHC + M	0.0	0.0	0.22	0.05	0.07
T126	0.0	0.0	0.0	0.168	0.184
F1	0.0	0.0	0.0	0.0	0.20
KSFO + 0.12 KOH[2]	0.0	0.115	0.055	0.05	0.08

1 Acidity groups are defined by heat of adsorption included between limits as follows:

A_1: $26 < -\Delta H$; A_2: $19 < -\Delta H < 26$;

A_3: $16 < -\Delta H < 19$; A_4: $14 < -\Delta H < 16$;

A_5: $11 < -\Delta H < 14$

2 KSFO titrated with 0.12 mmol/g. catalyst KOH in aqueous solution before pretreatment

Table 6

Basicity Distribution of Various Catalysts

Catalyst	Basicity[1] mmol/g. catalyst				
	B_1	B_2	B_3	B_4	B_5
KSFO	0.0	0.22	0.15	0.13	0.045
KSFO + M	0.12	0.03	0.05	0.09	0.035
KSF	0.0	0.05	0.03	0.02	0.050
F49	0.11	0.09	0.09	0.06	0.025
ALC	0.0	0.06	0.21	0.06	0.03
AHC	0.0	0.044	0.014	0.041	0.03
AHC + M	0.035	0.08	0.014	0.03	0.04
T126	0.066	0.064	0.06	0.06	0.04
F1.	0.04	0.045	0.144	0.19	0.03

1 Basicity groups are defined by heat of adsorption included between limits as follows:

B_1: $11 < -\Delta H < 13$; B_2: $9 < -\Delta H < 11$;
B_3: $7 < -\Delta H < 9$; B_4: $5 < -\Delta H < 7$;
B_5: $4 < -\Delta H < 5$;

Table 7

Determination of Best Model Fit for Ethylene Formation

s_{ij}	sum of weighted residual χ^2*
A_i	0.444
$A_i * (B_5)$	0.0618
$A_i * (B_4 + B_5)$	0.0045
$A_i * (B_3 + B_4 + B_5)$	0.630
$A_i * (B_2 + B_3 + B_4 + B_5)$	0.395
$A_i * B_{total}$	0.292

* sum of weighted χ^2 is evaluated by:

$$\chi^2 = \sum_j \frac{\left(r_{observed,\ j} - r_{predicted,\ j}\right)^2}{r_{observed,\ j}}$$

Table 8

Group Analysis Fit for Ethylene Formation

Catalyst	Predicted Rate by Group Analysis[1] $r \times 10^4$	Observed Rate $r \times 10^4$
KSF	33.8	33.8
KSFO	100.5	105.3
KSFO + M	62.96	62.40
F49	28.1	26.9
AHC	1.11	1.10
AHC + M	0.993	1.00
T126	0.105	0.105
F1	0.027	0.027
ALC	5.576	5.66

1 Specific rates for best model fit are:

$f_1 = 11933.7$ $f_2 = 2379$ $f_3 = 63.01$

$f_4 = 5.608$ $f_5 = 0.614$

Table 9

Details of Group Analysis for Ethylene Formation

Catalyst	Group Contributions ($r_{ij} \times 10^4$)				
j	$f_1 s_{1j}$	$f_2 s_{2j}$	$f_3 s_{3j}$	$f_4 s_{4j}$	$f_5 s_{5j}$
KSF	27.44	6.37	0.07	0.008	0.0008
KSFO	-	99.92	0.56	0.04	0.006
KSFO + M	-	62.45	0.48	0.036	0.007
F49	-	27.50	0.57	0.03	0.005
AHC	-	-	1.073	0.033	0.006
AHC + M	-	-	0.975	0.02	0.003
T126	-	-	-	0.094	0.011
F1	-	-	-	-	0.027
ALC	-	4.282	1.25	0.042	0.006

Table 10

Best Model Fit for Diethyl Ether Formation

	X_i	Y	sum of weighted residual χ^2
Set A			
	A_i	1.0	0.349
	A_i	(B_1)	4.008
	A_i	$(B_1 + B_2)$	0.287
	A_i	$(B_1 + B_2 + B_3)$	1.209
	A_i	$(B_1 + B_2 + B_3 + B_4)$	0.903
	A_i	B_{total}	0.742
Set B			
	$(A_i) * (B_4 + B_5)$	(B_1)	4.02
	$(A_i) * (B_4 + B_5)$	$(B_1 + B_2)$	0.409
	$(A_i) * (B_4 + B_5)$	$(B_1 + B_2 + B_3)$	1.371
Set C			
	$(A_i) * (B_4 + B_5)$	$(B_1 + B_2) * (A_5)$	0.0256
	$(A_i) * (B_4 + B_5)$	$(B_1 + B_2) * (A_5 + A_4)$	0.0215
	$(A_i) * (B_4 + B_5)$	$(B_1 + B_2) * (A_5 + A_4 + A_3)$	0.0749

Sum of weighted residual is evaluated by:

$$\chi^2 = \sum_j \left[\frac{r_{ob,j} - r_{pr,j}}{r_{ob,j}} \right]^2$$

s_{ij} is calculated from (X_i, Y) for j^{th} catalyst

Table 11

Group Analysis Fit for Diethyl Ether Formation

Catalyst	Predicted Rate[1] $r \times 10^3$	Observed Rate $r \times 10^3$
KSF	2.98	2.98
KSFO	32.04	29.9
KSFO + M	22.30	24.0
F49	13.53	14.20
AHC	1.267	1.20
AHC + M	1.493	1.54
T126	2.267	2.27
F1	0.129	0.129
ALC	2.59	2.39

1 Specific rates for best model fit are:

$f_1 = 914797$ $f_2 = 32852.1$ $f_3 = 6322.86$

$f_4 = 2778.07$ $f_5 = 172.44$

Table 12

Group Analysis for Methanol Dehydration

Catalyst	Predicted Rate[1] ($r \times 10^3$)	Observed Rate ($r \times 10^3$)
KSF	3.05	3.05
KSFO	30.53	30.98
KSFO + M	21.6	25.1
F49	13.88	12.47
AHC	2.01	2.00
AHC + M	2.34	2.69
T126	4.54	4.58
F1	0.197	0.197
ALC	3.620	3.25

1 Specific rates for best model fit are:

$f_1 = 937827$ $f_2 = 30046.5$ $f_3 = 9586.5$

$f_4 = 5613.8$ $f_5 = 263.32$

Table 13

Details of Group Analysis for Ethyl Ether Formation

Catalyst	Group Contribution ($r_{ij} \times 10^3$)				
j	$f_1 s_{1j}$	$f_2 s_{2j}$	$f_3 s_{3j}$	$f_4 s_{4j}$	$f_5 s_{5j}$
KSF	2.853	0.115	0.009	0.002	0.002
KSFO	-	30.355	1.217	0.443	0.04
KSFO + M	-	20.70	1.138	0.431	0.055
F49	-	11.393	1.677	0.440	0.040
AHC	-	-	1.092	0.166	0.020
AHC + M	-	-	1.349	0.139	0.013
T126	-	-	-	2.123	0.144
F1	-	-	-	-	0.129
ALC	-	0.745	1.577	0.261	0.024

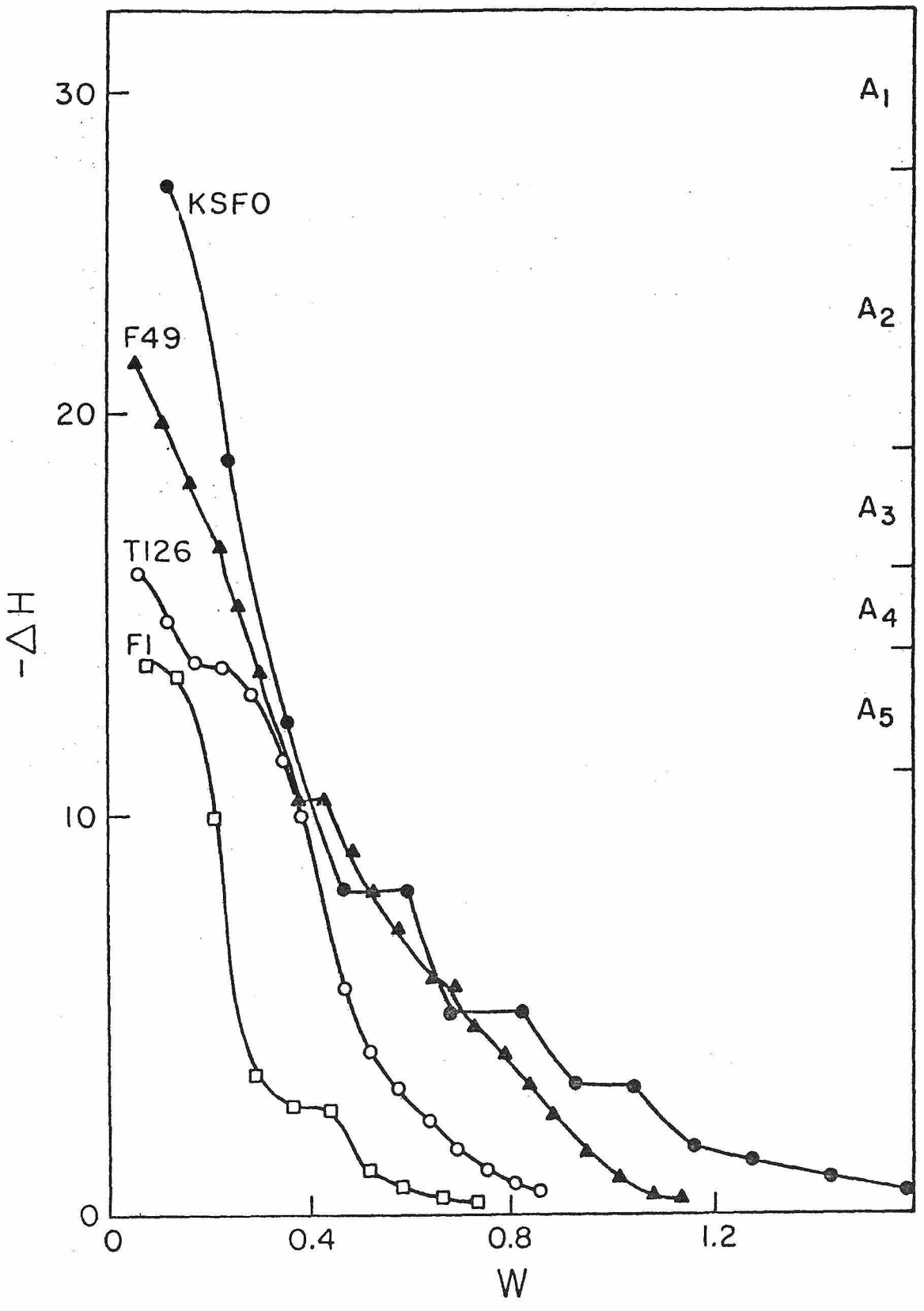

Figure 1. Heat of adsorption versus n-butylamine coverage.

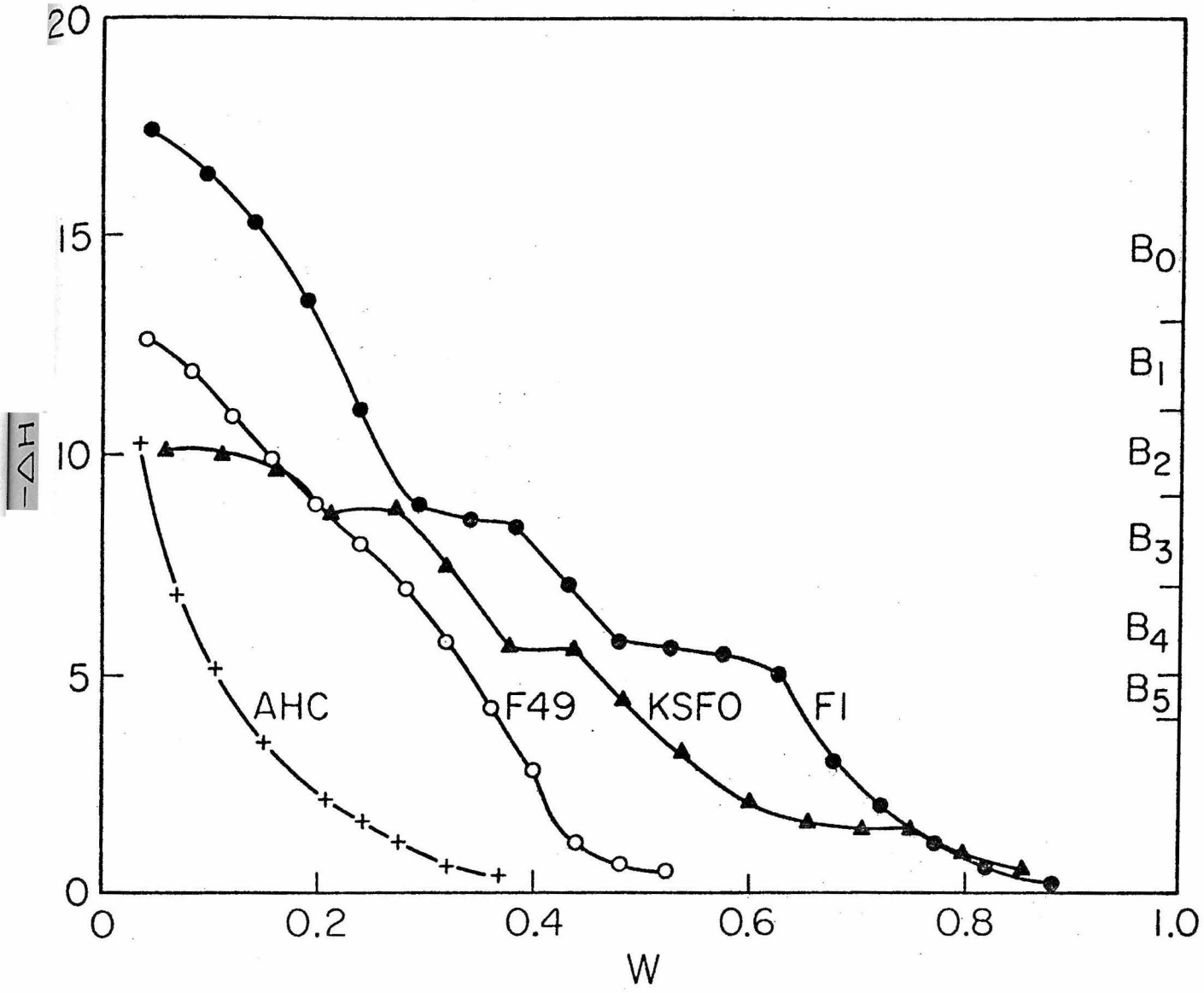

Figure 2. Heat of adsorption versus trichloroacetic acid coverage.

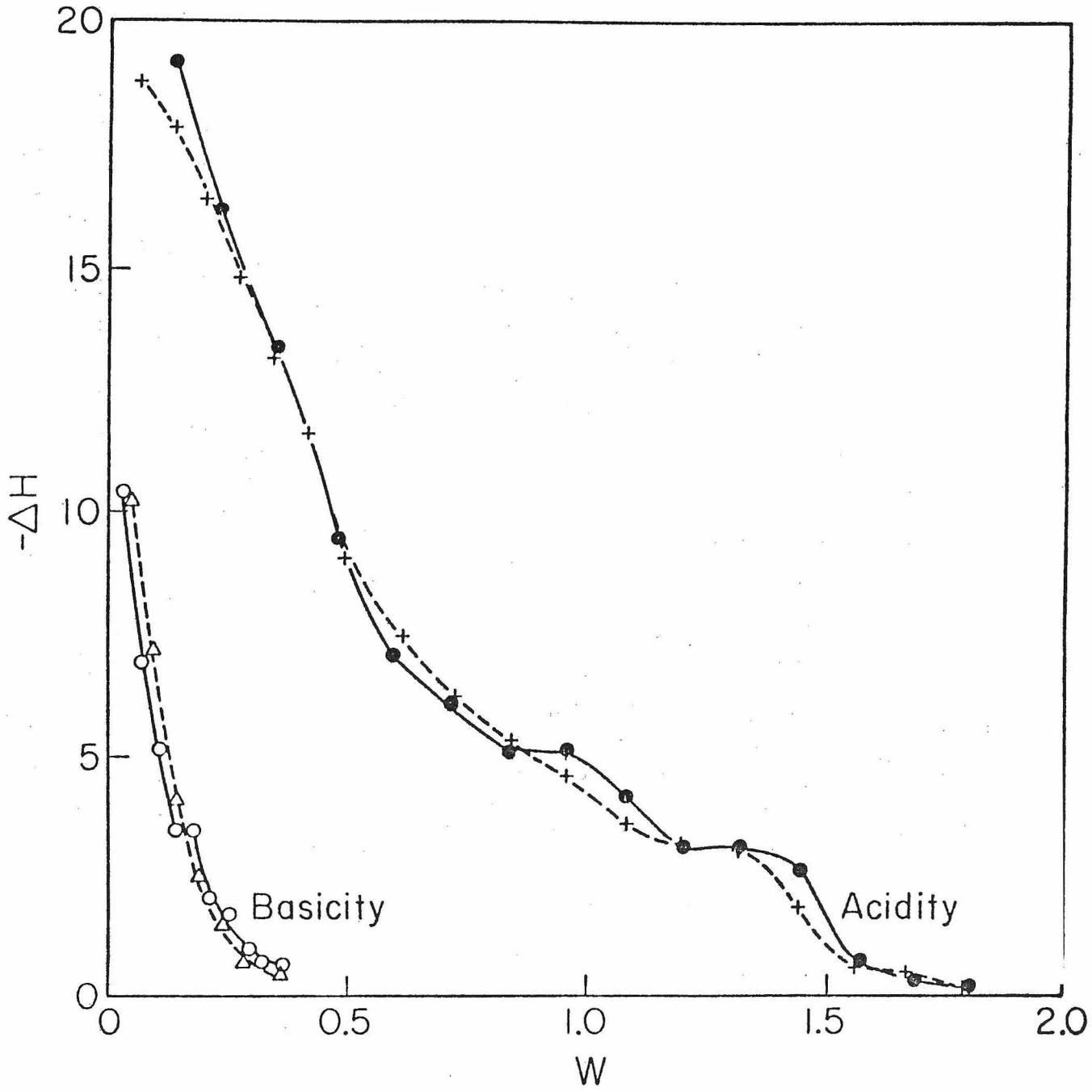

Figure 3. Effect of titer increment on the heat of adsorption curves of AHC

(●) Titer increment = 0.120 mmol/g catalyst
(+) Titer increment = 0.0705 mmol/g catalyst
(△) Titer increment = 0.0458 mmol/g catalyst
(o) Titer increment = 0.0358 mmol/g catalyst

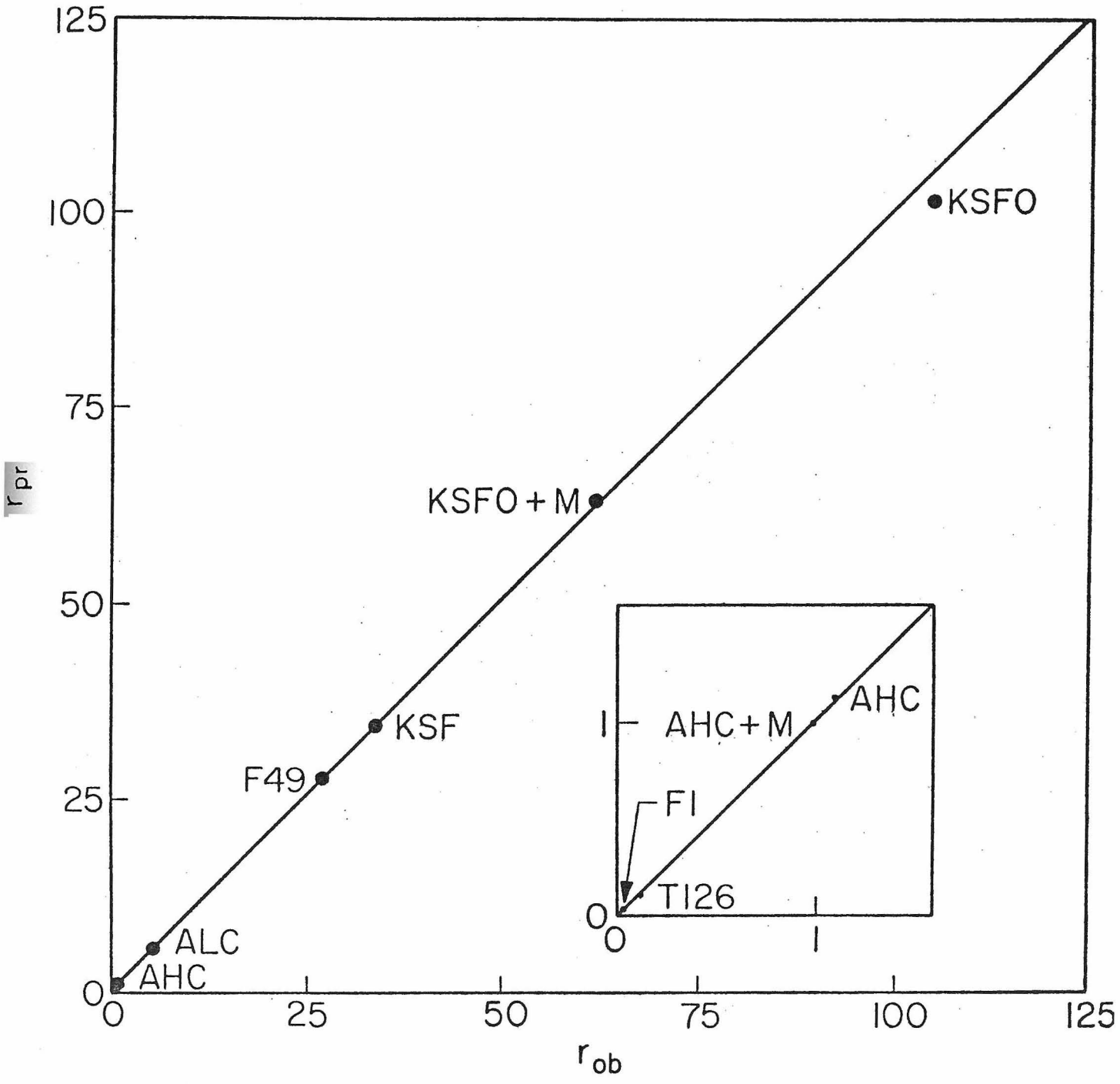

Figure 4. Group analysis fit for rates of ethylene formation

Experimental conditions:
Alcohol concentration = 6.64×10^{-3} moles/liter
Reaction temperature = 200^{o}

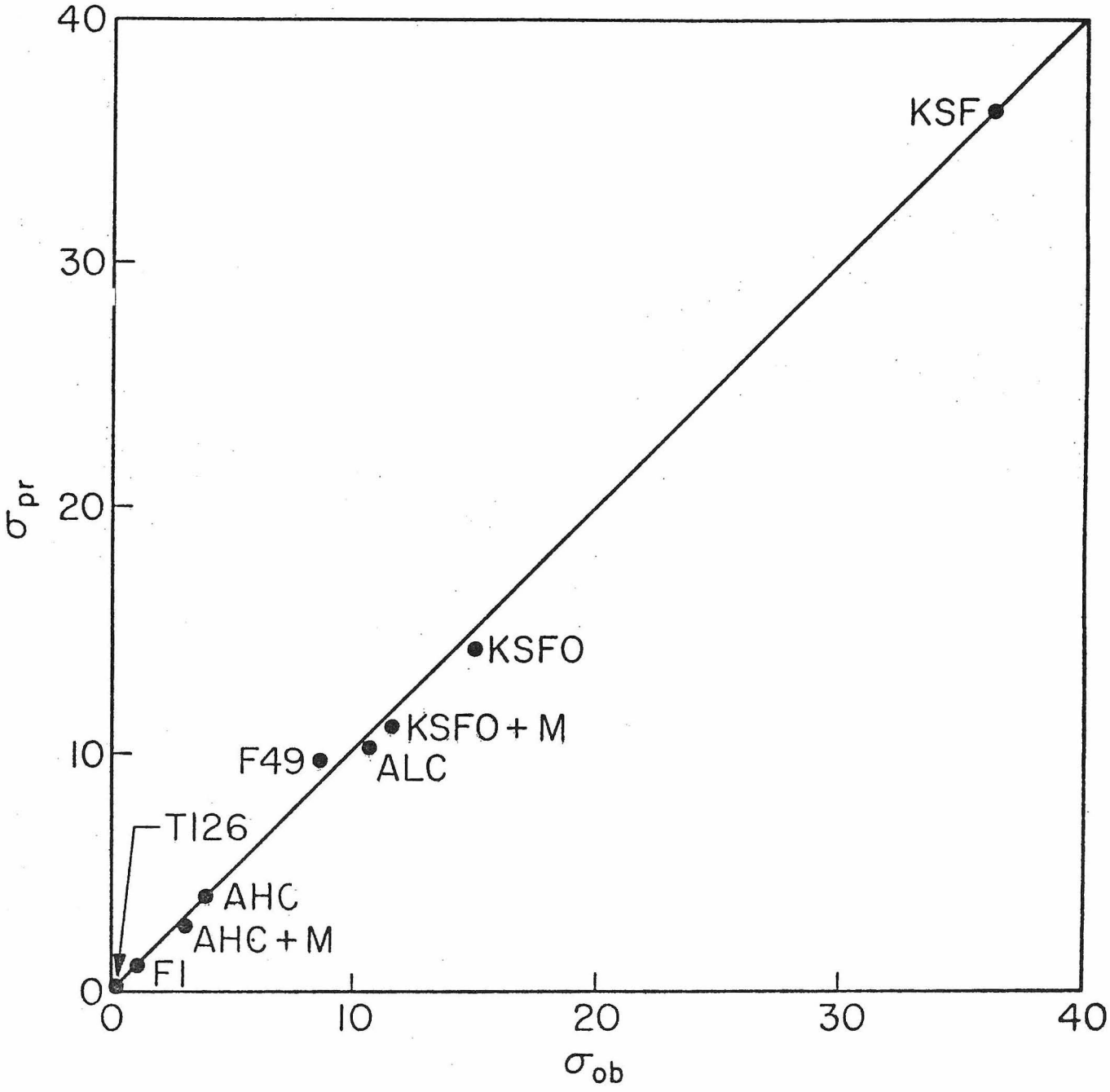

Figure 5. Group analysis fit for selectivity

Experimental conditions:
Alcohol concentration = 6.64×10^{-3} moles/liter
Reaction temperature = 200°C

IV.

Characterization of Acid-Base Catalysts by Calorimetric Titration

II. Effect of Poisoning on Titration Curves and Alcohol Dehydration Activity

K. R. Bakshi and G. R. Gavalas*

Division of Chemistry and Chemical Engineering
California Institute of Technology
Pasadena, California 91125

ABSTRACT

Several commercial aluminas, silica-aluminas and clays have been subjected to poisoning by ammonia and organic bases and subsequently characterized (1) by calorimetry, yielding the heat of adsorption of bases and acids as a function of coverage (2) activity in ethanol and methanol dehydration reactions. A correlation developed in a previous paper by Bakshi and Gavalas (1974b) describing the activity of fresh catalysts in terms of their acidity and basicity distributions has been used to describe the activity of the poisoned catalysts. Certain rather subtle selectivity changes caused by poisoning have been explained by the corresponding changes in the acidity and basicity distributions.

* To whom correspondence should be directed

INTRODUCTION

Most of the literature on catalyst poisoning has been concerned either with utilizing poison adsorption as a tool to elucidate reaction mechanisms or in relation to industrial catalytic processes. Thus the dynamics of poisoning and other deactivation processes in catalytic reactors and the resulting changes in activity and selectivity have all received considerable attention, see e.g. the review of Butt (1970). Whether from the fundamental or applied standpoint, however, an investigation of catalyst poisoning brings to focus two important issues

(a) The change of the catalyst state brought about by poison adsorption.

(b) The effect of the change in the catalyst state on the reaction kinetics; especially on the catalyst activity and selectivity.

These aspects of catalyst poisoning are intimately related to catalyst characterization, a very difficult problem at the center of current catalytic research.

In the case of acidic catalysts, acidity has provided a measure for characterization and correlation with catalytic activity (Tanabe, 1970; Covini et al., 1967). In an earlier paper, Bakshi and Gavalas (1974b), we have used the heat of adsorption as a function of coverage to characterize the acidity and basicity distributions of a number of commercial aluminas. Almost all catalysts tested were found to possess non-uniform acidic and basic sites in agreement with similar behavior reported for other commercial catalysts (Hirschler, 1963; Tanabe, 1970). A group analysis involving determination of the relative activity of sites of different strengths was then developed to correlate the acid-base distributions with the activity

of catalysts in alcohol dehydration reactions.

Since acidity and basicity distributions were found to be a suitable means of catalyst characterization, capable of describing the dehydration activity and selectivity of fresh catalysts, the present work is devoted to extend these results to poisoned catalysts. It includes a study of the effects of different poisons on the catalyst acidity and basicity distributions and attempts to explain quantitatively in terms of these distributions the activity and selectivity towards alcohol dehydration reactions.

EXPERIMENTAL

1. Reagents: All chemicals used in this investigation were high purity reagent grade and were used without further purification. Benzene used for calorimetric titrations was dried over molecular sieve before use.

2. Catalysts: Commercial catalysts used for this investigation were: KSFO Montmorillonite Clay obtained from Chemetron Corporation; Filtrol Grade 49 (F49) containing 4.5% MgO, 17.5% Al_2O_3 and 74% SiO_2 obtained from Filtrol Corporation; Aerocat Low Cracking (ALC) containing 13% Al_2O_3 and 87% SiO_2 obtained from American Cyanamid Company.

3. Catalyst Pretreatment and Poisoning: All catalysts were pretreated at 300°C for five hours in a dry nitrogen atmosphere before further use. The pretreated dry catalyst samples were partially poisoned by stepwise titrating at room temperature with a known amount of a standardized solution of an amine in dry benzene. The catalyst suspension was stirred during titration to obtain a uniform poisoning. The poisoned catalyst was dried at 200°C and stored under dry conditions before further use.

4. Activity Measurements: Evaluation of the catalyst activity for alcohol dehydration was carried out in a differential microreactor suspended in a well mixed air bath. The reactor temperature was maintained within ± 0.2°C of the reported values by a proportional temperature controller. Alcohol, fed by a multispeed infusion pump, was vaporized and mixed with dry nitrogen to attain the desired feed concentration. The reaction products were analyzed by a flame ionization detector after separation on a 10% Carbowax 20 M column. The details of the experimental set-up are described elsewhere (Bakshi and Gavalas, 1974a).

5. Calorimetric Titrations: Acidity and basicity distributions of both fresh and poisoned catalysts were carried out by calorimetric titrations

described elsewhere (Bakshi and Gavalas, 1974). The titrations were used to evaluate the heats of adsorption of n-butylamine and trichloroacetic acid as a function of coverage.

RESULTS

1. Activity Measurements: Activities for alcohol dehydration of fresh and partially deactivated catalysts were determined under identical conditions and the observed rates of olefin and ether formation are given in Table 1. Poisoning was observed to affect both ether and olefin formation in all cases and as shown in Table 1, the decrease in the relative rates of olefin and ether formation depends on the poison used to deactivate the catalyst. Weak bases such as aniline, pyridine and ammonia affect ethylene formation more than ether formation, thereby decreasing the selectivity σ of the fresh catalyst. Strong bases such as n-butylamine and triethylamine in most cases affect ether formation more than ethylene formation, resulting in a higher selectivity relative to the fresh catalyst. This behavior is not general, however, since the adsorption of n-butylamine on the ALC catalyst decreases the selectivity towards ethylene. These results suggest that the effect of poisoning on catalyst selectivity depends on the strength of the poison as well as the nature of the catalyst surface in its fresh state.

The changes in selectivity upon poisoning by weak bases such as pyridine and aniline follow the same trend as in the results of Figueras et al. (1971) for ethanol dehydration and of Jain and Pillai (1967) for isopropyl alcohol dehydration. The decrease in σ upon poisoning by weak bases is not surprising considering the stronger dependence of olefin formation on acidic

strength as compared to ether formation (Bakshi and Gavalas, 1974b).

The change in selectivity upon poisoning by strong bases shows a more complex pattern. The rate data on the poisoned KSFO and F49 shown in Table 1 suggest that poisoning the catalyst by a fixed molar amount of either a weak or a strong base affects ethylene formation to the same extent. However, the reduction in ether formation is stronger so that the overall selectivity shifts in favor of ethylene formation. To investigate this rather unexpected behavior, the effect of n-butylamine poisoning on the selectivity of KSFO was tested at various poisoning levels. The results shown in Table 2 indicate that at all poisoning levels, ether formation is affected more than olefin formation. As the amount of adsorbed poison increases, the selectivity towards ethylene increases at first and then approaches a constant level.

2. Acidity and Basicity Distributions: The catalysts tested in this investigation have been characterized by their acidity and basicity distributions obtained by calorimetric titrations. The same characterization can be applied to the poisoned catalysts and the changes in their acidity and basicity distributions may be invoked to explain the unusual selectivity changes attendant upon poisoning.

The acidity distributions of KSFO, F49 and ALC catalysts in their fresh and poisoned states are shown in Figures 1-3 in terms of their differential heat of adsorption curves obtained by calorimetric titrations. The differential heat curves are divided into various groups bounded by heat of adsorption limits as indicated in Figure 1. The corresponding group acidities in the strongest acidic group for the fresh and poisoned catalysts suggests that in all three catalysts tested, partial poisoning affects the

stronger acidic sites preferentially and the loss in strong acidities determined by the calorimetric titrations is in good correspondence with the poisoning level.

The basicity distributions of the fresh and poisoned states of the three catalysts are shown in Figures 1-3 in terms of their differential heat of adsorption curves. A comparison of these curves suggests that in all three catalysts, the maximum basic strength increases upon poisoning by n-butylamine. However, the total basicities obtained at the end of the calorimetric titrations are not affected by the adsorption of the poison. A division of the differential heat curves into groups of basicities as indicated in Figure 2 leads to the basicity distributions given in Table 4.

A comparison of the basicity distributions for fresh and poisoned catalysts indicates that the adsorption of a strong base on an acidic site results in an increase in the strength of the neighboring basic sites for all three catalysts tested. The basicity distributions of the poisoned catalysts show an increase in the sites of the B_0 group at the expense of sites in B_1, B_2 and B_3 groups. Comparing the basicity distributions for the KSFO catalyst poisoned by a weak base such as pyridine with the basicity distribution of KSFO in its fresh state, it is apparent that there is a small increase in basicity although as shown by Table 4, the number of sites in each group remains essentially unaltered.

GROUP ANALYSIS

The acidity and basicity distributions of the fresh catalysts have been utilized in a previous paper (Bakshi and Gavalas, 1974b) to develop a quantitative correlation for the rate of dehydration reactions. The group

analysis attempted to determine the relative contribution of each group towards the total catalyst activity, and the specific rates were determined by least squares for both olefin and ether formation. The specific rates for the fresh catalysts are given in Table 5. Since the acid and base distributions of the poisoned catalysts are available, a group analysis may be attempted using these specific rates to predict the total catalyst activity for both ether and olefin formation. The effective group site densities s_{ij}, defined in Table 5 for both reactions, are estimated for poisoned catalysts using their acidity and basicity distributions. The evaluation of s_{ij} from the product of densities of acidic and basic sites possessing optimal strengths follows a correlation developed for fresh catalysts (Bakshi and Gavalas, 1974b) and inherently assumes a random association of the acidic and basic sites on the catalyst surface. The rates predicted by group analysis are in satisfactory agreement with the experimentally observed rates for all three catalysts in their fresh and poisoned states. The details of the group analysis are shown in Table 7 in terms of the actual contribution of each group for all the catalysts. A comparison of the various group contributions in the fresh states of KSFO and F49 catalysts indicates that the contribution from Group 2 is the most significant towards the rates of both olefin and ether formation. Upon poisoning by n-butylamine, part of the acidity in this group is lost with a simultaneous shift in the basicity distribution as shown in Table 4. The total change in weak basicities (B_4 and B_5) is insignificant with the result that olefin formation is affected in accordance to the loss of acidic sites. The effect of poisoning on ether formation is more pronounced since aside from affecting the strong acidic sites, there is a shift in the basicity distribution resulting in an increase in the B_0 group and a decrease in

the B_1 and B_2 groups. Since the B_1 and B_2 basicity plays an important role in alkoxide formation (Bakshi and Gavalas, 1974b), a decrease in the strong basicity affects ether formation more than olefin formation because the latter does not require an alkoxide intermediate.

In order to investigate the importance of the changes in basicity distribution upon poisoning by n-butylamine, two different models are employed to evaluate s_{ij} for the group analysis. Model A evaluates s_{ij} from the actual acid-base distributions obtained from titrations of poisoned catalysts whereas Model B evaluates s_{ij} by assuming that the poison decreases the acidity distribution by destroying an equimolar amount of strong sites and does not affect the basicity distribution of the fresh catalyst. Model B thus obtains the acid-base distributions of the poisoned catalyst state without an actual titration. The results of group analysis using these two models are shown in Table 8 for both dehydration products. Both models predict olefin formation rates satisfactorily with the predictions of Model A being slightly better based on overall least squares. In the case of ether formation, the predictions of Model B are good for catalysts poisoned by weak bases, in agreement with the fact that the basicity distribution is only slightly altered by weak bases as shown in Table 4. In contrast, the predictions of Model B for ether formation on catalysts poisoned by strong bases are high by a factor of two or so of the observed rates. Model A, on the other hand, provides satisfactory predictions for ether as well as ethylene formation independently of the strength of the adsorbed poison.

DISCUSSION

The results of calorimetric titrations of a catalyst in its fresh and

poisoned states reveal that chemisorption of a poison affects both acidity and basicity distributions. The change in the acidity distribution is predictable from the amount of adsorbed poison and does not specifically depend on the strength of the poison. The change in the basicity distribution, on the other hand, is more complex. The basicity distributions of all poisoned catalysts show an increase in number density of the B_0 group at the expense of the B_1, B_2 and B_3 groups. This behavior may be explained by surface induction phenomena whereby a base molecule adsorbed on an acidic site may affect the neighboring basic sites. The effectiveness of such induction depends on the strength of the chemisorbed poison and the proximity of basic sites to the poisoned acidic site. Results of calorimetric titrations indicate that the effect of a weak base is indeed less pronounced as compared to the effect of a strong base. To investigate the proximity requirement, the relative spacing between the active sites may be estimated by assuming a uniform distribution on the available catalyst surface. The maximum spacing between an acid site and its nearest base site for a catalyst with 1 mmol./g. of total acid and base sites distributed uniformly over 200 m^2/g of surface is about 6Å. Although the maximum acid-base site spacing appears to be large, assumption of uniform distribution of the active sites is probably erroneous in view of the existence of patches of active sites observed by Hirschler (1969) for alumina and silica-alumina catalysts. Invoking the existence of such clusters, the spacing between acid-base sites may be expected to be significantly less thereby providing the required proximity for surface induction.

As reported in our earlier investigation of the kinetics of dehydration reactions on fresh and poisoned F49 catalysts (Bakshi and Gavalas, 1974a), the

increase in the value of the "adsorption constant" for alcohol upon poisoning by n-butylamine could be explained by invoking a surface induction effect resulting in an increase in the strength of the basic sites. The results of titrations are in good agreement with such an inductive effect.

The importance of the change in basicity distribution by induction in correlating the catalyst activity for dehydration reactions is well established by the success of Model A over Model B in explaining the selectivity changes upon poisoning for all the catalysts tested. The change in basicity distribution explains the increase in the selectivity of KSFO and F49 catalysts upon poisoning by n-butylamine. The decrease in the ALC selectivity however indicates that the change in basicity distribution alone is not sufficient to explain the effects of poisoning by a strong base. The results of group analysis detailed in Table 7 show that the relative contributions of the various groups to the total activity play an important role. The main contribution to the KSFO and F49 activities are derived from Group 2 for both dehydration products. Poisoning of these catalysts by n-butylamine destroys acidic sites within this group such that olefin formation is affected almost proportionately to the level of poisoning. The effect on ether formation is more pronounced due to the decrease in the $(B_1 + B_2)$ group through surface induction. The overall effect is an increase in the selectivity.

In contrast, the acidity distribution of the fresh ALC catalyst shows higher number density in A_3 as compared to A_2. However, as shown in Table 7, the main contribution to the activity for olefin formation still derives from Group 2 due to a considerable difference in the specific rates f_2 and f_3. Since poisoning completely destroys the acidic sites in Group 2

the activity for olefin formation decreases considerably. On the other hand, the main contribution for ether formation on fresh ALC catalyst derives from Group 3 because the relative values of activity constants k_2 and k_3 for ether formation do not compensate sufficiently for the higher number density in Group 3. Destruction of the contribution of Group 2 upon poisoning by n-butylamine results in a less pronounced effect on ether formation, thus resulting in a lower selectivity of the poisoned catalyst. This difference in behavior of the ALC and KSFO, F49 catalysts upon poisoning indicates that the detailed acid-base distributions of the fresh catalyst and the modifications due to poisoning are both important in determining the selectivity variations upon poisoning.

The evaluation of s_{ij} from specific models involving acid-base site pairs of specific strengths assumes a random distribution of the acidic and base sites on the catalyst surface. Such an assumption appears to lead to consistent results for fresh catalysts in as much as the s_{ij} determined by invoking this assumption leads to a successful quantitative correlation for the catalyst activities (Bakshi and Gavalas, 1974b). Chemisorption of a strong base may lead to certain bias in the strengths of neighboring acidic and basic sites. The fact that the predicted activities for ether formation are somewhat higher than the observed values for all poisoned catalysts may arise from such a bias induced by the chemisorbed base.

CONCLUSIONS

A correlation developed in Part I by Bakshi and Gavalas (1974b) describing the dehydration activities of several commercial catalysts in terms of their acidity and basicity distributions has been found to provide good results for the catalysts poisoned by ammonia and organic bases. The ad-

sorption of weak bases preferentially removes the strongest acidic sites but has little effect on the basicity distribution. The adsorption of strong bases in addition to removing the stronger acidic sites causes a shift in the basicity distribution towards higher strengths. This shift reduces the density of sites having an intermediate basicity responsible for ether production and hence increases the catalyst selectivity towards ethylene production. These results show that selective poisoning can be used to produce rather subtle selectivity changes for the catalysts studied.

Table 1

Effect of Partial Catalyst Poisoning on Dehydration Activity and Selectivity[1]

Catalyst	Rate of Ethylene Formation $r \times 10^4$	Rate of Ether Formation $r \times 10^3$	Selectivity* σ%
Group A			
KSFO	105.3	29.9	14.97
KSFO + aniline	46.08	11.57	16.61
KSFO + pyridine	28.56	9.96	12.53
KSFO + n-butylamine	48.0	8.61	21.80
KSFO + triethylamine	49.9	4.95	33.5
Group B			
F49	26.9	14.2	8.65
F49 + aniline	17.92	12.7	6.59
F49 + ammonia	12.78	9.94	6.04
F49 + pyridine	12.43	8.64	6.71
F49 + n-butylamine	10.74	2.64	16.9
F49 + triethylamine	11.58	3.08	15.8
Group C			
ALC	5.66	2.39	10.60
ALC + n-butylamine	0.987	0.828	5.62

* $\sigma = \frac{\text{amount of alcohol converted to ethylene} \times 100}{\text{total alcohol conversion}}$

1 Run conditions:

Feed concentration: $6.64 * 10^{-3}$ moles/liter
Reaction temperature: 200°C

Table 2

Effect of Poisoning Level on
Dehydration Activity of KSFO Catalyst

Poisoning level $\left(\frac{\text{mmol of n-butylamine}}{\text{g catalyst}}\right)$	Rate of Ethylene Formation $r \times 10^4$	Rate of Ether Formation $r \times 10^3$	Selectivity $\sigma\%$
0	105.3	29.9	14.97
0.0145	82.38	16.93	19.57
0.0909	60.22	8.57	26.00
0.1454	37.59	4.36	30.12
0.2000	16.22	1.94	29.48

Table 3

Acidity Distribution of Fresh and Poisoned Catalysts

Catalyst[2]	Acidity[1] mmol/g catalyst				
	A_1	A_2	A_3	A_4	A_5
KSFO	0.0	0.24	0.05	0.04	0.06
KSFO + n-butylamine (0.12)	0.0	0.125	0.06	0.04	0.06
F49	0.0	0.136	0.104	0.06	0.09
F49 + n-butylamine (0.10)	0.0	0.03	0.09	0.08	0.16
ALC	0	0.02	0.22	0.08	0.13
ALC + n-butylamine (0.10)	0	0	0.14	0.07	0.11

1 Acidity groups are defined by heat of adsorption included between limits as follows:

A_1: $26 < -\Delta H$ A_2: $19 < -\Delta H < 26$ A_3: $16 < -\Delta H < 19$

A_4: $14 < -\Delta H < 16$ A_5: $11 < -\Delta H < 14$

2 The numbers in parentheses represent poisoning level in mmol/g catalyst.

Table 4

Basicity Distribution of Fresh and Poisoned Catalysts

Catalyst	Basicity[1] mmol/g catalyst					
	B_0	B_1	B_2	B_3	B_4	B_5
KSFO	0.0	0.0	0.22	0.15	0.13	0.045
KSFO + pyridine	0.0	0.0	0.225	0.14	0.14	0.04
KSFO + n-butylamine	0.13	0.05	0.07	0.10	0.12	0.05
F49	0.0	0.11	0.09	0.09	0.06	0.025
F49 + n-butylamine	0.14	0.05	0.03	0.08	0.06	0.05
ALC	0.0	0.0	0.06	0.21	0.06	0.03
ALC + n-butylamine	0.05	0.015	0.03	0.16	0.06	0.05

1 Basicity groups are defined by heat of adsorption included between limits as follows:

B_0: $13 < -\Delta H$ B_1: $11 < -\Delta H < 13$ B_2: $9 < -\Delta H < 11$

B_3: $7 < -\Delta H < 9$ B_4: $5 < -\Delta H < 7$ B_5: $4 < -\Delta H < 5$

Table 5

Specific rates for Alcohol Dehydration[1,2,3]

Group	$f_{ethylene}$	f_{ether}
1	11933.7	914797.0
2	2379.0	32852.1
3	63.01	6322.86
4	5.608	2778.07
5	0.614	172.44

1 Run conditions:

Feed concentration: $6.64 * 10^{-3}$ moles/liter
Reaction temperature: 200°C

2 Effective site density s_{ij} for j^{th} catalyst is evaluated as follows:

a. Ethylene: $s_{ij} = (A_i) * (B_4 + B_5)$ for j^{th} catalyst

b. Ether: $s_{ij} = (A_i) * (B_4 + B_5) * (B_1 + B_2) * (A_4 + A_5)$ for j^{th} catalyst

3 Specific rates obtained by Bakshi and Gavalas (1974b)

Table 6

Group Analysis of Fresh and Poisoned Catalysts

Catalyst	Rate of Ethylene Formation $r \times 10^4$		Rate of Ether Formation $r \times 10^3$		Percentage Selectivity $\sigma\%$	
	Predicted	Observed	Predicted	Observed	Predicted	Observed
KSFO	100.52	105.3	32.04	29.9	13.56	14.97
KSFO + n-butylamine	51.23	48.0	9.40	8.61	21.41	21.80
F49	28.1	26.9	13.53	14.20	9.41	8.65
F49 + n-butylamine	8.51	10.74	3.00	2.64	12.42	16.9
ALC	5.578	5.66	2.595	2.39	9.72	10.60
ALC + n-butylamine	1.02	0.987	0.976	0.828	4.97	5.62

Table 7

Details of Group Analysis for Various Catalysts

Catalyst j	Product	Group Contributions@ f_1s_{1j}	f_2s_{2j}	f_3s_{3j}	f_4s_{4j}	f_5s_{5j}
KSFO	Ether	-	30.355	1.217	0.443	0.04
	Ethylene	-	99.92	0.56	0.04	0.006
KSFO + $BuNH_2$	Ether	-	8.377	0.78	0.241	0.02
	Ethylene	-	50.55	0.65	0.03	0.005
F49	Ether	-	11.393	1.677	0.44	0.35
	Ethylene	-	27.50	0.57	0.03	0.005
F49 + $BuNH_2$	Ether	-	1.675	0.914	0.391	0.045
	Ethylene	-	7.85	0.60	0.052	0.007
ALC	Ether	-	0.745	1.577	0.261	0.022
	Ethylene	-	4.282	1.25	0.042	0.006
ALC + $BuNH_2$	Ether	-	-	0.789	0.179	0.016
	Ethylene	-	-	0.970	0.045	0.007

@ Total rate predicted by group analysis is given by

$$r_j = \sum_{i=1}^{5} f_i \cdot s_{ij} \quad \text{for } j^{th} \text{ catalyst}$$

Table 8

Comparison of Group Analysis on Different Models' Observed Rates

Catalyst*	Rate of Ethylene Formation			Rate of Ether Formation		
	Predicted by Model A	Predicted by Model B	Observed	Model A	Model B	Observed
KSFO + $BuNH_2$ (0.12)	51.23	52.71	48.0	9.40	17.56	8.61
KSFO + pyridine (0.17)	30.55	29.74	28.56	10.85	10.53	9.96
F49 + $BuNH_2$ (0.10)	8.51	6.6	10.74	3.00	4.66	2.64
ALC + $BuNH_2$ (0.10)	1.02	0.84	0.987	0.976	1.26	0.828

*The values in parentheses represent W in mmol/g catalyst.

NOMENCLATURE

A_i	Acidity in i^{th} group defined by Table 3
B_i	Basicity in i^{th} group defined by Table 4
f_i	Specific rate for i^{th} group
r	Rate of product formation, mole of product/hr-g catalyst
s_{ij}	Effective group density for i^{th} group in j^{th} catalyst, defined by Table 5
σ	Selectivity defined by Table 1
W	Amount of titer adsorbed, mmol/g. catalyst
$-\Delta H$	Heat of adsorption kcal/mole

LITERATURE CITED

Bakshi, K. R., Gavalas, G. R., AIChE Journal (Submitted for publication, 1974a)

Bakshi, K. R., Gavalas, G. R., J. Catalysis (Submitted for publication, 1974b)

Butt, J. B., in "Chemical Reaction Engineering," Advances in Chemistry Series, No. 109, pp. 259-496 (1972)

Covini, R., Fattore, V., Giordano, N., J. Catalysis, 9, 315 (1967)

Figueras, F., Nohl, A., DeMourges, L., Trambouze, Y., Trans. Faraday Soc., 67, 1155 (1971)

Hirschler, A. E., J. Catalysis, 2, 428 (1963)

Hirschler, A. E., Preprints of Am. Chem. Soc., New York Meeting, 14, No. 3, B-68 (1969)

Jain, J. R., Pillai, C. N., J. Catalysis, 9, 322 (1967)

Tanabe, K., "Solid Acids and Bases," Academic Press, New York (1970)

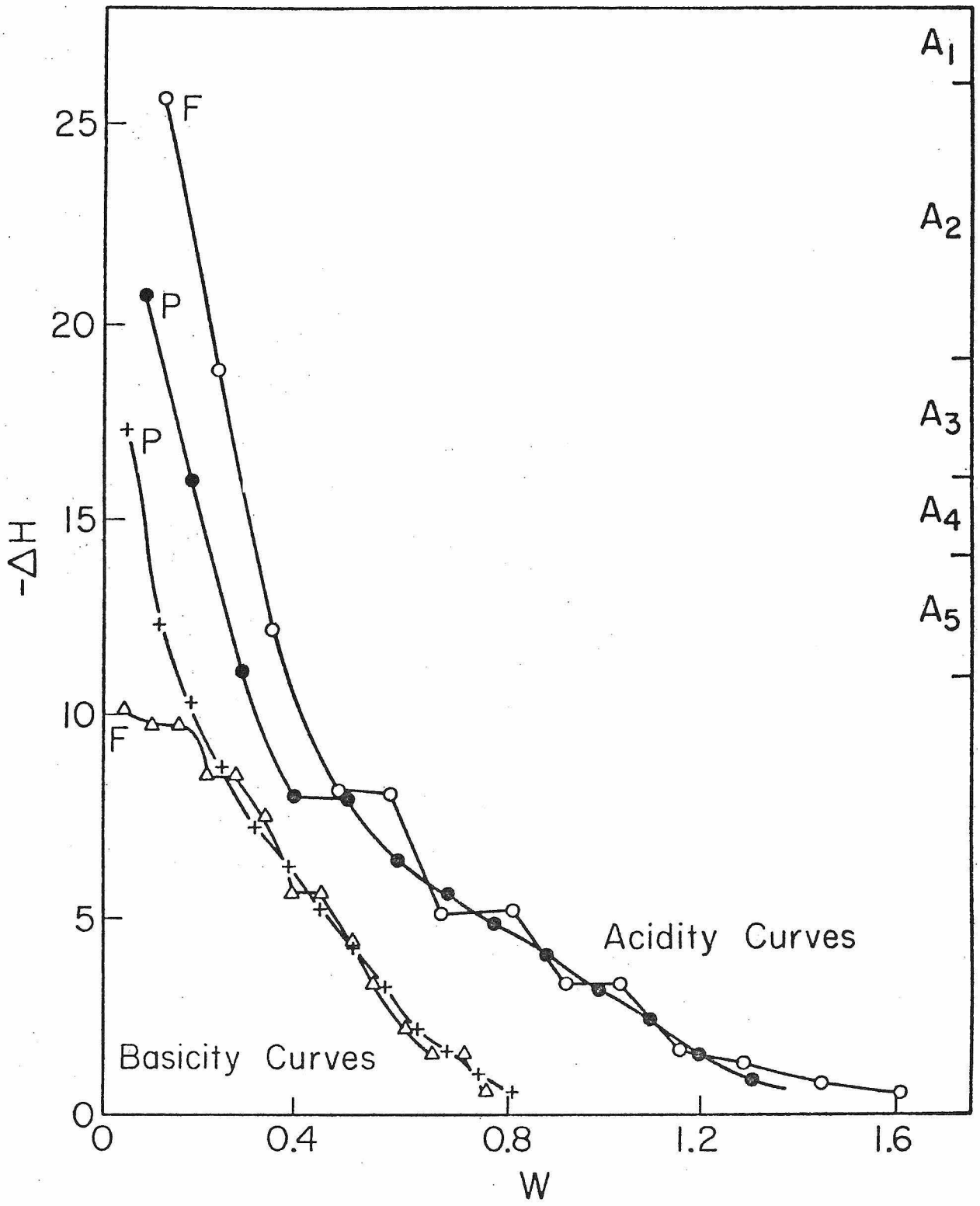

Figure 1. Effect of n-butylamine poisoning on the heat of adsorption curves of KSFO.

(o) Fresh KSFO: acidity measurement
(●) Poisoned KSFO: acidity measurement
(△) Fresh KSFO: basicity measurement
(+) Poisoned KSFO: basicity measurement

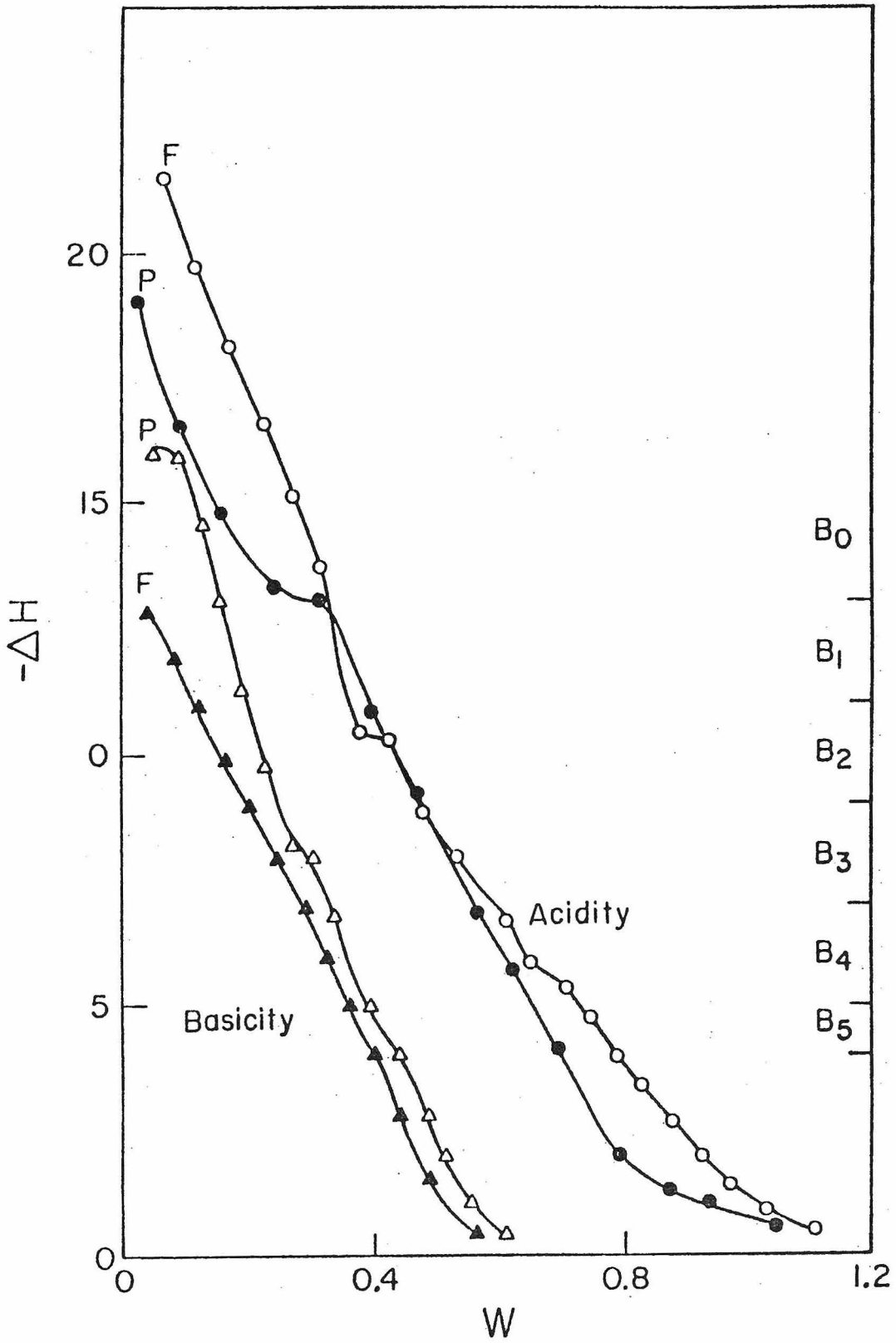

Figure 2. Effect of n-butylamine poisoning on the heat of adsorption curves of F49.

(o) Fresh F49: acidity measurement
(●) Poisoned F49: acidity measurement
(▲) Fresh F49: basicity measurement
(△) Poisoned F49: basicity measurement

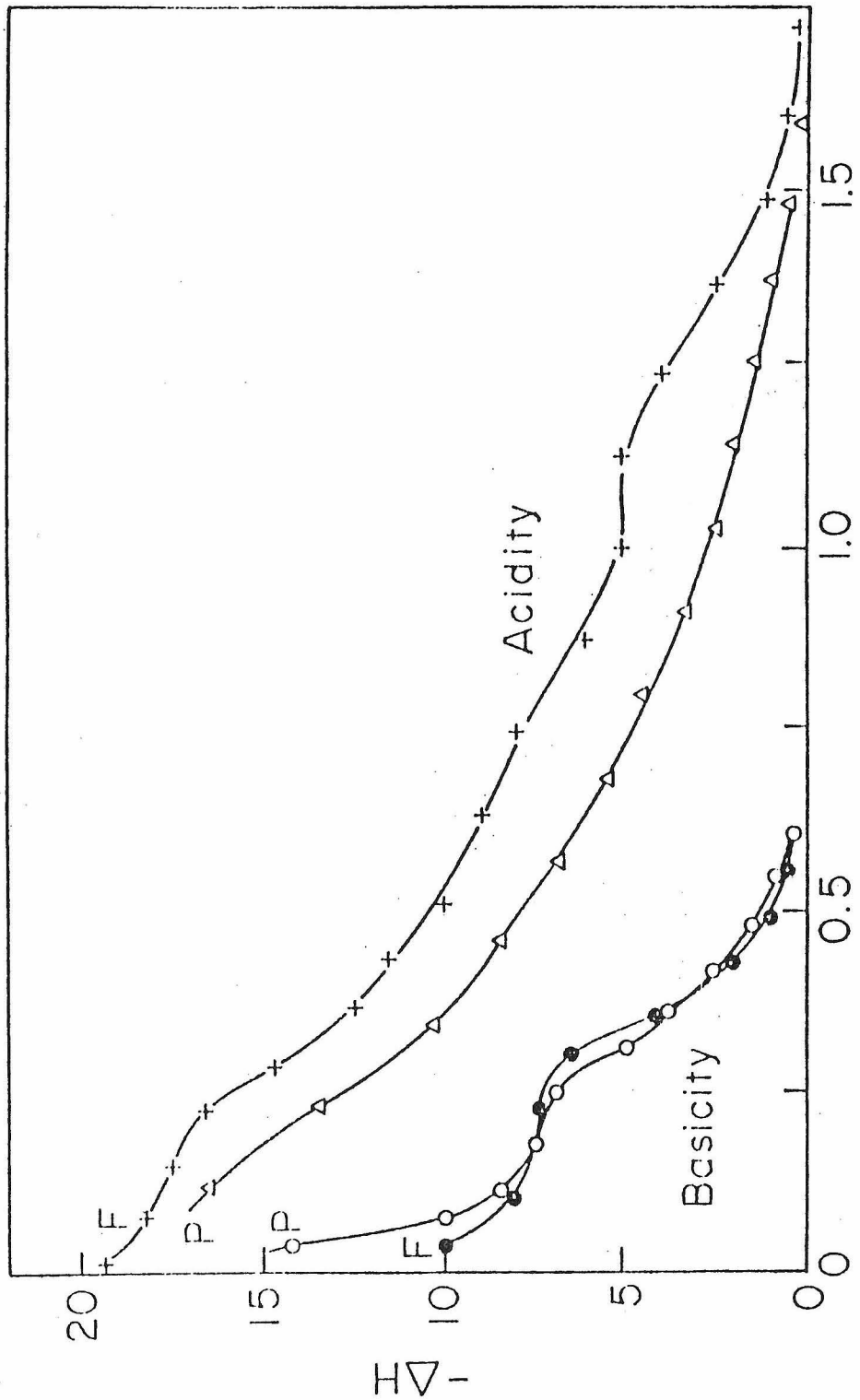

Figure 3. Effect of n-butylamine poisoning on the heat of adsorption curves of ALC.

(+) Fresh ALC: acidity measurement
(Δ) Poisoned ALC: acidity measurement
(●) Fresh ALC: basicity measurement
(○) Poisoned ALC: basicity measurement

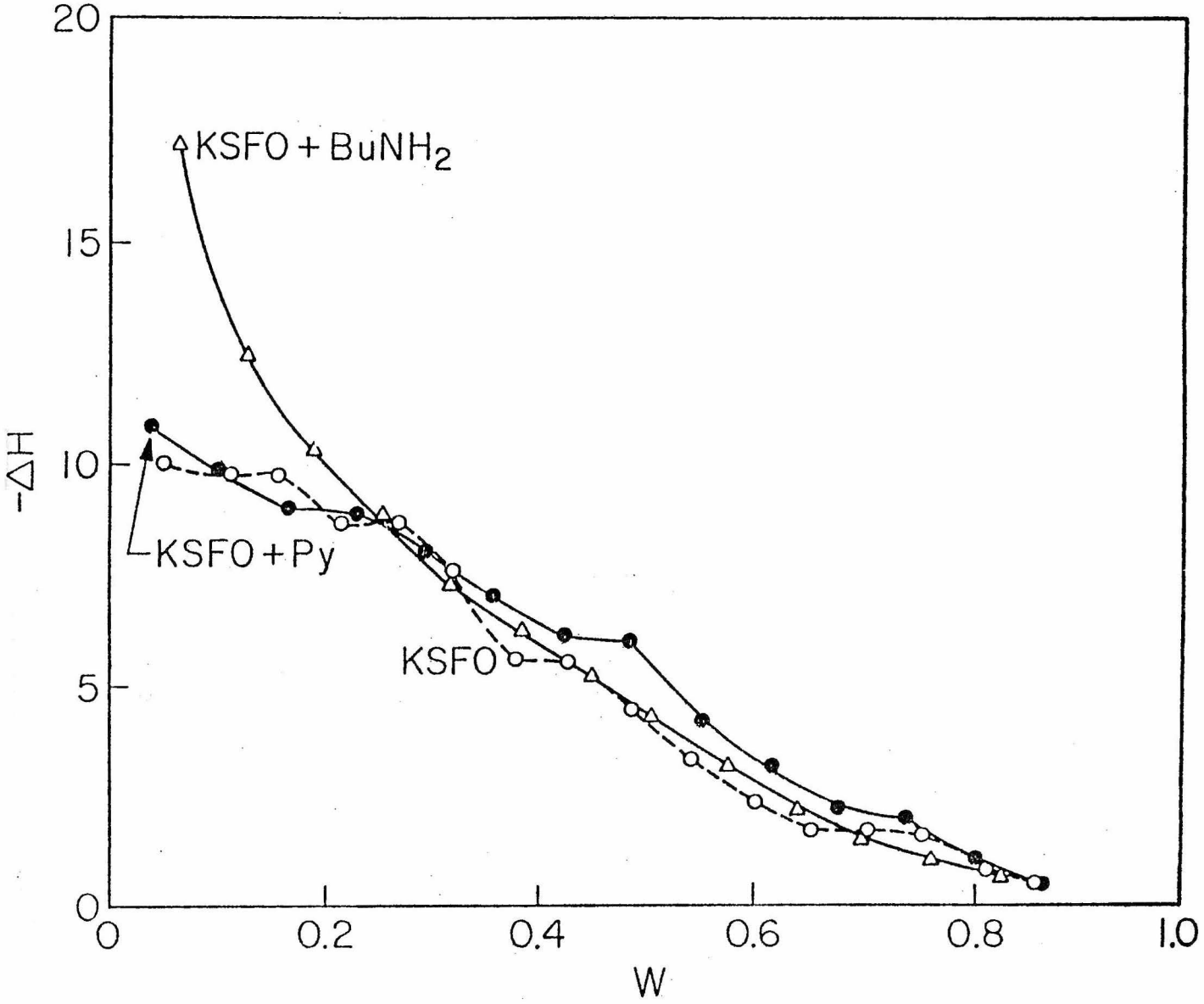

Figure 4. Effect of various poisons on the heat of trichloroacetic acid adsorption curve for KSFO.

V.
Concluding Remarks

Present investigation on various aluminas and silica-aluminas shows that these catalysts exhibit considerable variation in their acid-base distributions, which in turn govern their activities and selectivities for dehydration of primary alcohols. Success of the group analysis in correlating the observed activities indicate that the catalyst states may be operationally defined in terms of their corresponding acid-base distributions. As illustrated in this work, the transformation of the catalyst state by partial poisoning can also be followed by the resultant acid-base distributions. Certain subtle variations in selectivities are observed upon such changes in the catalyst state. These results suggest further investigations on the use of selective poisoning to improve the product distribution in other industrially important reaction systems.

Aside from poisoning by feed impurities, commercial catalysts undergo transformation in their states due to a variety of processes such as variations in catalyst pretreatment, incorporation of moderators or promoters, and deactivation by coking. Each of these transformations and their effects on the catalyst activity may be studied by following their resultant acid-base distributions. Future investigations may include a study of the kinetics of these transformation processes by utilizing the acid-base distributions as a measure to follow the reaction path.

It should be pointed out here that although this operational definition of the catalyst state appears to be useful in applied catalysis, it does not suffice to obtain a complete understanding of the processes that lead to changes in the catalyst state. A clear understanding of the process of coking, for example, would require investigation of the coke structure and

its effect on the catalyst as well. Incorporation of results from more sophisticated analyses such as IR and NMR should be of immense help to obtain a clear understanding of the catalyst state.

Appendix I. Estimation of Mass Transfer Limitations in the Dehydration Reaction.

The observed rate of reaction in heterogeneous catalysis results from three distinct steps:

(1) gas phase mass transfer of reactant to the external catalyst surface;

(2) diffusion of reactant and products through the catalyst pores; and

(3) surface reaction.

Effects of mass transfer limitations on the observed kinetic data should hence be determined before assigning the observed kinetic behavior to the surface reaction alone.

(a) Effect of gas phase mass transfer:

Rate of mass transfer in gas phase may be estimated from:

$$r = k_G a_m \Delta P \quad , \qquad (1)$$

where

k_G = mass transfer coefficient in moles/hr.cm^2 atm

a_m = specific external surface area of the catalyst in cm^2/g catalyst

and

ΔP = driving force for mass transfer to the catalyst particles in atm.

For F49 catalyst, the following kinetic data is observed for methanol dehydration:

temperature: 182^{o}C

total pressure: 1.1 atm.

total flow rate @ 182^{o}C: 7.5 cc/sec

average particle size of the catalyst: 0.25 mm

concentration of feed: 2.44×10^{-2} moles/liter

total rate of dehydration: 5.68×10^{-3} moles/g. hr

In order to compare the observed rate with the rate of gas phase mass transfer, k_G is estimated using correlations reported by Bird, Stewart and Lightfoot (1960), as follows:

From the above conditions, the Reynolds number, Re, based on catalyst particle is estimated to be 2.288. For Re < 50, k_G is correlated by:

$$\frac{k_G \cdot P_F}{G_m} = 0.91\ Re^{-0.51} \cdot \psi \cdot S_c^{-2/3} \qquad (2)$$

where G_m is the molar velocity of gas, P_F is the pressure of the inert, such as N_2 in our experiment, ψ is the shape factor for the catalyst particle, and S_c is the gas phase Schmidt number.

From the experimental data, k_G is estimated to be 0.947 moles/hr $\cdot$ cm^2 $\cdot$ atm, and a_m to be 90.57 cm^2/g. Now if a further assumption is made that the gas phase mass transfer is rate limiting, the surface concentration of alcohol is negligible due to fast reaction. Hence, ΔP equals the partial pressure of alcohol in the gas phase, or 0.091 atm in our case. The rate of gas phase mass transfer is then estimated from (1) to be 7.81 moles/hr.g. Comparing this with the observed rate shows that the above assumption is erroneous and that under the experimental conditions, the gas phase mass transfer is not rate limiting.

(b) Mass transfer effects due to pore diffusion:

Weisz (1954) has developed a criterion to assess the importance of pore diffusion. Defining a modulus Φ by,

$$\Phi = - \frac{r}{C_o} \frac{Rp^2}{D_{eff}} \qquad (3)$$

where r = Observed rate, moles/cc. sec

C_o = Reactant concentration, moles/cc.

Rp = Radius of catalyst particle, cm.

D_{eff} = Effective diffusivity of reactant in catalyst pores, cm^2/sec

The effective diffusivity for alcohol in a catalyst with average pore of 42Å may be estimated to be about 10^{-3} cm^2/sec using a tortuosity factor of 3 in the expression reported by Satterfield (1970). The corresponding value for the modulus Φ using the experimental data is $\Phi \sim 10^{-2}$. As reported by Weisz, pore diffusion does not affect the kinetics substantially for $\Phi < 0.1$.

The above considerations thus indicate that the kinetic data obtained for this system represent the true reaction kinetics and are not affected by any mass transfer limitations.

LITERATURE CITED

Bird, R. B., Stewart, W. E., Lightfoot, E. N., "Transport Phenomena," Wiley, New York (1960)

Satterfield, C. N., "Mass Transfer in Heterogeneous Catalysis," MIT Press, Massachusetts (1970)

Weisz, P. B., Prater, C. D., Advan. Catalysis, 6, 167 (1954)

Table A1*

Properties of KSF

Surface area:	47 m^2/g
Bulk density:	0.81 g/cc
Classification:	Montmorillonite Clay (activated)

Typical analysis: (% by weight)

SiO_2	53.2
Al_2O_3	18.8
Fe_2O_3	5.1
CaO	2.9
MgO	2.8
H_2SO_4	6.0
Loss on ignition	8.1

* Properties of various catalysts (Tables A1 - A7) are determined by their suppliers.

Table A2

Properties of KSFO

Surface area:	215 m^2/g
Bulk density	0.351 g/cc
Classification:	Montmorillonite Clay (activated)

Typical Analysis: (% by weight)

SiO_2	69.8
Al_2O_3	14.2
Fe_2O_3	3.2
CaO	0.8
MgO	0.9
Loss on ignition	6.1
H_2SO_4	5.0

Table A3

Properties of F49

Typical analysis:

1.	Volatile content (wt. % after 1700°F ignition)	17.00
2.	Specific gravity (after 1000°F heating)	2.65
3.	Surface area (N_2 adsorption, B.E.T., sq. meters/gm.)	290.00
4.	Pore size diameter, angstorms	
	"most frequent"	42.00
	median 50% of surface	42.00
	average	50.00
5.	Pore size distribution	
	Pore diameter, angstorms	% surface area
	0 to 40	41.00
	40 to 60	47.60
	60 to 80	5.80
	80 or more	3.60
6.	Chemical analysis (dry basis, wt. %)	
	SiO_2	74.00
	Al_2O_3	17.50
	MgO	4.50
	Fe_2O_3	1.40
7.	Particle porosity, ml./gm.	0.42

Table A4

Properties of AHC

Surface area:	450 m^2/g
Bulk density:	0.38 g/cc
Classification:	High Alumina Cracking Catalyst

Typical analysis: (% weight, dry basis)

SiO_2	75.9
Al_2O_3	24
Na_2O	0.02
Fe	0.05
Ca	0.02
Loss on ignition (% by weight)	18

Table A5

Properties of ALC

Surface area:	500 m^2/g
Bulk density:	0.44 g/cc
Classification	Fluid Cracking Catalyst

Typical analysis: (% weight, dry basis)

SiO_2	87.4
Al_2O_3	12.5
Na_2O	0.02
Fe	0.05
Ca	0.02
Loss on ignition (% by weight)	16

Table A6

Properties of T-126

Surface area:	216 m^2/g
Mean crystallite size:	59Å
Classification:	r-Al_2O_3

Table A7

Properties of F-1

Surface area:	210 m^2/g
Bulk density:	0.83 g/cc
Classification:	r-Alumina
Typical analysis:	
Al_2O_3	92
Na_2O	0.9
Fe_2O_3	0.08
SiO_2	0.09
Loss on ignition	6.50

Table A8

Directional Effects on Ethanol Dehydration[@]

	Forward Direction[1]			Reverse Direction		
c_A ($\times 10^3$)	$r_{ethylene}$ ($\times 10^5$)	r_{ether} ($\times 10^4$)	σ	$r_{ethylene}$ ($\times 10^5$)	r_{ether} ($\times 10^4$)	σ
4.48	8.73	6.52	6.3	9.07	6.8	6.45
2.30	8.59	4.17	9.34	9.24	4.16	10.2
1.15	6.90	2.60	11.6	7.64	2.56	13.0
0.575	6.47	1.46	18.0	7.08	1.39	20.2
0.305	6.22	1.01	23.2	6.77	0.93	26.67
0.155	5.40	0.70	27.5	5.89	0.625	32.00

[@] Catalyst: F49

Experimental conditions: Temperature 170°C

1 Forward direction implies fresh F49 followed by partially poisoned F49

Table A9

Directional Effects on Ethanol Dehydration at Different Conversion Levels@

Total Conversion %	Percentage Selectivity change upon flow reversal %
11.5	2.5
15.0	8.6
19.5	12.0
22.5	12.2
30.6	15.1
44.4	16.5

@ Experimental conditions:

Catalyst: F49
Temperature: 170°C

Table A10

Kinetic Data for Methanol Dehydration on Fresh F49 at 160°C

A. $c_W = 0$

$c_A \times 10^2$	0.12	0.17	0.20	0.32	0.44	0.64	0.90	1.20	1.85	2.41
$r \times 10^3$	0.559	0.639	0.702	0.766	0.870	1.061	1.152	1.338	1.539	1.589

B. $c_W = 2.5 \times 10^{-4}$

$c_A \times 10^2$	0.09	0.15	0.25	0.33	0.46	0.60	0.93	1.18	1.75	2.41
$r \times 10^3$	0.42	0.47	0.597	0.719	0.800	0.929	1.051	1.122	1.339	1.469

C. $c_A = 1.01 \times 10^{-2}$

$c_W \times 10^3$	0.249	0.481	0.716	1.195	1.683	2.437
$r \times 10^3$	1.110	0.987	0.906	0.758	0.669	0.5865

Table A11

Kinetic Data for Methanol Dehydration on Fresh F49 at 170°C

A. $c_W = 0$

$c_A \times 10^2$	0.12	0.16	0.23	0.31	0.43	0.61	0.805	1.22	1.67	2.42
$r \times 10^3$	1.023	1.100	1.202	1.401	1.592	1.795	1.967	2.362	2.695	3.119

B. $c_W = 1.24 \times 10^{-3}$

$c_A \times 10^2$	0.09	0.15	0.25	0.32	0.40	0.58	0.82	1.18	1.64	2.37
$r \times 10^3$	0.495	0.64	0.80	0.88	1.001	1.139	1.262	1.522	1.796	2.04

C. $c_A = 1.02 \times 10^{-2}$

$c_W \times 10^3$	0.28	0.50	0.73	0.95	1.21	1.70	1.95
$r \times 10^3$	2.002	1.818	1.672	1.538	1.429	1.250	1.163

Table A12

Kinetic Data for Methanol Dehydration on Fresh F49 at 182°C

A. $c_W = 0$

$c_A \times 10^2$	0.092	0.162	0.230	0.340	0.425	0.60	0.85	1.15	1.63	2.44
$r \times 10^3$	1.479	1.919	1.08	1.60	3.001	3.2	3.96	4.32	4.879	5.68

B. $c_W = 1.30 \times 10^{-3}$

$c_A \times 10^2$	0.08	0.15	0.22	0.30	0.445	0.63	0.86	1.21	1.68	2.41
$r \times 10^3$	0.879	1.16	1.239	1.595	1.88	2.04	2.401	2.88	3.402	3.722

C. $c_A = 1.01 \times 10^{-2}$

$c_W \times 10^3$	0.286	0.514	0.747	0.985	1.223	1.464	1.708	1.956
$r \times 10^3$	3.763	3.322	3.062	2.915	2.704	2.50	2.328	2.237

Table A13

Kinetic Data for Methanol Dehydration on Poisoned F49 at 160°C

A. $c_W = 0$

$c_A \times 10^2$	0.115	0.185	0.210	0.32	0.45	0.66	0.88	1.18	1.84	2.11	2.4
$r \times 10^4$	3.90	4.50	5.05	5.89	6.50	7.197	7.60	8.39	9.3	9.796	10.25

B. $c_W = 2.5 \times 10^{-4}$

$c_A \times 10^2$	0.095	0.162	0.24	0.32	0.45	0.58	0.97	1.16	1.68	2.45
$r \times 10^4$	2.35	3.0	3.6	4.05	4.70	5.00	6.20	6.55	7.50	8.35

C. $c_A = 1.01 \times 10^{-2}$

$c_W \times 10^3$	0.255	0.485	0.719	1.196	1.684
$r \times 10^4$	6.523	5.128	4.405	3.597	2.530

Table A14

Kinetic Data for Methanol Dehydration on Poisoned F49 at 170°C

A. $c_W = 0$

$c_A \times 10^2$	0.11	0.18	0.26	0.32	0.44	0.62	0.82	1.24	1.65	2.43
$r \times 10^3$	0.66	0.84	1.00	1.06	1.138	1.30	1.40	1.68	1.76	1.982

B. $c_W = 1.10 \times 10^{-3}$

$c_A \times 10^2$	0.09	0.16	0.25	0.32	0.40	0.56	0.83	1.18	1.62	2.39
$r \times 10^3$	0.22	0.319	0.352	0.438	0.451	0.542	0.65	0.719	0.839	1.002

C. $c_A = 1.02 \times 10^{-2}$

$c_W \times 10^3$	0.28	0.50	0.73	0.95	1.21	1.70	1.95
$r \times 10^3$	1.22	1.031	0.87	0.746	0.658	0.532	0.490

Table A15

Kinetic Data for Methanol Dehydration on Poisoned F49 at 182°C

A. $c_W = 0$

$c_A \times 10^2$	0.085	0.17	0.25	0.37	0.43	0.62	0.84	1.18	1.65	2.42
$r \times 10^3$	1.202	1.68	1.80	2.08	2.28	2.48	2.72	3.00	3.32	3.763

B. $c_W = 1.20 \times 10^{-3}$

$c_A \times 10^2$	0.09	0.15	0.23	0.31	0.45	0.64	0.87	1.22	1.69	2.42
$r \times 10^3$	0.46	0.597	0.72	0.78	0.96	1.10	1.36	1.56	1.639	1.920

C. $c_A = 1.01 \times 10^{-2}$

$c_W \times 10^3$	0.312	0.535	0.762	0.991	1.228	1.467	1.712	1.96
$r \times 10^3$	2.451	2.08	1.786	1.60	1.373	1.235	1.165	1.132

Table A16

Kinetic Data for Ethanol Dehydration on Fresh F49 at 155°C

A. $c_W = 0$

$c_A \times 10^2$	0.08	0.12	0.16	0.23	0.32	0.45	0.635	0.865	1.210	1.725
$r_{ethylene} \times 10^4$	0.421	0.465	0.484	0.531	0.542	0.58	0.62	0.64	0.67	0.689
$r_{ether} \times 10^3$	0.50	0.586	0.695	0.767	0.951	1.007	1.129	1.171	1.340	1.560
σ%	4.04	3.82	3.36	3.34	2.77	2.80	2.67	2.66	2.44	2.16

B. $c_A = 1.28 \times 10^{-2}$

$c_W \times 10^3$	0.475	0.871	1.284	1.700	2.104	2.952
$r_{ethylene} \times 10^4$	0.37	0.256	0.208	0.167	0.139	0.104
$r_{ether} \times 10^3$	1.22	1.075	1.00	0.926	0.833	0.735
σ%	1.49	1.18	1.029	0.894	0.827	0.704

Table A17

Kinetic Data for Ethanol Dehydration on Poisoned F49 at 155°C

A. $c_W = 0$

$c_A \times 10^2$	0.08	0.12	0.16	0.23	0.32	0.45	0.635	0.865	1.21	1.725
$r_{ethylene} \times 10^4$	0.241	0.28	0.293	0.301	0.320	0.329	0.345	0.352	0.368	0.372
$r_{ether} \times 10^4$	1.82	2.125	2.25	2.513	2.576	3.48	3.77	3.825	4.416	6.150
σ%	6.21	6.18	5.29	5.63	5.85	4.52	4.38	4.40	4.00	2.94

B. $c_A = 1.28 \times 10^{-2}$

$c_W \times 10^3$	0.08	0.475	0.871	1.284	1.70	2.104	2.952
$r_{ethylene} \times 10^4$	0.333	0.189	0.133	0.109	0.0893	0.0725	0.0543
$r_{ether} \times 10^4$	4.39	3.55	3.25	3.05	2.94	2.52	2.38
σ%	3.65	2.59	2.00	1.76	1.50	1.42	1.13

Table A18

Kinetic Data for Ethanol Dehydration on KSFO at 225°C

A. $c_W = 0$

$c_A \times 10^2$	0.047	0.098	0.14	0.202	0.405	0.582	0.794
$r_{ethylene} \times 10^2$	1.02	1.13	1.184	1.26	1.34	1.37	1.38
$r_{ether} \times 10^2$	1.20	1.75	2.03	2.27	3.36	3.82	4.52
σ%	29.82	24.41	22.58	21.73	16.62	15.2	13.24

B. $c_A = 1.11 \times 10^{-2}$

$c_W \times 10^3$	0.67	1.03	1.41	2.17	2.93	4.07
$r_{ethylene} \times 10^2$	1.10	1.00	0.88	0.76	0.63	0.50
$r_{ether} \times 10^2$	4.50	4.20	3.99	3.59	3.26	2.92
σ%	10.89	10.64	9.93	9.57	8.81	7.89

Table A19

Kinetic Data for Ethanol Dehydration on F49 at 225°C

A. $c_W = 0$

$c_A \times 10^2$	0.066	0.0936	0.195	0.389	0.772
$r_{ethylene} \times 10^2$	0.432	0.480	0.502	0.530	0.565
$r_{ether} \times 10^2$	1.02	1.23	1.72	2.30	3.11
σ%	17.48	16.33	12.73	10.33	8.33

B. $c_A = 1.017 \times 10^{-2}$

$c_W \times 10^3$	0.71	0.89	1.26	2.41	4.27	6.15	8.08
$r_{ethylene} \times 10^2$	0.466	0.448	0.414	0.326	0.248	0.200	0.178
$r_{ether} \times 10^2$	3.30	3.21	3.05	2.80	2.43	2.00	1.82
σ%	6.61	6.52	6.36	5.50	4.85	4.76	4.66

Table A20

Kinetic Data for Ethanol Dehydration on AHC at 225°C

A. $c_W = 0$

$c_A \times 10^2$	0.038	0.052	0.108	0.153	0.220	0.436	0.621	0.850	1.194
$r_{ethylene} \times 10^3$	0.300	0.358	0.420	0.446	0.482	0.520	0.538	0.550	0.562
$r_{ether} \times 10^2$	1.12	1.28	1.68	2.00	2.22	2.67	2.93	3.15	3.22
σ%	11.81	12.27	11.11	10.03	9.79	8.87	8.41	8.03	8.03

B. $c_A = 1.127 \times 10^{-2}$

$c_W \times 10^3$	0.43	1.20	1.98	2.75	3.92	5.87
$r_{ethylene} \times 10^3$	0.388	0.253	0.188	0.142	0.112	0.076
$r_{ether} \times 10^2$	2.42	1.57	1.21	0.94	0.70	0.54
σ%	7.39	7.46	7.21	7.02	7.41	6.57

Table A21

Kinetic Data for Ethanol Dehydration on F1 at 225°C

A. $c_W = 0$

$c_A \times 10^2$	0.0276	0.0394	0.0542	0.077	0.225
$r_{ethylene} \times 10^5$	0.437	0.450	0.488	0.52	0.57
$r_{ether} \times 10^4$	1.15	1.25	1.30	1.37	1.82
$\sigma\%$	1.87	1.77	1.84	1.86	1.54

B. $c_A = 1.176 \times 10^{-2}$

$c_W \times 10^3$	0.40	0.60	0.80	0.98	1.18
$r_{ethylene} \times 10^5$	0.252	0.209	0.184	0.164	0.125
$r_{ether} \times 10^4$	1.02	0.81	0.71	0.63	0.54
$\sigma\%$	1.22	1.27	1.28	1.285	1.14

Table A22

Determination of Time Required for Adsorption during Titration of T126

Time after Titer Addition (minutes)	Temperature (Beckman Reading) ^{o}C	Total Temperature Increase* ^{o}C	$\Delta T^{@}$ ^{o}C
0	2.420	--	--
0.5	2.445	0.025	0.024
1.0	2.470	0.050	0.048
1.5	2.490	0.070	0.067
2.0	2.513	0.097	0.093
2.5	2.520	0.100	0.95
3.0	2.525	0.105	0.099
4.0	2.528	0.108	0.100
5.0	2.530	0.110	0.100
6.0	2.532	0.112	0.100
8.0	2.536	0.116	0.100
10.0	2.540	0.120	0.100

* Includes temperature change due to mixing which is observed to be $0.002^{o}C$/minute.

@ Note that time required for adsorption of n-butylamine is of the order of 2.5-3 minutes.

Table A23

Acidity Titration for KSF

W	ΔT	-ΔH
0.0135	0.058	29.4
0.027	0.053	26.8
0.0405	0.048	24.3
0.054	0.041	20.8
0.0675	0.038	19.2
0.081	0.033	16.7
0.0945	0.028	14.2
0.108	0.023	11.6
0.1215	0.018	9.1
0.135	0.014	7.07
0.1485	0.011	5.56
0.1620	0.010	5.05
0.1755	0.008	4.05
0.1890	0.004	2.05
0.2025	0.003	1.52
0.2160	0.002	1.02

Table A24

Acidity Titrations for KSFO

W	ΔT	-ΔH
0.115	0.255	25.7
0.230	0.185	18.7
0.345	0.120	12.17
0.460	0.08	8.15
0.575	0.08	8.16
0.690	0.05	5.13
0.805	0.05	5.14
0.920	0.03	3.10
1.035	0.030	3.11
1.15	0.012	1.25
1.265	0.015	1.57
1.380	0.012	1.27
1.495	0.003	0.316

Table A25

Acidity Titrations for KSFO + M

W	ΔT	-ΔH
0.0782	0.148	24.04
0.1564	0.127	20.84
0.2346	0.105	17.13
0.3128	0.085	13.9
0.3910	0.07	11.47
0.4692	0.06	9.86
0.5474	0.055	9.06
0.6256	0.035	5.78
0.7038	0.035	5.78
0.7820	0.026	4.31
0.8602	0.015	2.49
0.9384	0.01	1.66
1.0166	0.005	0.83
1.0948	0.003	0.50
1.1730	0.002	0.34

Table A26

Acidity Titrations for F49

W	ΔT	-ΔH
0.0516	0.135	21.34
0.1032	0.125	19.80
0.1548	0.115	18.30
0.2064	0.105	16.71
0.2580	0.095	15.15
0.3096	0.085	13.59
0.3612	0.065	10.42
0.4128	0.065	10.42
0.4654	0.055	8.84
0.5160	0.050	8.07
0.5676	0.045	7.28
0.6192	0.036	5.83
0.6708	0.035	5.69
0.7224	0.030	4.85
0.7740	0.025	4.08
0.8256	0.020	3.27
0.8772	0.015	2.46
0.9288	0.010	1.64
0.9804	0.005	0.82
1.032	0.002	0.33

Table A27

Acidity Titration for AHC

W	ΔT	-ΔH
0.0705	0.115	18.79
0.1410	0.110	17.95
0.2115	0.10	16.40
0.282	0.09	14.82
0.3525	0.08	13.20
0.4320	0.072	11.88
0.4935	0.057	9.50
0.6110	0.075	7.49
0.7285	0.062	6.22
0.8460	0.052	5.24
0.9635	0.045	4.55
1.0810	0.035	3.56
1.1985	0.03	3.06
1.3160	0.03	3.06
1.4335	0.018	1.87
1.5510	0.005	0.52
1.6685	0.005	0.52
1.7860	0.002	0.21

Table A28

Acidity Titration for AHC + M

W	ΔT	-ΔH
0.0852	0.110	17.91
0.1704	0.110	17.91
0.2556	0.099	16.2
0.3408	0.065	10.65
0.4260	0.065	10.65
0.5112	0.05	8.23
0.5964	0.05	8.24
0.6816	0.03	4.96
0.7668	0.028	4.64
0.852	0.02	3.32
0.9372	0.01	1.66
1.0224	0.005	0.83
1.1076	0.003	0.50

Table A29

Acidity Titrations for ALC

W	ΔT	-ΔH
0.01	0.02	19.4
0.073	0.11	18.2
0.146	0.105	17.4
0.219	0.10	16.54
0.292	0.09	14.98
0.365	0.075	12.51
0.438	0.07	11.7
0.511	0.06	10.02
0.633	0.09	9.1
0.755	0.08	8.1
0.877	0.06	6.1
0.999	0.05	5.1
1.122	0.05	5.1
1.244	0.04	4.13
1.366	0.025	2.59
1.488	0.01	1.15
1.610	0.005	0.57

Table A30

Acidity Titration for T126

W	ΔT	-ΔH
0.0557	0.100	15.90
0.1114	0.092	14.78
0.1671	0.085	13.68
0.2228	0.085	13.70
0.2785	0.08	12.94
0.3342	0.07	11.34
0.3899	0.062	10.07
0.4456	0.035	5.7
0.5013	0.025	4.08
0.5570	0.02	3.27
0.6127	0.015	2.46
0.6684	0.010	1.64
0.7241	0.007	1.15
0.7798	0.005	0.82
0.8355	0.003	0.5

Table A31

Acidity Titrations for F1

W	ΔT	-ΔH
0.0725	0.132	13.68
0.1450	0.130	13.45
0.2175	0.095	9.954
0.2900	0.03	3.35
0.3771	0.032	2.81
0.435	0.028	3.71
0.5075	0.01	1.065
0.580	0.004	0.43
0.6525	0.005	0.53
0.725	0.003	0.32

Table A32

Basicity Titration for KSF

W	ΔT	-ΔH
0.034	0.043	9.77
0.068	0.033	7.54
0.102	0.022	5.05
0.136	0.019	4.38
0.170	0.009	2.09
6.204	0.001	0.23

Table A33

Basicity Titrations for KSFO

W	ΔT	-ΔH
0.056	0.048	10.186
0.112	0.044	9.374
0.168	0.046	9.839
0.224	0.040	8.59
0.280	0.041	8.84
0.336	0.035	7.574
0.392	0.025	5.591
0.448	0.025	5.612
0.564	0.020	4.379
0.560	0.015	3.3
0.616	0.01	2.21
0.672	0.007	1.55
0.728	0.01	2.22
0.784	0.007	1.56
0.84	0.003	0.672
0.896	0.002	0.45
0.952	0.002	0.45

Table A34

Basicity Titrations for KSFO + M

W	ΔT	-ΔH
0.0413	0.055	18.12
0.0826	0.04	13.21
0.1239	0.035	11.59
0.1652	0.033	11.05
0.2065	0.033	11.06
0.2478	0.026	8.67
0.2891	0.022	7.35
0.3304	0.017	5.69
0.3717	0.015	5.09
0.4130	0.012	4.36
0.4543	0.007	2.36
0.4956	0.005	1.70
0.5369	0.004	1.35
0.5782	0.003	1.02
0.6195	0.001	0.34

Table A35

Basicity Titrations for F49

W	ΔT	-ΔH
0.0326	0.041	12.9
0.0652	0.038	12.48
0.0978	0.035	11.45
0.1304	0.033	10.7
0.1630	0.029	9.88
0.1956	0.027	9.02
0.2282	0.024	8.11
0.2608	0.022	7.50
0.2934	0.02	7.12
0.3260	0.018	5.99
0.3586	0.015	4.90
0.3912	0.01	3.50
0.4238	0.007	2.10
0.4564	0.004	1.34
0.489	0.002	0.67
0.5216	0.001	0.33

Table A36

Basicity Titration for AHC

W	ΔT	-ΔH
0.0358	0.03	10.37
0.0716	0.02	6.83
0.1074	0.015	5.20
0.1432	0.01	3.48
0.1790	0.01	3.48
0.2148	0.006	2.10
0.2506	0.005	1.75
0.2084	0.003	1.05
0.3222	0.002	0.70
0.3580	0.002	0.70

Table A37

Basicity Titrations for AHC + M

W	ΔT	-ΔH
0.05	0.08	15.38
0.10	0.078	15.18
0.15	0.07	13.74
0.20	0.052	10.21
0.25	0.053	10.24
0.30	0.039	7.73
0.35	0.022	4.37
0.40	0.012	2.40
0.45	0.006	1.19
0.50	0.004	0.79

Table A38

Basicity Titrations for ALC

W	ΔT	-ΔH
0.038	0.03	9.95
0.102	0.04	8.0
0.166	0.037	7.44
0.230	0.036	7.30
0.294	0.032	6.49
0.358	0.02	4.07
0.422	0.01	2.04
0.486	0.006	1.23
0.55	0.003	0.62

Table A39

Basicity Titrations for T126

W	ΔT	-ΔH
0.0316	0.05	16.63
0.0632	0.04	13.33
0.0948	0.04	13.33
0.1264	0.04	13.33
0.1580	0.035	11.75
0.1596	0.035	11.75
0.2212	0.03	10.11
0.2528	0.027	9.12
0.2844	0.025	8.47
0.3160	0.02	6.79
0.3476	0.015	5.1
0.3792	0.015	5.1
0.4108	0.01	3.42
0.4424	0.01	3.42
0.4740	0.01	3.42
0.5056	0.008	2.73
0.5372	0.008	2.73
0.5688	0.007	2.40
0.6004	0.005	1.73
0.6320	0.003	1.04
0.6636	0.003	1.04
0.6952	0.001	0.35

Table A40

Basicity Titrations for F1

W	ΔT	-ΔH
0.0475	0.08	17.34
0.095	0.075	16.31
0.1425	0.07	15.28
0.1900	0.062	13.58
0.2375	0.05	10.99
0.2850	0.04	8.82
0.3325	0.038	8.42
0.3800	0.038	8.42
0.4275	0.032	7.13
0.475	0.025	5.59
0.5525	0.025	5.60
0.5700	0.03	6.76
0.6175	0.023	5.21
0.665	0.013	2.95
0.7125	0.009	2.05
0.760	0.005	1.16
0.8075	0.003	0.69
0.855	0.002	0.46
0.9025	0.002	0.46

Table A41

Acidity Titrations for KSFO + B_uNH_2

W	ΔT	-ΔH
0.10	0.13	20.68
0.20	0.095	15.15
0.30	0.065	10.39
0.40	0.05	8.02
0.50	0.05	8.00
0.60	0.04	6.44
0.70	0.035	5.64
0.80	0.03	4.85
0.90	0.025	4.05
1.00	0.02	3.25
1.10	0.015	2.45
1.20	0.009	1.47
1.30	0.005	0.82
1.40	0.003	0.49

Table A42

Acidity Titrations for F49 + B_uNH_2

W	ΔT	-ΔH
0.0290	0.044	19.17
0.0772	0.065	17.11
0.1544	0.09	14.82
0.2316	0.082	13.49
0.3088	0.080	13.17
0.3860	0.065	10.77
0.4632	0.055	9.14
0.5404	0.04	6.66
0.6176	0.035	5.84
0.6948	0.025	4.18
0.7720	0.011	1.84
0.8492	0.007	1.18
0.9264	0.007	1.18
1.0036	0.003	0.51

Table A43

Acidity Titrations for ALC + B_uNH_2

W	ΔT	-ΔH
0.114	0.165	16.52
0.228	0.135	13.6
0.342	0.100	10.1
0.456	0.085	8.62
0.570	0.07	7.13
0.684	0.054	5.53
0.798	0.045	4.62
0.912	0.033	3.40
1.026	0.023	2.38
1.140	0.02	2.08
1.254	0.013	1.36
1.368	0.008	0.84
1.482	0.005	0.53
1.596	0.002	0.21

Table A44

Acidity Titrations for KSFO + KOH

W	ΔT	-ΔH
0.1	0.125	19.67
0.2	0.095	15.00
0.3	0.08	12.66
0.4	0.055	8.72
0.5	0.055	8.72
0.6	0.04	6.37
0.7	0.035	5.58
0.8	0.03	4.80
0.9	0.026	4.17
1.0	0.02	3.22
1.1	0.016	2.57
1.2	0.009	1.45
1.3	0.005	0.81
1.4	0.004	0.65
1.5	0.002	0.33

Table A45

Basicity Titrations for KSFO + B_uNH_2

W	ΔT	-ΔH
0.063	0.084	17.26
0.126	0.06	12.38
0.189	0.05	10.36
0.252	0.042	8.74
0.315	0.035	7.32
0.378	0.03	6.30
0.441	0.025	5.27
0.504	0.02	4.24
0.567	0.015	3.19
0.630	0.01	2.14
0.693	0.007	1.50
0.756	0.005	1.07
0.819	0.003	0.65

Table A46

Basicity Titrations for KSFO + Pyridine

W	ΔT	-ΔH
0.038	0.032	10.80
0.102	0.05	9.87
0.166	0.045	9.02
0.230	0.045	9.03
0.294	0.04	8.00
0.358	0.035	7.03
0.422	0.03	6.05
0.486	0.03	6.06
0.550	0.02	4.07
0.614	0.015	3.07
0.678	0.01	2.05
0.742	0.01	2.06
0.806	0.005	1.03
0.870	0.002	0.42

Table A47

Basicity Titration for F49 + B_uNH_2

W	ΔT	-ΔH
0.0363	0.05	16.10
0.0726	0.05	16.10
0.1089	0.045	14.56
0.1452	0.04	12.94
0.1815	0.035	11.37
0.2178	0.03	9.77
0.2541	0.025	8.16
0.2904	0.025	8.17
0.3267	0.02	6.56
0.3630	0.015	4.93
0.3993	0.012	3.95
0.4356	0.007	2.31
0.4719	0.005	1.66
0.5082	0.003	1.00
0.5445	0.001	0.37

Table A48

Basicity Titrations for ALC + B_uNH_2

W	ΔT	-ΔH
0.038	0.043	14.33
0.076	0.03	10.02
0.113	0.025	8.37
0.176	0.038	7.67
0.239	0.036	7.30
0.302	0.032	6.52
0.365	0.019	3.89
0.428	0.01	2.05
0.491	0.005	1.03
0.554	0.003	0.62

Nomenclature for Tables A10 - A48

c_A	Alcohol concentration, moles/liter
c_W	Water concentration, moles/liter
$-\Delta H$	Heat of adsorption, kcal/mole
r	Rate of product formation, moles/hr. g catalyst
ΔT	Temperature change due to adsorption
W	Amount of titer adsorbed, mmol/g catalyst
σ	Selectivity for ethylene formation, as defined in earlier sections

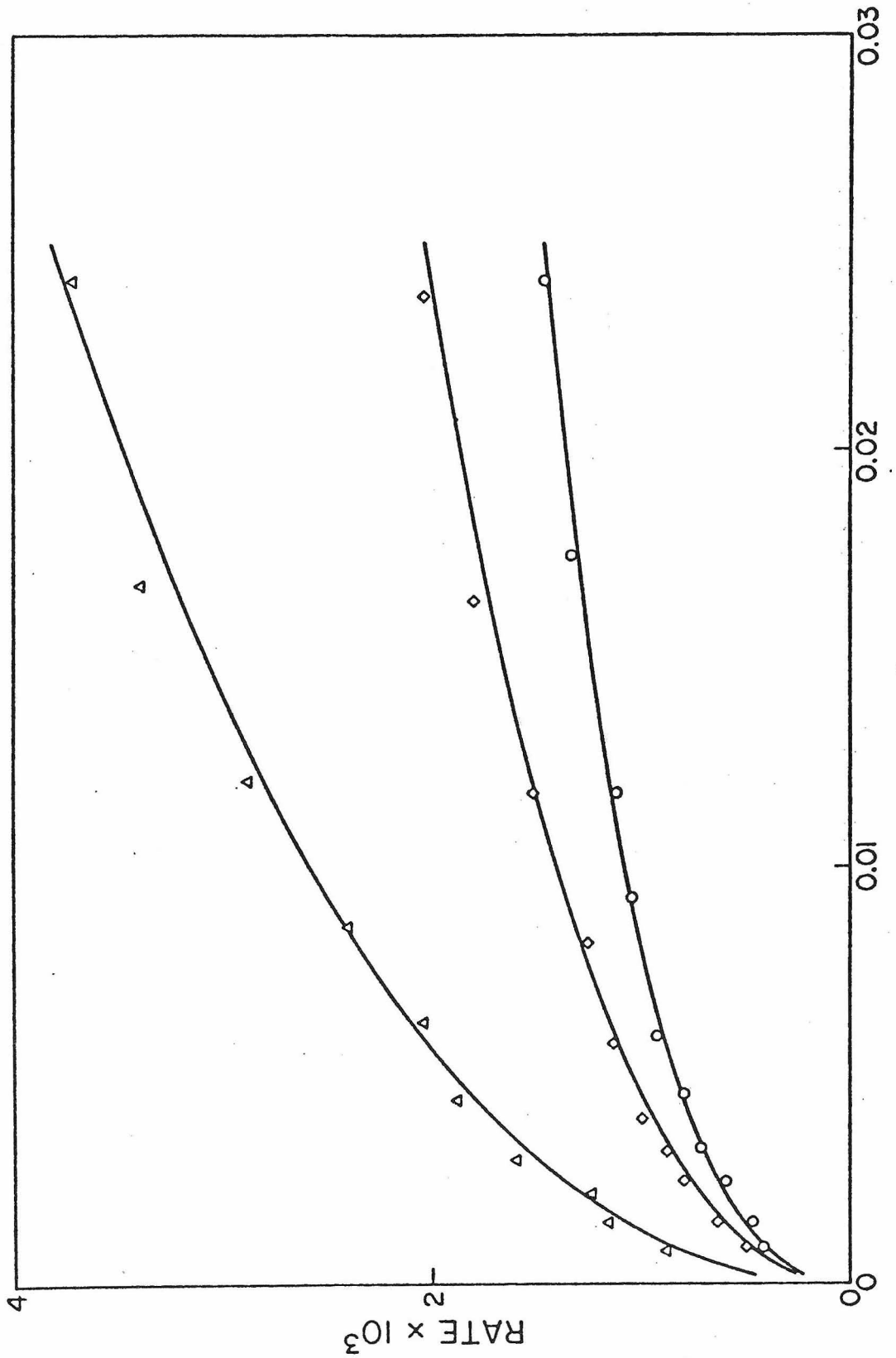

Figure A1 Kinetics of methanol dehydration on fresh catalyst

Run conditions

(△) T = 182°C; c_W (feed) = 0.0013
(◇) T = 170°C; c_W (feed) = 0.00124
(o) T = 160°C; c_W (feed) = 0.00025

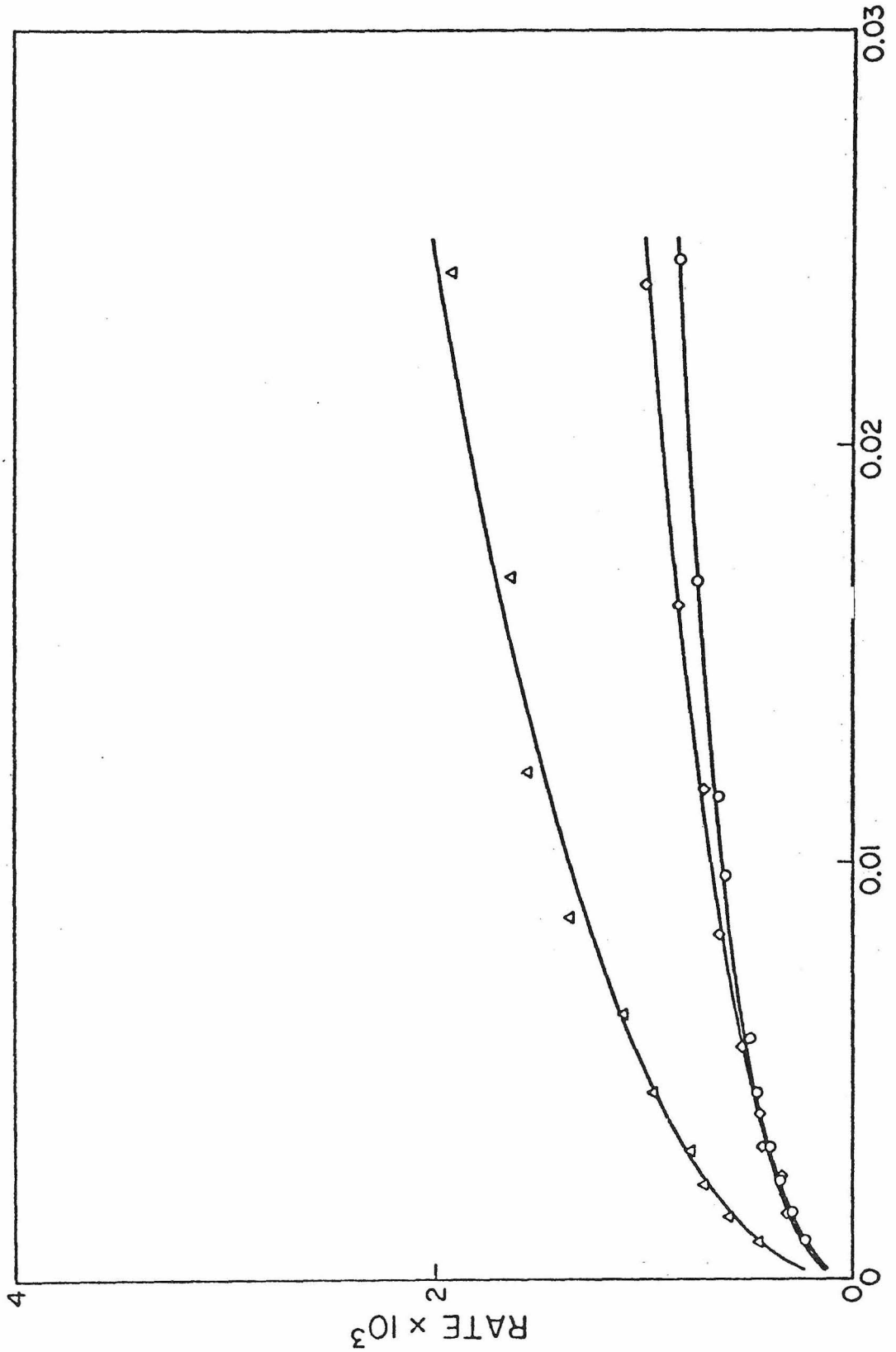

Figure A2 Kinetics of methanol dehydration on poisoned catalyst

Run conditions

(△) T = 182°C; c_W (feed) = 0.0012
(◇) T = 170°C; c_W (feed) = 0.0011
(○) T = 160°C; c_W (feed = 0.00025

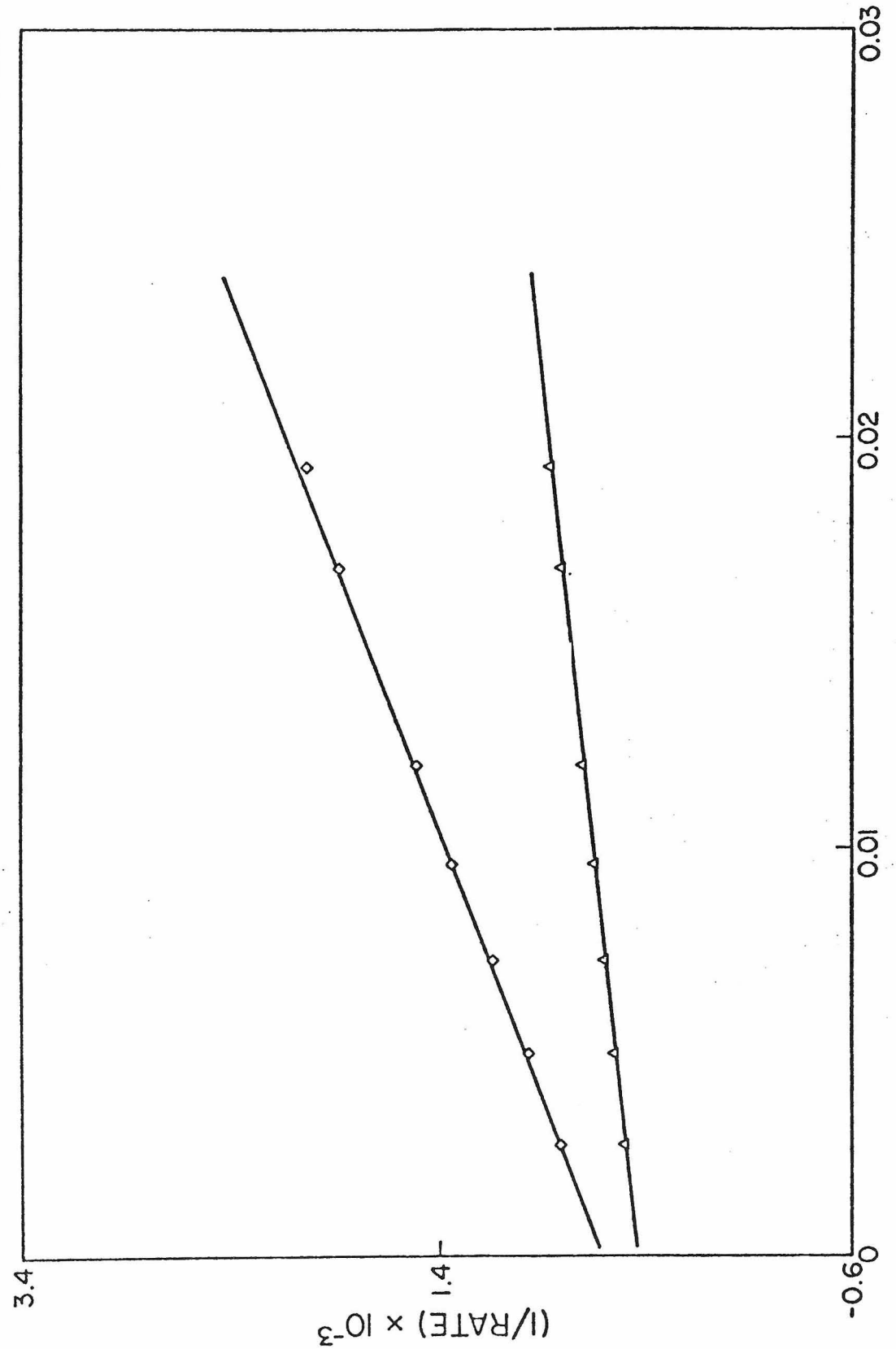

Figure A3 Effect of water on methanol dehydration.

Run conditions; c_A = 0.0102; T = 170°C

(◇) Poisoned catalyst
(△) Fresh catalyst

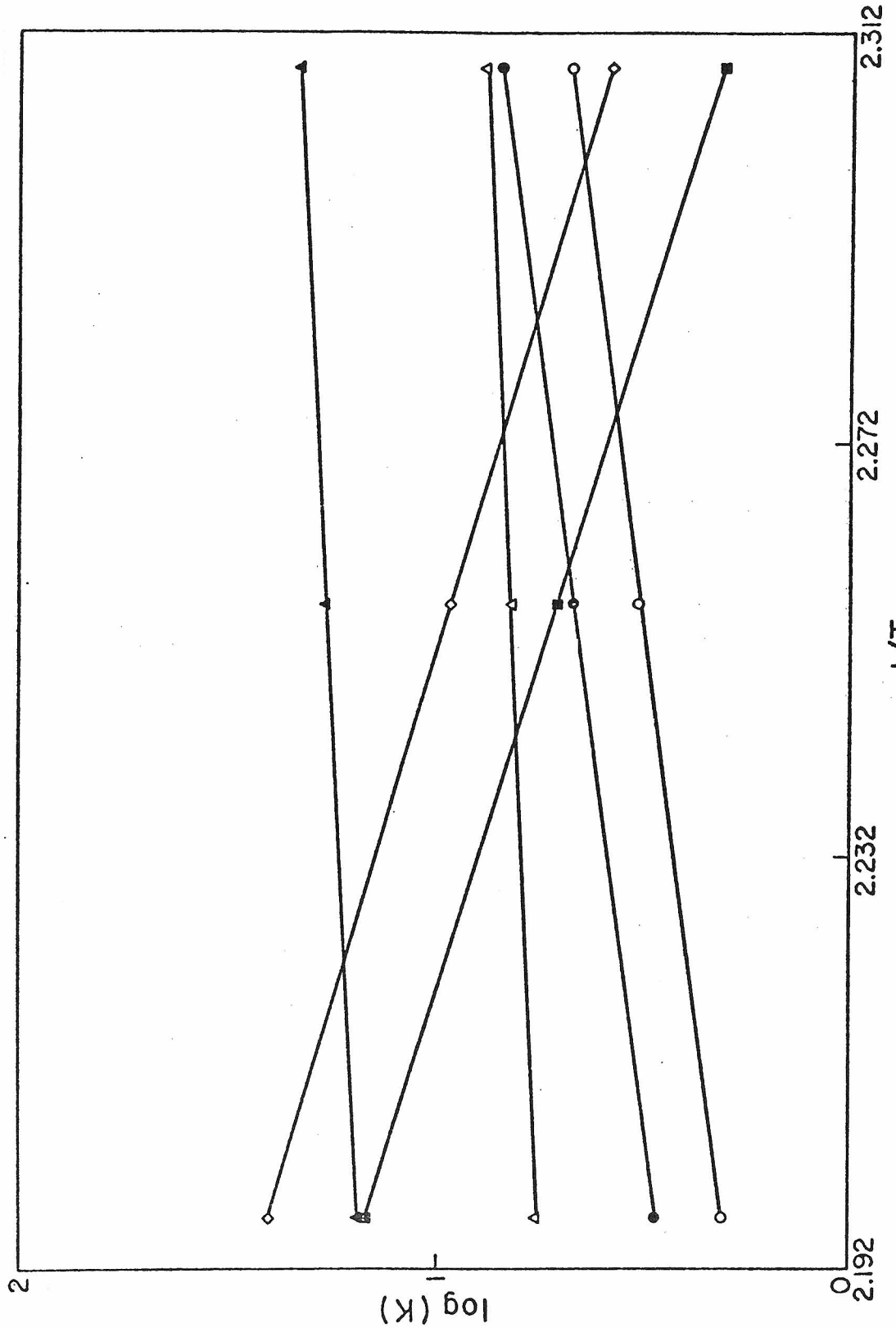

Figure A4 Temperature effect on model constants for methanol dehydration

(a) Fresh catalyst: (□) k x 10^3; (○) K_A ; (△) K_W x 10^{-2}
(b) Poisoned catalyst: (■) k x 10^3; (●) K_A ; (▲) K_W x 10^{-2}

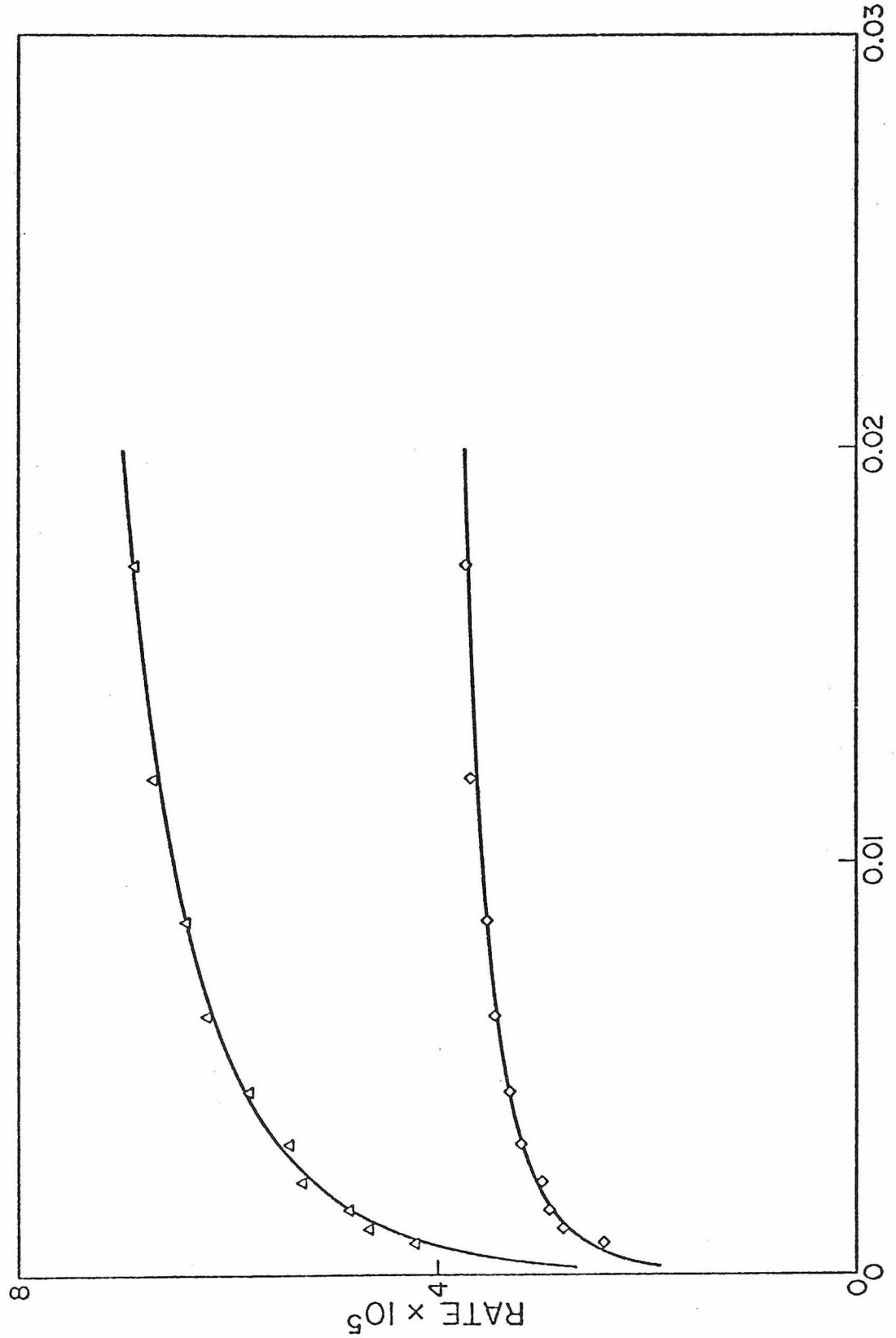

Figure A5 Kinetics of ethylene formation at 155°C

Run conditions: c_W (feed) = 0; (△) fresh catalyst;
(◇) poisoned catalyst

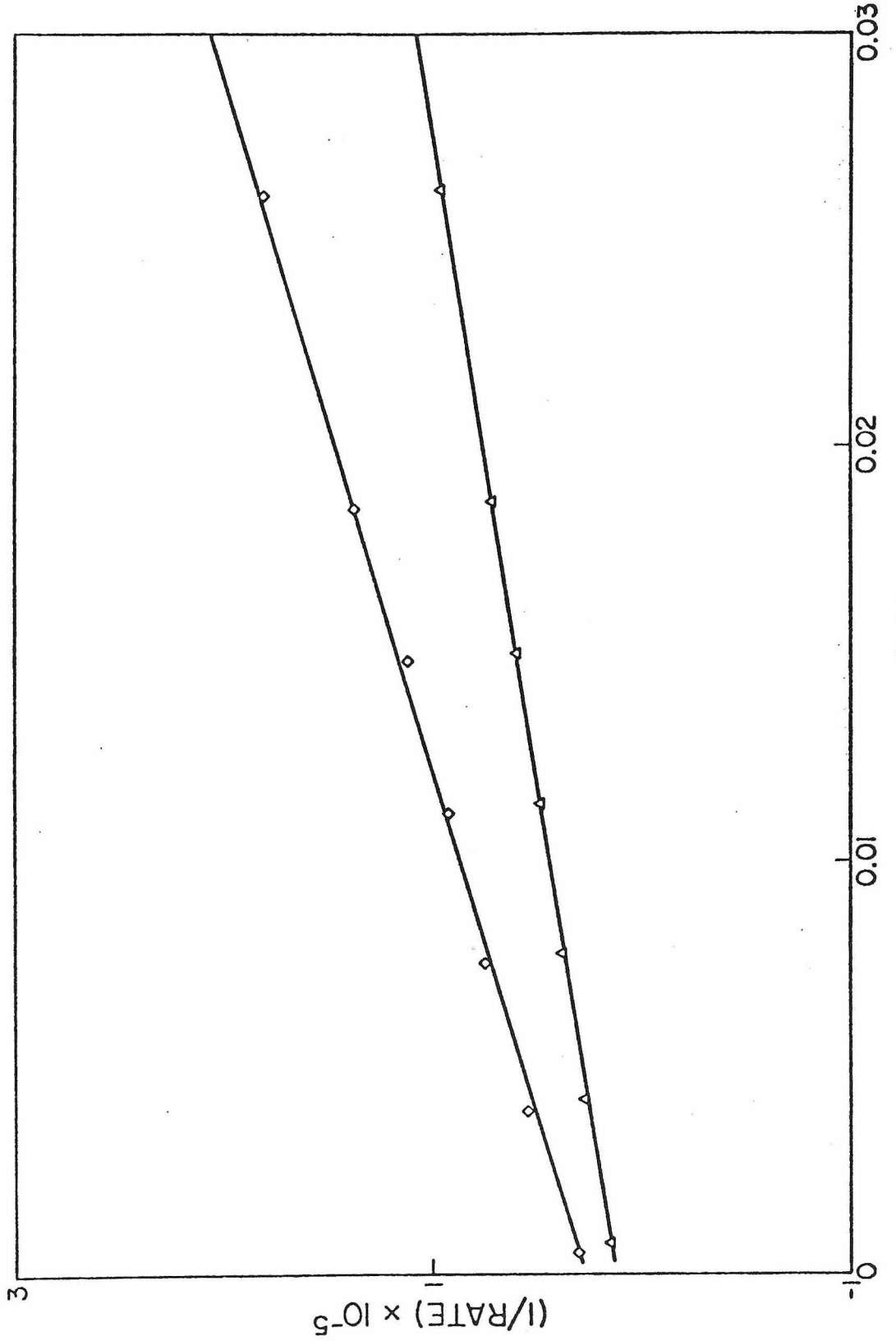

Figure A6 Effect of water on ethylene formation at 155°C.

Run conditions: c_A = 0.0128; (△) fresh catalyst; (◇) poisoned catalyst

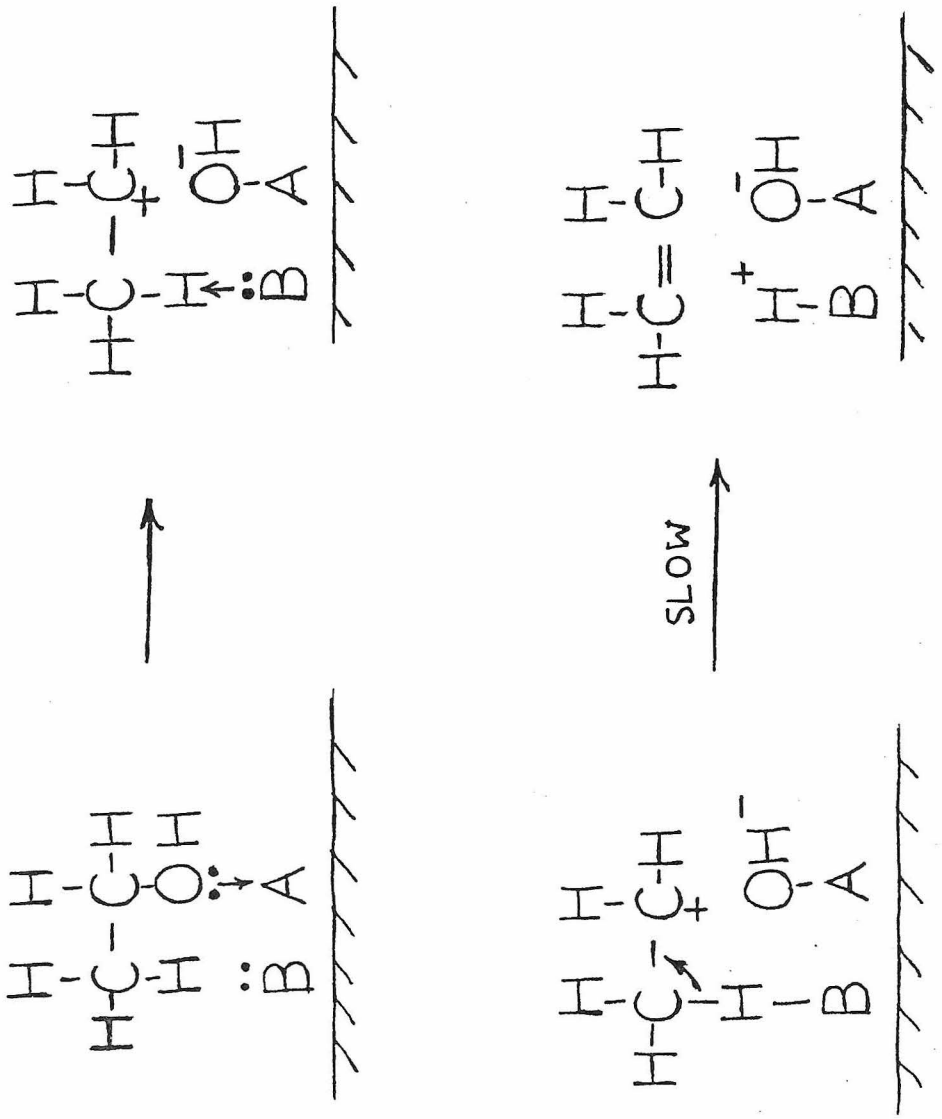

Figure A7 Mechanism Proposed for Ethylene Formation

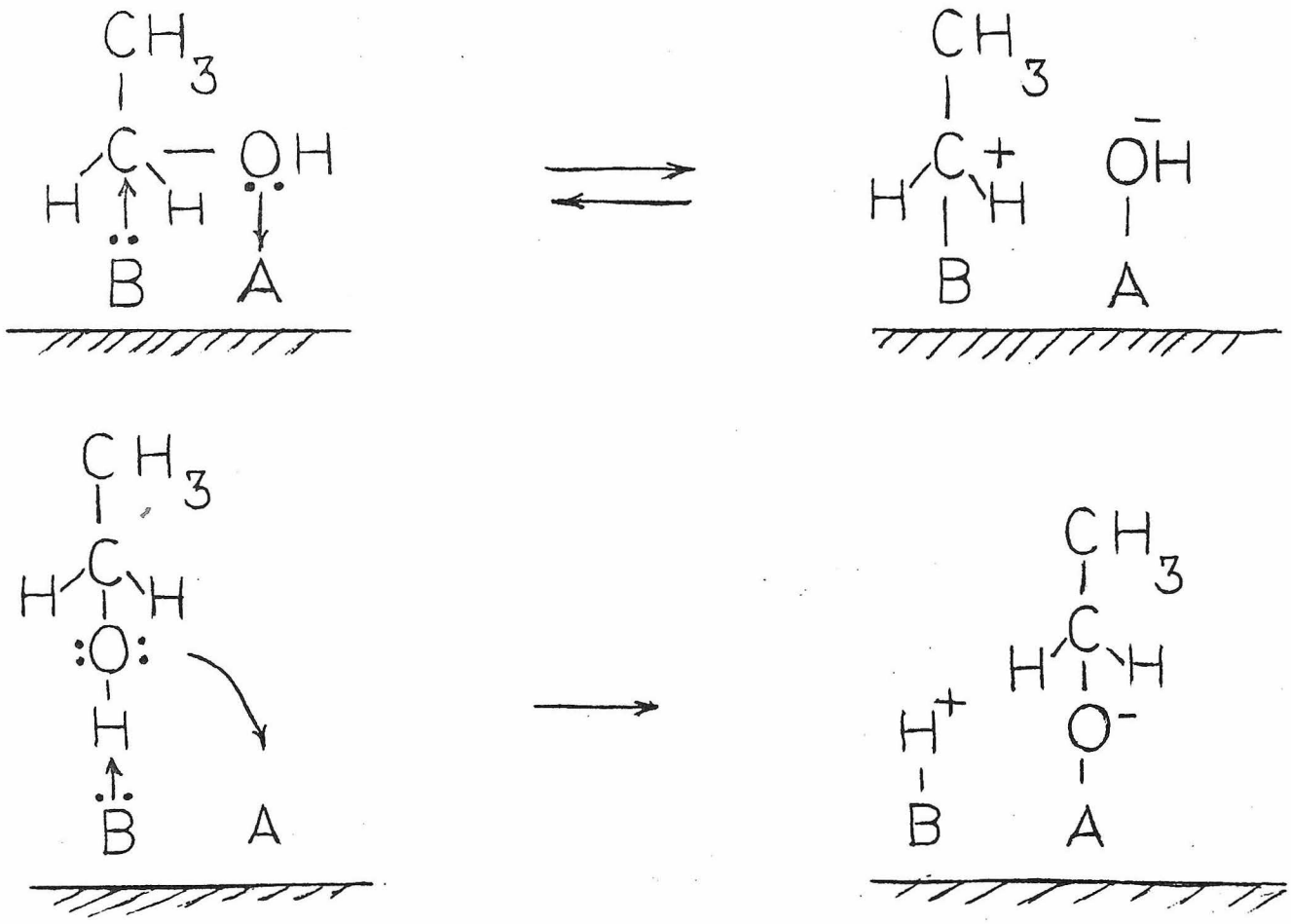

Figure A8 Mechanism Proposed for Ether Formation